Final Report

Modular Multipurpose Research UAV

J.M. Bakker	4016076	M. van Rijsingen	4078357
S. Potkamp	4154304	J.J.P. van den Berg	4094166
R.L. Bokdam	4178122	M. Baars	1506668
S.A. Doesburg	4144317	P.M. Nijman	4180178
J.M. de Wilde	4087372	M.J. Perdeck	4078799

Design Synthesis Exercises

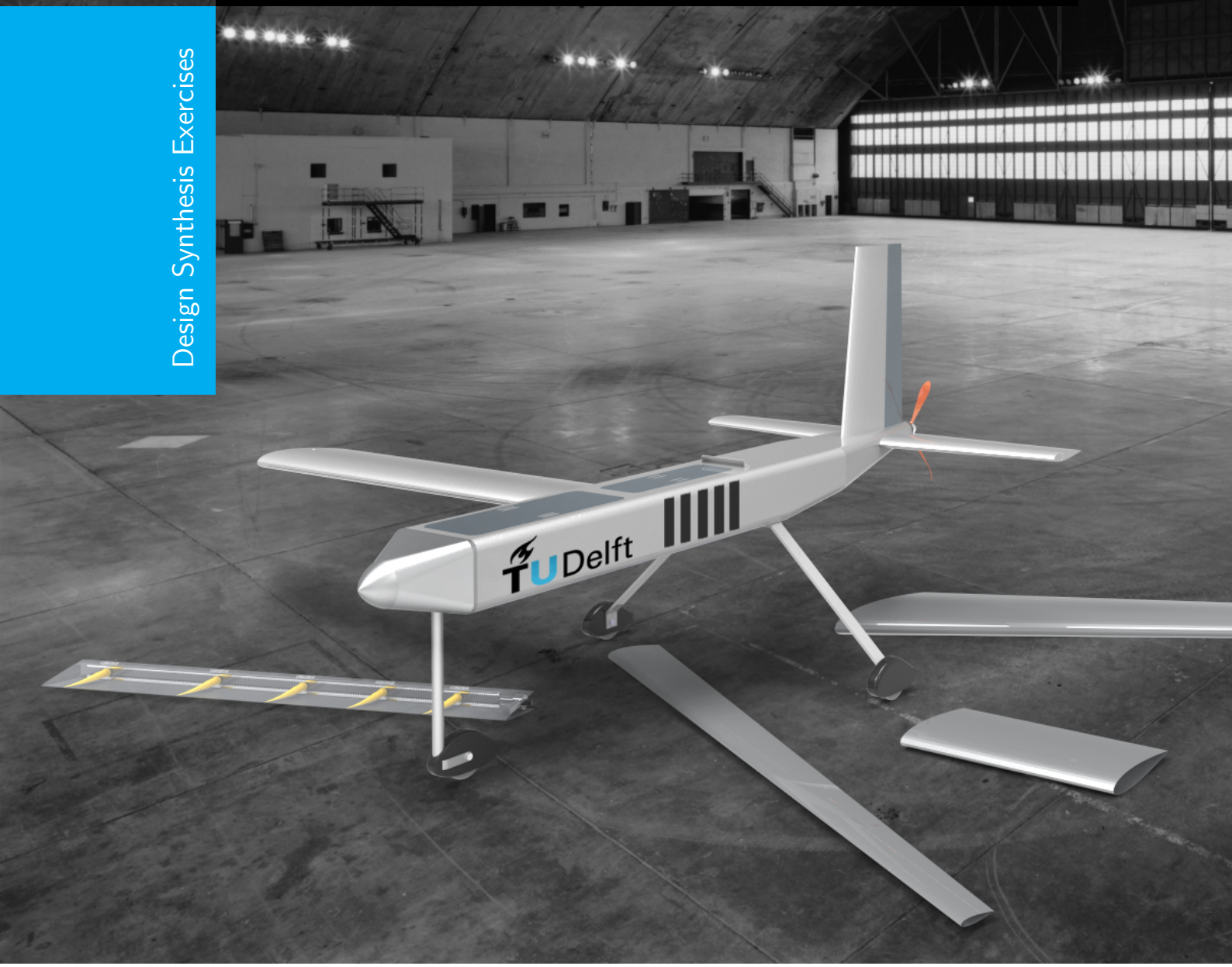

TU Delft Delft University of Technology

Aerospace Engineering

Revision 4

January 26, 2016

Summary

Modern day aeronautical testing is done with multiple means; wind tunnels, flight simulators and research aircraft are all used to test new aeronautical concepts. All have one thing in common, the high costs to make use of these facilities. Especially the use of research aircraft is very capital intensive and prone to stringent regulations. The research gap from wing testing in wind tunnels and actual flight testing is also very big, which leads to thorough safety measures which bring even more cost.

A promising solution for solving these issues and filling the research gap is the use of a Modular Unmanned Aerial Vehicle (MUAV). A MUAV has lower costs and more lenient regulations than conventional test aircraft. Therefore the Delft University of Technology has assigned a team of ten students to design a Modular Multipurpose Research UAV as test platform for innovative aeronautical concepts.

The MUAV will be a modular platform supporting a range of wing configurations, high lift device modules, wing tip modules, custom flight control schemes, interchangeable propeller and accommodation of a box wing. This modularity was the main priority during the design of the MUAV.

The first step was to select a concept to design. A trade-off was done between three different concepts; an MUAV with a fixed wing position, a MUAV with a movable wing position, and a MUAV consisting of modular fuselage blocks. After a thorough trade-off the movable wing concept was found to be the best concept and was to be designed in more detail.

All subsystems were preliminarily designed in various depths with the main focus on modularity interface details. The propulsion, power, safety, and electrical subsystems were all designed using off-the-shelf components while the empennage, landing gear, and structural design were mainly done numerically. Most detail was put into the empennage and structural design of the wing, fuselage and payload bay to account for a variety of wing configurations, modules, and payload.

A box wing module has been investigated concluding that it is feasible to design one for the MUAV. A Seamless High Lift Device module has been designed with a preliminary model to show the MUAV's capability to accommodate state of the art high lift devices.

To ensure quality of the MUAV all the subsystems have been verified and validated thoroughly. Risk and Reliability, Availability, Maintainability, and Safety (RAMS) were analysed to get an insight to the risk mitigation methods as well as the RAMS of the MUAV.

The MUAV is an innovative design with a lot of modular features. A business case has been set up to showcase the possibilities and sustainability of the MUAV to add to the attractiveness of the MUAV.

Concluding, the MUAV design is a necessary and attractive solution for aeronautic concept testing as well as for other research purposes. With the state of the current design the project can move on to more detailed design of the subsystems with the prospect of an eventual working prototype and further production.

Contents

Nomenclature

Greek symbols

α	Angle of attack	$^\circ$
α_{stall}	Stall angle of attack	$^\circ$
ε	Downwash angle at tailplane	$^\circ$
η	Aerodynamic efficiency parameter	-
Γ	Dihedral angle	$^\circ$
Λ	Sweep	$^\circ$
λ	Taper ratio	–
λ_h	Horizontal tail taper ratio	–
λ_r	Failure rate	$1/\text{hrs}$
ρ	Density of air	kg/m^3
Θ	Angle	rad
$\ddot{\Theta}$	Angular acceleration	rad/s^2

Roman symbols

A	Wing aspect ratio	–
$\bar{a}$	Average acceleration	m/s^2
A_h	Horizontal tail aspect ratio	–
b	Wing span	m
b_r	Rudder span	m
b_v	Vertical tail span	m
C	Minimal cut set	–
c	Climb rate	m/s
$\bar{c}$	Mean aerodynamic chord	m

$C_{D_{max}}$	Maximum drag coefficient	–
c_f	HLD chord length	m
C_h	Horizontal tail chord	m
C_L	Lift coefficient	–
C_L	Lift coefficient	-
C_{L_α}	lift coefficient slope curve	–
$C_{L_{\alpha_h}}$	Tail lift coefficient slope curve	–
$C_{L_{\alpha V}}$	Vertical tail lift slope	–
$C_{L_{des}}$	Design lift coefficient	–
C_{L_h}	3D tail lift coefficient	–
$C_{L_{max}}$	Design lift coefficient	–
C_{m_α}	Moment coefficient w.r.t. angle of attack	–
$C_{m_{ac}}$	Pitching moment coefficient about aerodynamic centre	–
$C_{m_{\delta_e}}$	Moment coefficient w.r.t. elevator deflection	–
C_{m_u}	Moment coefficient w.r.t. airspeed	–
C_{N_α}	Normal force coefficient slope curve	–
$C_{n_{\delta r}}$	Rudder deflection moment coefficient	–
C_{N_f}	Normal force coefficient HLD	–
$C_{N_{h_\alpha}}$	Tail normal force coefficient slope curve	–
c_r	Root chord	m
c_{wing}	Wing chord	m
C_{X_α}	Axial body force coefficient w.r.t. angle of attack	–
C_{X_u}	Axial body force coefficient w.r.t. airspeed	–
C_{Z_0}	Normal body force coefficient at 0 angle of attack	–
C_{Z_α}	Normal body force coefficient w.r.t. angle of attack	–
$C_{Z_{\delta_e}}$	Normal coefficient w.r.t. elevator deflection	–
C_{Z_u}	Normal body force coefficient w.r.t. airspeed	–
d_i	Moment arm	m
F_i	Aerodynamic force	N
h/b	Stagger	–

I_m	Mass moment of inertia	kgm^2
I_{mg}	Mass moment of inertia around the main landing gear	kgm^2
I_{mxx}	Mass moment of inertia around the x-axis through the centre of gravity	kgm^2
I_{mxz}	Mass x-z-product of inertia around the the centre of gravity	kgm^2
I_{mzz}	Mass moment of inertia around the z-axis through the centre of gravity	kgm^2
K	Number of ribs	–
L	Lift force	N
l_h	Horizontal tail length	m
l_v	Vertical tail length	m
r	mass	kg
$MTTF$	Mean time to failure	hrs
$MTTF_s$	Mean time to failure system	hrs
N_c	Number of components	–
N_{SR}	Spin recovery moment	[Nm]
N_t	Normal force on the trailing edge devices	N
P	Probability	–
R	Reliability	–
r	Distance	r
R_s	Reliability of system	–
S	Wing surface surface	m^2
$s_{airland}$	Landing airborne distance	m
s_{airTO}	Take-off airborne distance	m
$s_{groundland}$	Landing ground distance	m
$s_{groundTO}$	Take-off ground distance	m
S_h	Horizontal tailplane surface	m^2
s_{land}	Landing distance	m
s_{TO}	Take-off distance	m
S_v	Vertical tail span	m
t	Time	s
t_s	System life time	hrs

V	Airspeed	m/s
V_A	Approach speed	m/s
V_a	Manoeuvering speed	m/s
V_B	Maximum speed with gust	m/s
V_c	Design cruise speed	m/s
$V_{Cruisemax}$	Maximum cruise speed	m/s
V_d	Maximum dive speed	m/s
V_h	Horizontal tailplane speed	m/s
V_{Lof}	Lift off speed	m/s
V_s	Stall speed	m/s
V_{scr}	Screen speed	m/s
V_{Sland}	Landing speed	m/s
V_{TD}	Touch down speed	m/s
V_v	Vertical tail volume coefficient	–
W	Weight of the MUAV	N
x_{ac}	Position of aerodynamic centre from nose of aircraft	m
x_{cp}	Position of control point from nose of aircraft	m
x_{LE}	Root chord leading edge x-coordinate	m
x_{np}	Position of neutral point from nose of aircraft	m
τ_r	Control surface to lifting surface ratio	–

List of Abbreviations

CFD	Computational Fluid Dynamics	38
c.g.	centre of gravity	12
c.p.	centre of pressure	18
DOT	Design Option Tree	11
DUT	Delft University of Technology	1
EDS	Extreme Design Space	19
EOL	End of Life	122
ESDU	Engineering Sciences Data Unit	36
FBS	Functional Breakdown Structure	6
FEM	Finite Elements Method	35
FFD	Functional Flow Diagram	6
FMEA	Failure Mode and Effect Analysis	102
FW	Fuel Weight	20
GFRP	Glass Fiber Reinforced Polymer	74
GPS	Global Positioning System	103
HLD	High Lift Device	4
IDS	Independent Design Space	10
IMU	Inertial Measurement Unit	60
LE	Leading Edge	9
MAC	Mean Aerodynamic Chord	18
MAI	Manufacturing Assembly and Integration	118
MIT	Massachusetts Institute of Technology	21
MTOW	Maximum Take-Off Weight	15
MUAV	Modular Unmanned Aerial Vehicle	iii
NACA	National Advisory Committee for Aeronautics	86
n.p.	neutral point	12
OEW	Operational Empty Weight	15
PDU	Power Distribution Unit	58
POS	Project Objective Statement	2

PW	Payload Weight	20
RAMS	Reliability, Availability, Maintainability and Safety	101
RPN	Risk Priority Number	107
SEAD	Systems Engineering and Aircraft Design	18
SHLD	Seamless High-lift Devices	1
SIMONA	Simulation, Motion and Navigation	1
SWOT	Strength Weakness - Opportunities Threats	111
s.m.	stability margin	18
TE	Trailing Edge	9
UAV	Uninhabited Aerial Vehicle	2
WP	Weight over Power ratio	20
MTTF	Mean Time To failure	102
NLR	Netherlands Aerospace Centre	113

Chapter 1

Introduction

The faculty of aerospace engineering located in Delft is the largest and most sophisticated faculty with respect to aeronautical and space engineering in Northern-Europe. This is mainly due to the extensive research facilities available to researchers and students. The high speed and low speed wind tunnels provide the researchers the opportunity to accurately analyse the flow around wings and even complete small aircraft. The research simulator Simulation, Motion and Navigation (SIMONA) is able to test new flight control schemes and can simulate in-flight conditions. Furthermore the research aircraft of the faculty, a Cessna Citation II which combines the capabilities of the wind tunnel and the simulator can be used. All have one thing in common, the high costs to make use of these facilities. Especially the use of the Cessna is very capital intensive and subject to stringent regulations. A promising solution for solving these issues is the use of a Modular Unmanned Aerial Vehicle (MUAV). The investments and operational costs are much lower, and the regulations are more lenient. It is therefore that the Delft University of Technology (DUT) has assigned a team of ten students to design a MUAV that can be used as a platform to test new and innovative aeronautical concepts.

The main purpose of this report is to provide the reader with the preliminary design of the MUAV, as well as to give an overview of the total design process. The design process starts with the conceptual design phase, where in six weeks a suitable concept was generated. The last four weeks of the ten week project were dedicated to the preliminary design phase, where the subsystems were designed in more detail. Besides the design of the MUAV a preliminary box wing and Seamless High-lift Devices (SHLD) module have been designed to show the relevance of the MUAV. An extensive analysis of the business case is also provided to the reader to show the opportunities.

This report is structured as follows: first the mission outline and the conceptual design phase are presented in chapter 2 and 3. The latter will provide, among other subjects, the reader with valuable knowledge on how to approach a design of a modular platform. In chapter 4 and 5, the design of the subsystems and the design of the modules are presented respectively. This will be the core of this report, as the final design follows from this. Chapter 6 provides the reader with the integration process of the subsystems, as well as the evaluation of the flight and aerodynamics performance of the MUAV. In chapter 7 the risk management can be found. In chapter 8 the extensive analysis of the business case can be found, and in chapter 9 a conclusion is presented. This report concludes with chapter 10, where some important recommendations are given.

Chapter 2

Design of a modular UAV: project outline

Developing a modular multipurpose research Uninhabited Aerial Vehicle (UAV) or any similar complex vehicle requires a lot of resources. To make good use of these resources, a clear overview of what has to be done is needed. This chapter will discuss the approach used for this project. In this chapter the scope of the project is discussed in section 2.1 after which the mission profile and possible test scenarios are discussed in section 2.2 and 2.3 respectively. A functional analysis of the MUAV is done in section 2.4. In section 2.5 the most important requirements are highlighted. In section 2.6, the design philosophy behind the MUAV is discussed. the final section of this chapter will treat the general verification and validation procedures taken during the design.

2.1 Project scope

The Project Objective Statement (POS) is: to develop a low-cost modular platform for in-flight testing of aeronautic concepts with 10 students in 10 weeks.

The main point of focus during the design phase will be the modularity of the flying platform, as this is the most innovative part of the project and also the most interesting for the client. Because of the limited available time of 10 weeks and the strong focus on modularity, other parameters of the vehicle will be designed with less detail. Off-the-shelf solutions will be chosen for some subsystems of the platform like the control systems, software, and the engine. To put the modularity to the test, two example modules will be designed; a boxed wing concept and an SHLD.

2.2 Mission profile

Since the MUAV is both a testing tool as well as an aircraft, its mission profile should describe a typical testing day. It is assumed that a test day starts and ends in a workshop at the university which is not at the testing site. The complete mission profile is displayed as a block diagram in figure 2.1. The testing phase in figure 2.1 is done in-flight. For this purpose a nominal flight diagram is made.

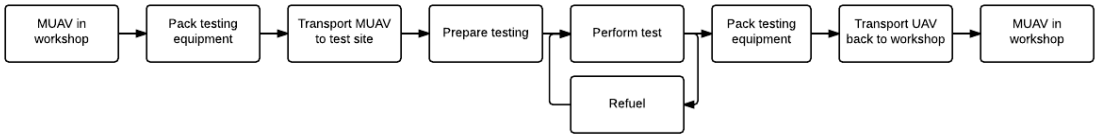

Figure 2.1: Mission profile

In figure 2.2, the nominal flight diagram can be found. This diagram consists of the following segments:

- **Take-off** Take-off time includes time to accelerate to climb speed. The vertical distance covered will be around half the maximum flight altitude.
- **Climb** The time needed to climb to the operational altitude depends on the climb gradient and climb rate. The climb gradient, operational altitude and time to climb to operation altitude are restricted by regulations.
- **Cruise** Cruise time depends on the time needed to calibrate the testing equipment.
- **Manoeuvres** Manoeuvre time depends on the type of research being conducted as well as the amount of energy left to fly according to the endurance of the UAV. More on test profiles can be found in section 2.3.
- **Descent and landing** The descent and landing is performed according to a specified schedule with a speed limit restriction, just like the climb.

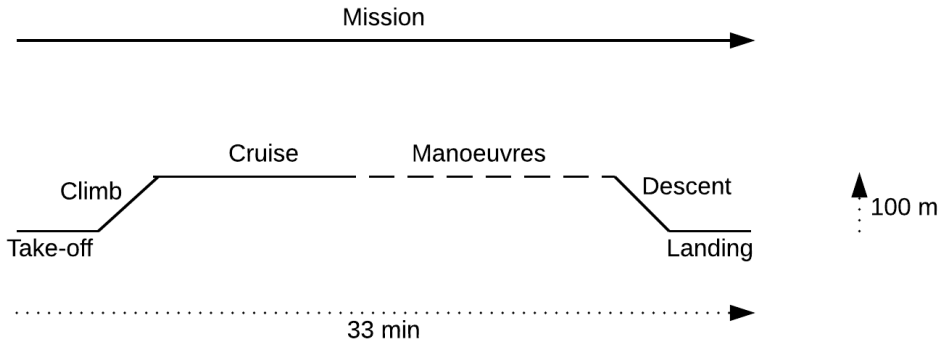

Figure 2.2: Flight diagram, start and end position may be the same location

It is important to consider the situation of an unforeseen circumstance occurring during the descent, approach or landing phase. To still safely land the aircraft in these situations, it is important to have the option to perform a new landing approach. To facilitate this new landing approach a reserve in the amount of fuel capacity has to be incorporated in the total fuel capacity required for the mission. In figure 2.3 the reserve flight diagram is shown. In this figure one can see the second landing approach and its estimated duration.

2.3 Test profiles

The MUAV will be used for a multitude of goals of which the test profile varies widely. This variety of test profiles will be analysed in this section. The MUAV can accommodate different types of modules and payload. Under normal testing conditions only one type of payload or module will be used. For instance, a new wing concept and a new High Lift Device (HLD) concept are not likely to be tested simultaneously unless both have been tested separately already. Furthermore the combination of modules and configuration will result in a combined test profile. Eight different test profiles are in more detail:

HLD testing

HLDs are mainly used to reduce take-off and landing speeds and runway lengths. Therefore HLD tests will usually be performed by doing multiple take-offs and landings, or by just doing the airborne part of the take-off and landing. The MUAV has to decelerate and climb more than once with such a test profile. The take-off and landing are not load intensive so these tests will not drive the structural design.

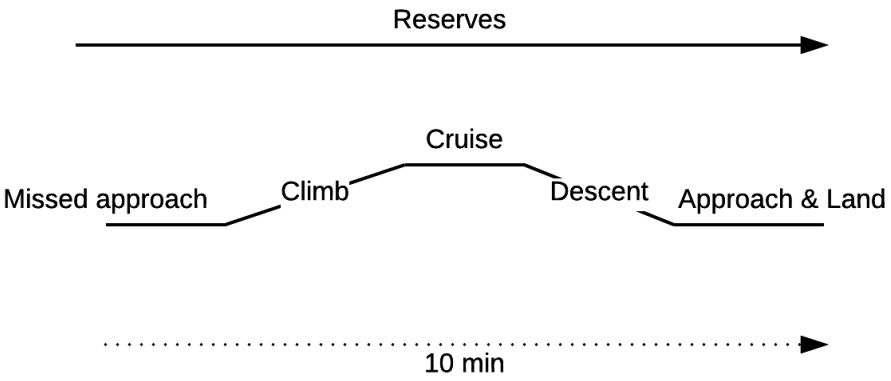

Figure 2.3: Reserve flight diagram

Control surface testing

Control surfaces are used to make manoeuvres or recover from unstable flight modes. Some possible basic aircraft manoeuvres are:

- Fast turn (high bank angle)
- Roll
- Spiral
- Pull up

Manoeuvres are often performed by acrobatic and fighter aircraft, and are a combination of the basic manoeuvres above. These manoeuvres can be very load intensive and will be driving the structural design. The aircraft may use empennage control surfaces, aileron modules, or both to achieve these manoeuvres. The tests are done to see how well the module controls the aircraft and how it deals with the aerodynamic loads. Therefore the test profile of control surface modules is manoeuvre intensive, which also makes it load intensive.

Wing tip testing

Wingtip modules may be used to achieve varying results. Below are some examples of possible wingtip modules.

- Winglets
- Active winglets
- Raked wingtips
- Tip mounted tanks

Wing tips increase climb performance and fuel efficiency. Therefore the test profile of wingtip modules will have few manoeuvres.

Wing configuration testing

Wing configurations vary greatly with the mission profile varying between gliding flight to intensive manoeuvring flight. The variation of wing configurations results in an unpredictable test profile. One configuration might subject the MUAV to a manoeuvre intensive flight while an other configuration will only have the MUAV cruise and loiter.

Control scheme testing

Control scheme testing may be done to test new autopilots, smoother control of aircraft, automatic take-off and landing and stabilising of unstable configurations. To test most control schemes perturbations in the flight path are necessary, as the aircraft response is the required data for analysis. These tests consist of short, low loading (below 2g) manoeuvres. However, the user might want to push the MUAV to its limits to see if the control scheme works under the worst flight conditions.

Propeller testing

Propellers may be tested for efficiency, variable pitch, climb performance, and engine failure performance. These tests might subject the MUAV to low loading (below 2g). The tests profile will consist of climbing, cruising and possibly gliding as well.

Research with payload

Just like with the wing configurations, payloads can be used for different missions. Sometimes it is to test a component under certain load factors, other times it is to perform research with a camera for example. The former example will have a manoeuvre intensive flight profile while the latter will have a flight profile consisting of cruise and loiter.

Multi-module testing

Of course many test cases can be combined which will result in different flight profiles. For example some payload instruments can be installed to measure certain parameters for a wing module or configuration. However, the most extreme test profiles have already been pointed out. Any combination of test profiles is expected to fall within the range of test profiles that have been analysed.

2.4 Functional analysis of the MUAV

From the mission profile discussed in section 2.2 and the customer requirements a Functional Flow Diagram (FFD) can be made. In the FFD all the functions of the MUAV are listed. The FFD is shown in figure 2.4.

The Functional Breakdown Structure (FBS) that follows from the FFD is shown in figure 2.5. The FBS contains more detail than the FFD. The functions in the FFD and FBS are either inspired by requirements or inspire requirements themselves. To relate the requirements with the FFD or the other way around, table 2.1 is made. The codes of the requirements that are used in the third and fourth column of table 2.1 are listed in the requirement specification [1]. Some functions in the table do not inspire technical requirements on the design but on maintenance or operations and logistics procedures.

2.5 Requirements

The most important requirements, that follow from the requirement analysis and the functions identified in section 2.4, are highlighted in this section.

As stated in the scope in section 2.1 the main difference between the design of the MUAV and other designs is the requirement of modularity for research purposes. This means that the approach of the design for some of the systems aboard the MUAV is deviating from normal aircraft or UAV design principles

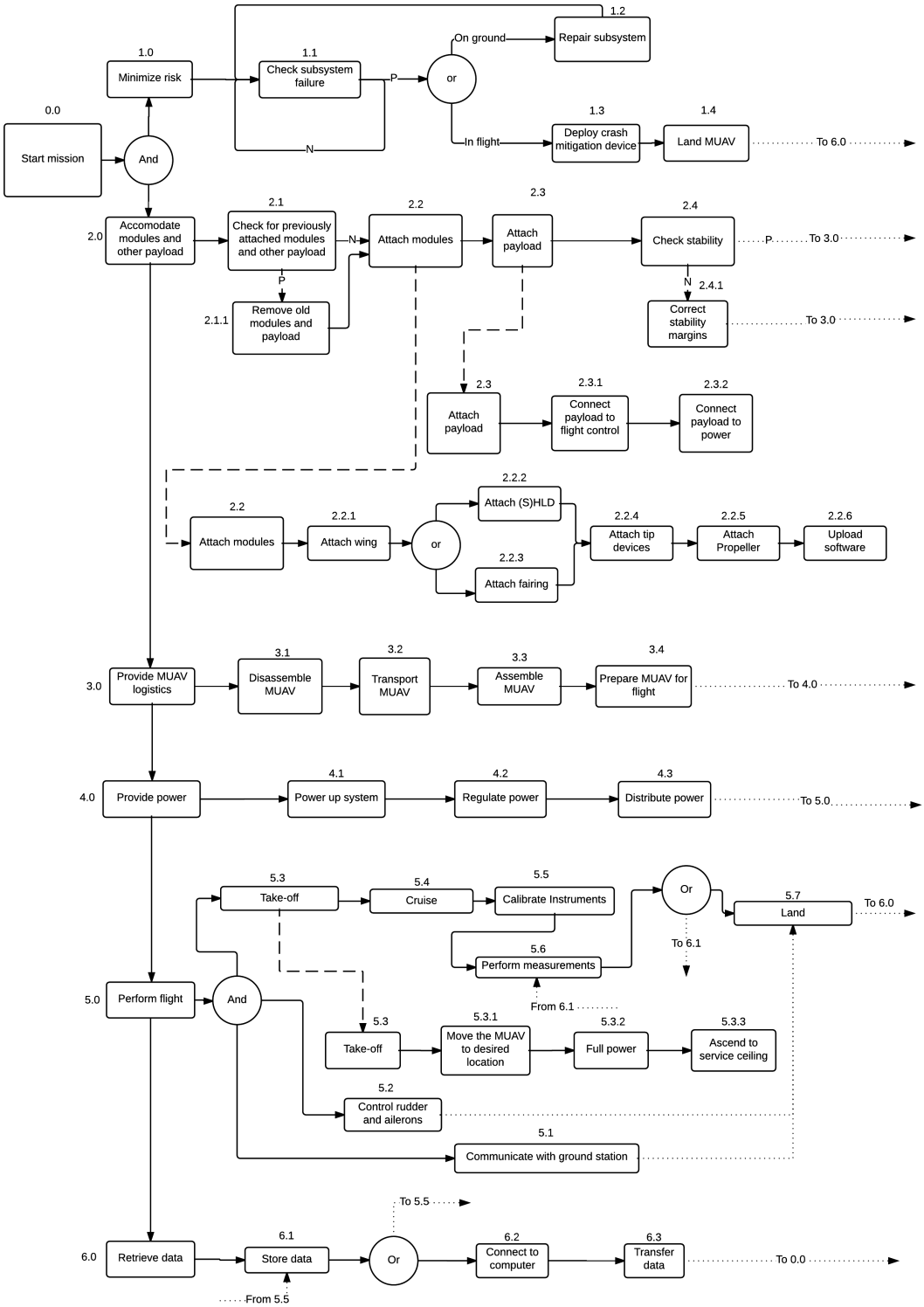

Figure 2.4: Functional Flow Diagram

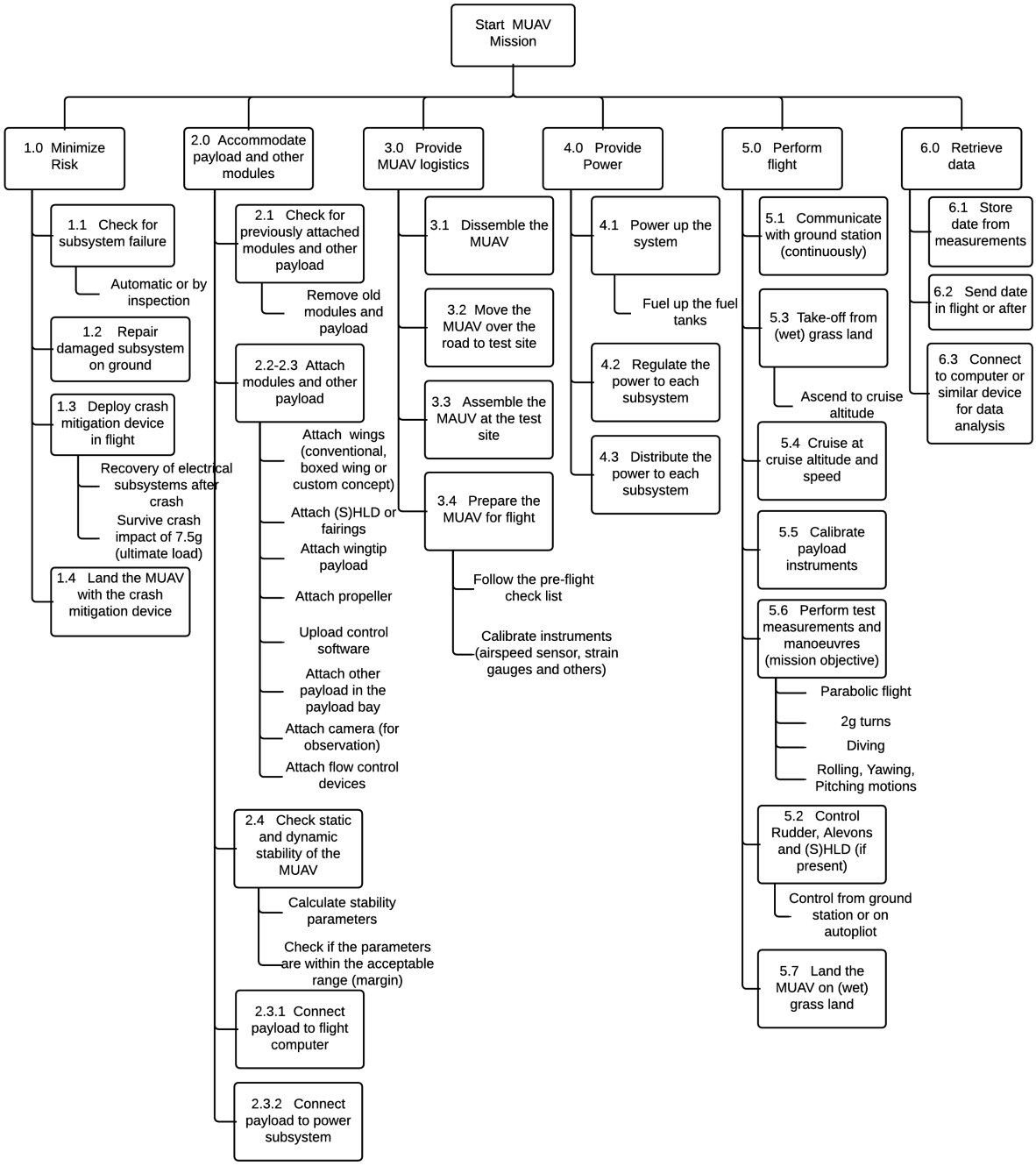

Figure 2.5: Functional Breakdown Structure

Table 2.1: Link between functions and requirements

Function ID	Function description	Inspired by		Inspires
1	Minimise technical risks	M2RU-ST-03		
1.1	Check subsystem failure			Maintenance procedures
1.2	Repair subsystems			Maintenance procedures
1.3	Deploy crash mitigation device	M2RU-SYS-S03-03		
1.4	Land MUAV in case of failure			M2RU-SYS-S03-04
2	Accommodate modules and other payload	M2RU-ST-01		
2.1	Check for previous attached modules and payload			Operations and logistics procedures
2.2	Attach modules			M2RU-SYS-S01-03, M2RU-SYS-S01-04
2.3	Attach payload			M2RU-SYS-S02-07-B3
2.4	Check stability			Operations and logistics procedures
3	Provide MUAV logistics	M2RU-ST-04		
3.1	Dissemble MUAV			Operations and logistics procedures
3.2	Transport MUAV			M2RU-SYS-S04-02
3.3	Assemble MUAV			Operations and logistics procedures
3.4	Prepare MUAV for flight			Operations and logistics procedures
4	Provide Power	M2RU-ST-02		
4.1	Power up system			Operations and logistics procedures
4.2	Regulate Power			M2RU-SYS-S01-16-P3
4.3	Distribute power			M2RU-SYS-S01-16-P3
5	Perform flight	M2RU-ST-02		
5.1	Communicate with ground station			M2RU-SYS-S01-09-E7
5.2	Control rudder and ailerons			M2RU-SYS-S01-12
5.3	Take-off			M2RU-SYS-S02-09
5.4	Cruise			M2RU-SYS-S02-01
5.5	Calibrate instruments	M2RU-SYS-S01-17		
5.6	Perform measurements	M2RU-ST-02		
5.7	Land MUAV			M2RU-SYS-S02-09
6	Retrieve data	M2RU-SYS-S01-06	to	
		M2RU-SYS-S01-11		
6.1	Store data	M2RU-SYS-S01-06	to	
		M2RU-SYS-S01-11		
6.2	Connect to computer	M2RU-SYS-S01-06	to	
		M2RU-SYS-S01-11		
6.3	Transfer data	M2RU-SYS-S01-06	to	
		M2RU-SYS-S01-11		

which will be further explained in section 2.6. The wings are the biggest part of the MUAV that is required to be modular. To show the modularity of the wings two additional modules next to the MUAV are designed: a boxed wing and SHLD. The standard platform of the MUAV comes with a set of wings that have a wingspan of 6 meters. The standard wing provides attachment points for HLD on the Leading Edge (LE) as well as on the Trailing Edge (TE) and attachment points for modules on the wingtips. This means that the customer has the ability to change the entire wing or part of the wings to test innovative wing concepts that otherwise would require them to design a whole new UAV or aircraft for in-flight testing.

Aside from the modularity requirement the following list contains the five most important requirements next to the modularity requirement:

- The MUAV must be usable to evaluate the performance of various subsystem concepts. Examples of such subsystems are high lift devices, wing tip devices, flow control devices, propellers and automated control systems.
- The unit cost shall not exceed €50,000.
- The telemetry and data acquisition systems shall survive a crash.
- The wingspan shall be larger or equal to 6 meter.
- The MUAV shall be able to perform under high load factors (> 5).

A complete overview of the requirements, on both system and subsystem level, can be found in the Requirement Specification [1]. This file is available via the TU Delft webdrive.

2.6 Non-conventional design philosophy

The design process is subject to various constraints, requirements and limits. However, there are two more uncommon concepts that should be addressed individually beforehand, to define their places in the project. In this section the philosophy regarding the platforms modularity and sustainability is discussed.

The most characterising technical requirement of this project is without doubt the modularity of the aircraft. While regular aircraft have their main requirements in domains as range, altitude, payload and velocity, this project should target to facilitate modularity. This non-conventional requirement requires a non-conventional design strategy. To develop an design strategy, first a clear definition of modularity is needed. The dictionary definition of a module is: ”a combinable, changeable part or component”. Taking this as a starting point and focusing on the project, modularity is defined in our particular case as ”the freedom for customers to test aeronautical concepts”. The reader should note that the difficulty of modularity in aircraft lies in the fact that so many parameters are interrelated. Changes in static, dynamic or structural properties that seem feasible at first sight, might render the aircraft completely unflyable.

Designing for ”freedom for users to test aeronautical concepts” implies two problems that have to be tackled in order to allow a sensible design process to take place. The first problem is that the objective is unrestricted and undirected. Although the project description steers towards a modular wing and propeller, this does not confine the focus area sufficiently to design for. More information about which parts exactly are valuable to be modular is vital for the process. The solution to this problem is rather straightforward: information gathering from people that understand the needs of potential customers. The second problem is that, contrary to the ’regular’ design objectives mentioned above, modularity is not quantifiable. However, to be able to compare different design options objectively it should be quantified. This is done by listing all different possible modular parameters and ranking them on their merit and range. A way of looking at the strategy is considering the subjectivity just to be moved: not quantifying modularity will yield a subjective trade-off, while an objective trade-off will be based on an inherently subjective quantification due to the ranking process. However, opposed to not quantifying at all, this process can very well be subjected to a logical structure, also input from external experts can provide valuable information on the range and merit of parameters.

To be more specific, the reader should view the strategy as follows: Each possible configuration of the aircraft can be regarded as a point in an N-dimensional space, wherein N is the number of parameters.

It is clear that not every single point in the design space is equally valuable. This implies that bluntly maximising the volume enclosing all feasible design points not necessarily yields the best design. The proposed strategy to cope with this is twofold. First, it is assumed that there exists a limited design space that will allow all modularity found to be required (during this research). This space is dubbed the Independent Design Space (IDS) (parameter values are seemingly independent of each other in this space). Meeting this space as efficiently as possible will be the first objective of the concepts. Second, there are the design points that have not been adequately assessed for their merit. There is no shame in that, it is inherent to designing a platform for testing new concepts. Given that the proposed aircraft concepts all cover the IDS, an additional modularity criterion is needed. To this end, another space is defined, the Extreme Design Space (EDS). This space, by definition a lot larger than the EDS, allows quantification of the coverage of design points lying outside the IDS.

Another key element in the design process is sustainability. As wide as the concept can be conceived, as wide will it be deployed throughout the design process. Environmental sustainability is driving all technical considerations throughout the design process. Recyclabiltiy and greenhouse gas emissions are clear areas where this concept will surface. More indirectly however, the entire project can catalyse sustainability in the aircraft industry as well. With commercial airliners basing a significant portion of their ticket fares on fuel consumption, research to drag and weight reductions are always economically interesting. The MUAV will be able to facilitate such research. Besides environmental sustainability, specific issues for this project will be addressed as well. Indeed, the public opinion on UAV's, or more commonly referred to as 'drones' by the media, is not unanimously positive. This should not surprise, given that most media report on drones either in combination with warfare or privacy invasion. This feeds public scepticism vastly. The definitions of modularity and sustainability will be used throughout the report. Both concepts distinguish the MUAV design from conventional UAV design, imposing unfamiliar requirements and resulting in an uncommon design process.

2.7 Verification and validation methodology

Verification corresponds to checking if something is functioning to the specifications while validation is checking if something is functioning as intended, they complement each other to ensure a good design. These are continuous processes and should be kept in mind throughout the design phase. This section will treat how these activities were handled in the current design stage. First the verification methods are treated followed by a short discussion on validation.

Numerical design verification

Numerical design revolves around performing calculations to determine an optimal design. This way complex calculations can be repeated easily to quicken the optimisation processes. Verification of this design method starts at the inputs as they are the base of all calculations. Every input parameter should be checked on their correctness, either by calculating it by hand or by looking up the value. Every individual calculation in the script should be checked by hand with a verification model to see if the numerical calculation is correct. Often multiple calculations are linked together to form functions. These functions should be checked individually by hand to ensure a correct functionality. Lastly the interconnection of functions should be verified since one wrong parameter assignment can be catastrophic.

Sensitivity analysis

Some sensitivity analyses will be performed as part of numerical code verification. Most numerical tools are programmed for a specific design space and therefore only work within a specific region of parameters. Important information can be obtained by analysing the behaviour of the numerical tool around deviations from the design point. Whether the numerical too will converge to the same design point and how the result changes with a different design point can be found out this way. Sensitivity is analysed for the relevant subsystems, with a general system sensitivity analysis in section 6.5

Existing numerical tool verification

Sometimes a numerical design can be greatly simplified by using existing numerical tools. There exists a wide variety of numerical tools for different purposes, some of which are well known such as JavaFoil. Using these tools is advised since a lot of hours have been put into verification and validation. Usually the tools have the verification and validation available as proof that the tool does the correct thing. This should be investigated before the tool is used. The discrepancies of the tool should be kept in mind while using it in case they are indicated by the tool creator.

Research design verification

Sometimes using numerical tools is unnecessary and using literature as well as engineering knowledge to get to a design is sufficient. This method can be verified by investigating the validity of the sources used to design. Good sources are well referenced and thoroughly explained. Multiple sources should be used to come to a proper design choice for a specific part. If it can be shown that these criteria are true than the part has been verified sufficiently. However, the part should be analysed and verified more thoroughly in further design phases.

Off-the-shelf design verification

Sometimes a subsystem design lies outside of the knowledge of the engineer, in this case off-the-shelf components should be selected to fulfil the subsystem design. Off-the-shelf components often come with data sheets containing detailed information on the characteristics and performance. When verifying a design made up of off-the-shelf components each individual component functionality should be documented, after which the functionality should be compared to the subsystem requirements to see if the components will suffice. One has to be aware components can interact; structurally, electrically, or other ways. Whether this happens correctly should be verified by testing or analysis. Drawing diagrams can be helpful in determining the correct interaction of a system of components.

Validation

Validation is done to see whether the right system was designed. This usually means comparing the resulting design with existing designs for similar missions. Validation at this stage of design proves to be hard as not much reference data is available for UAV, especially for modular ones. Validation should be done by testing the initial design prototypes to see if it matches the predicted modularity. Therefore validation is not treated at this design stage, some suggestions for future validation will be made for some subsystem designs however.

Chapter 3

Conceptual design

With the mission outline known, the next phase in the design of the MUAV is to select a suitable configuration to perform the mission. In order to select the proper configuration, all the functions and requirements that were identified in chapter 2 must be covered by the concepts. In this chapter different configurations are proposed and after the consideration of all possibilities the final concept is selected. This process is described in more detail in the baseline and mid-term report. In section 3.1 the design strategy for the conceptual phase will be explained. The process of concept generation will be discussed in section 3.2. The resulting concepts, described in section 3.4 are evaluated using the methodology discussed in section 3.3. The final trade-off is shown in section 3.5.

3.1 Design strategy

As the MUAV is modular, there exists a broad range of possible applications. The first step in generating the different concepts is the creation of an overview of every aspect of an aircraft the user might want to change. To accommodate for this modularity, the interfaces between the fuselage and the modular parts are crucial. To discover all possibilities a Design Option Tree (DOT) was made for each interface and other aspects, such as power generation and safety systems. After generating all possibilities, the next phase is the process of converging to the best possible solution. The clearly unfeasible concepts were excluded in the feasibility study, which was followed by an initial trade-off to find the best solutions from each DOT. These were combined in three concepts for the whole MUAV. To be able to select the best of the three concepts, these were analysed in more detail.

3.2 Concept generation

As mentioned in section 3.1, the design process started with exploring the design options. After collecting all options the search for the best option started. In this section this process up to the generation of concepts for the complete MUAV is summarised. First the modular parts will be treated in section 3.2.1. After that take-off and landing, safety systems, power generation and ground communication are discussed in section 3.2.2 to 3.2.5. Finally the complete concepts will be generated in section 3.2.6.

3.2.1 Modularity

Every aspect of the UAV one might want to change has been collected in the following tree, see figure 3.1. With this information, the question arose of how the platform could accommodate for that. It was found that the interfaces between the fuselage and the modular parts have the biggest influence on the modularity possibilities. The design options for the different interfaces, together with the options for changing the stability and manoeuvrability characteristics will be discussed in this section.

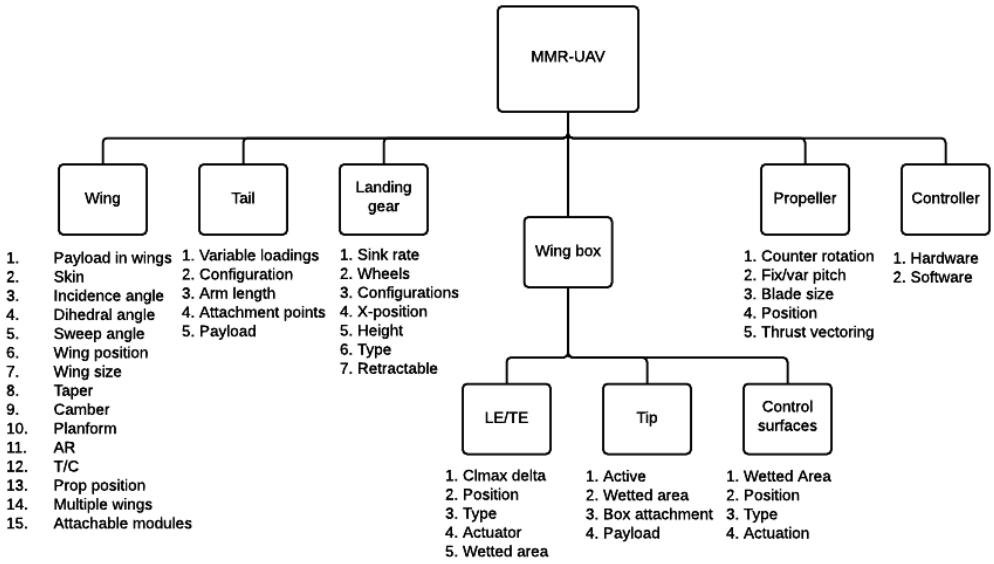

Figure 3.1: Aspects of the aircraft a user might want to change.

Fuselage-wing interface

Having exchangeable wings is one of the most important features of the MUAV. However, with the fuselage-wing interface more modularity options can be created. Options in which the position and the incidence angle of the wing can be changed, both continuous and discrete, were evaluated. After a feasibility study and an initial trade-off three options remained: a fixed centre wing box, modular fuselage blocks and multiple mounting positions (movable wings). One fixed centre wing box is the most straight-forward solution. However, with the other two concepts the position of the wing can be altered which gives more testing possibilities.

Fuselage-empennage interface

A modular empennage is not required, but it enlarges the testing options of the MUAV even further. Therefore the options were discovered and evaluated. The design options can be divided in three categories: a fixed empennage, a modular empennage, in which parts or the complete system can be replaced, and an adjustable empennage, in which parameters can be changed without replacing parts. The last category was discarded because it is very complex and does not have a large influence on the aircraft characteristics. After the initial trade-off the fixed empennage and the empennage that is replaceable as a whole remained.

Variable stability margins

To make sure the MUAV can accommodate different wing concepts, it should be possible to change the stability margins. This can be done by moving the neutral point (n.p.) and moving the centre of gravity (c.g.). The n.p. can be moved by altering the wing and tail position. The c.g. can be moved by moving around subsystems or adding dead weight. After the initial trade-off the options ”move wings”, ”move payload” and ”add dead weight” remained, since these are the most effective.

Variable manoeuvrability

When testing different control strategies, the user of the aircraft might want to change the manoeuvrability. This can be done by changing the mass moment of inertia or the control surfaces. As mentioned earlier, the empennage will be fixed or entirely modular. Therefore the control surfaces cannot be changed.

Changing the mass moment of inertia by moving payload is very hard, since they should stay within the payload bay. However, the default wings give the possibility of mounting extra weight on the wing tips.

Fuselage-propulsion interface

In the requirements it is stated that the MUAV should have a modular propeller. Additional options for the fuselage-propulsion interface concern the position of of the propeller and adjustable propeller characteristics. All adjustable options were removed, because they add too much complexity and weight. This leaves a choice between a modular and fixed engine position. In section 3.2.4 the choice for a combustion engine will be explained. This type of engine is not very suitable to mount at different positions since it is quite big and heavy. However, when modular fuselage blocks are being used, moving the engine might still be considered.

Landing gear interface

Although it is not required, the possibility of modular landing gear was investigated. It was concluded that this adds complexity with very little returns. Therefore it has been decided to use a fixed landing gear. What this will look like is discussed in section 3.2.2.

3.2.2 Take-off and landing

A large variety of take-off and landing options was evaluated. The requirements state that the MUAV should be able to take-off without assistance. In case this would impose problems, assisted take-offs were evaluated as well. Initial sizing showed that is not needed. Therefore a conventional take-off and landing on a (unpaved) runway will be used.

3.2.3 Safety systems

Since the UAV will be used for testing, component failure might occur relatively often. Therefore it is important to have safety systems on board to minimise the damage or prevent the crash all together. The evaluated safety systems can be divided in three categories: survive autopilot failure, survive component failure and crash tolerance.

For the first category a manual override is mandatory, since regulations do not allow completely autonomous vehicles. On top of that a safe mode, a basic full-proof autopilot, can be added. This will not be designed within this project. However, the MUAV will be designed to always be statically stable, so making such a controller is possible. To survive component failure a parachute will be installed, this is the only viable option. Making the complete aircraft crash resistant is impractical. Expensive or fragile components might be placed in a ”black box-like” structure. This will be decided in a later stage. These choices are independent of the chosen concept.

3.2.4 Power generation

In the requirements it is stated that the MUAV should have a propeller, limiting the design space of the power generation. Another requirement is that the vehicle should have zero emissions. Since that is not very common yet for aircraft, a feasibility study has been conducted. It was concluded that batteries are the only viable electric option at the moment, but using them still results in a vehicle exceeding the weight requirements. After the concern that a battery powered propulsion system would be too heavy was shared with the stakeholder he agreed that bio-fuel would be an option as well. This will not result in a zero emission vehicle, but all greenhouse gasses emitted were first absorbed by the vegetation or algae used to make the fuel. Therefore the vehicle has a zero net emission. Since a system using a combustion engine will be way lighter and cheaper, this concept was chosen.

3.2.5 Ground communication

To manually control the MUAV and have telemetry, ground communication is required. Designing a custom communication system is considered to be outside the scope of this project. Therefore an off-the-shelf unit will be used.

3.2.6 Final concepts

In the feasibility studies and trade-offs discussed above, a trend that could be seen was that fixed interfaces are the best in every way, except that they can not be changed. Making more elements modular adds weight and complexity, but also increases testing possibilities. It seems that this is only worth the trouble when a lot of extra options are being created. This resulted in a table with a few concepts left. These concepts can be seen in table 3.1.

Table 3.1: Remaining design options.

Function	Fuselage wing interface	Fuselage empennage interface	Change stability margins
Design options	Fixed wing Modular fuselage blocks Multiple mounting points	Fixed empennage Entire empennage modular	Move wings Move payload Add dead weight

With the remaining options three concepts have been generated. The first concept is the most conventional one with the following characteristics:

- Fixed wing
- Fixed empennage
- Move payload/add dead weight

The second concept gives a middle ground between the first and third:

- Multiple mounting points
- Fixed empennage
- Move wings/move payload/add dead weight

The third concept goes all the way in terms of modularity, with these characteristics:

- Modular fuselage blocks
- Entire empennage modular
- Move wings/move payload/add dead weight

These three concepts will be discussed in more detail later in this report. The fixed wing concept can be found in section 3.4.1, the movable wing concept in section 3.4.2 and the modular fuselage blocks in section 3.4.3.

3.3 Final trade-off methodology

To be able to choose the best concept generated in the previous section, they have to be designed in some more detail. First the trade-off criteria and scoring system will be shown in section 3.3.1. After that the methods used to analyse the different concepts will be discussed in sections 3.3.2 to 3.3.9.

3.3.1 Trade-off strategy for final concept

In this section the trade-off strategy is explained. In order to make an objective choice between the three concepts, trade-off criteria are established. For all concepts all these criteria were worked out in sufficient detail. The results will lead to three worked out concepts, from which all values can be used for the final trade-off and then a quantifiable decision can be made on which concept will be chosen as final concept.

Criteria

The trade-off criteria need to reflect the important differences between the concepts. If done properly these criteria include all the interesting differences. The reason for taking the criteria shall be shown as well. To fulfil this as good as possible, the following trade-off criteria have been defined, in order of importance:

- **IDS coverage**. A target design space, called IDS will be specified. Here the percentage of the IDS that is covered will be checked.
- **Performance**. There are currently two requirements on performance, namely stall speed shall be lower than 20 m/s and the cruise speed shall be higher than 55 m/s. The stakeholder has given these a relatively high importance.
- **Additional configurations**. Some concepts have room for configuration possibilities that lie outside of the targeted design space. To make sure that this is taken into account, this criterion is added.
- **Manufacturing cost**. Since affordability is a stakeholder requirement it is important to keep the manufacturing cost as low as possible. The requirements state that the manufacturing cost should stay below €50,000.
- **OEW**. The Operational Empty Weight (OEW) is used as a proxy to quantify the transportability and ease of handling and operating the vehicle. A low OEW means that the vehicle is easy to handle and operate, and is easier to transport from storage to the test location. The requirements state that the Maximum Take-Off Weight (MTOW) should be lower than 80 kg, from which has been interpreted that the OEW shall be lower than 60 kg.
- **Technical risk**. Technical risk is a combination of safety and reliability. The technical risk shall be low, which means that both the probability of the risk occurring and the effect should be as low as well. A risk matrix is used to asses this.
- **Project risk**. In order to get insight in the chances of making this project a success, the project risk has to be investigated. The project risk shall be low, which means that both the probability of the risk occurring and the effect should be as low as well. A risk matrix is used to asses this.
- **Development cost**. The development cost is dependent mainly on MTOW and difficulty of the project. Keeping the development cost low will be good for achieving a low market price and making sure the project can be finished in time.
- **Saleability**. There are certain aspects of the business case that have not yet been accounted for. These less quantifiable factors will be put together in the saleability criterion.
- **Deployment time**. It is important that the MUAV is easy to use and that testing does not take too much time. Therefore the time necessary to assemble the aircraft from clean platform (no wings, no payload) to take-off ready is important. From the requirements follows that the deployment time should be maximum 90 minutes.

For these criteria the requirements and the margin in which the deficiencies are deemed correctable are shown in table 3.2. From this table it can be noted that there is no margin in which the deficiencies are deemed correctable for the target configuration coverage requirement. This means that all concepts will be designed such that the 100% requirement is met. This will be included as a check in the final trade-off, but not as a criterion.

Table 3.2: Requirements and reasonable margins for all criteria

Criteria	**Requirement**	**Reasonable margin**
Target configuration coverage	100%	None
Performance	Stall speed <20 m/s. Cruise speed >55 m/s.	+ 10% - 10 %
Additional configurations	None. This is additional on top of the requirements.	The concept that scores average is taken as to fall within the reasonable margin.
Manufacturing cost	<€50,000. However, due to the approach of relative cost, the fixed wing concept is chosen as index 100.	+ 15%
Operational empty weight	From the requirement of MTOW <80 kg, it can be extrapolated that OEW <60 kg.	+15 %
Technical risk	The technical risk shall be low.	Between low and medium.
Project risk	The project risk shall be low.	Between low and medium.
Development cost	No requirement. Due to the approach of relative cost, the fixed wing concept is chosen as index 100.	+ 15%
Saleability	The saleability shall be high.	Between high and medium.
Deployment time	<90 minutes.	+ 30%

Scoring the concepts

In order to better compare the concepts to each other, the results of each criterion will be summarised as a score. This score goes from 1 to 5, where 5 is the best possible score. How these scores are assigned can be seen in table 3.3. These scores can be used together with the weight factors, that will be assigned in the next subsection, to numerically compare the three concepts to each other. As can be seen, the most important criteria are performance and additional configurations. This is because of the priority that has been given by the stakeholder to the performance parameters, and also the objective of modularity during this project. The low importance of deployment time can be explained by the fact that the higher deployment time goes hand in hand with additional modularity.

Table 3.3: Scores definitions

Score	Definition
5	Meets requirement
4	Within first half of reasonable margin
3	Within second half of reasonable margin
2	Within two times the reasonable margin
1	Outside two times the reasonable margin

Weight factors

The relative weights of these criteria have been established by using the method of swinging weights. These weights have then be normalised such that they can be transformed into a percentage. This results in the weights as can be seen in table 3.4.

Table 3.4: Criteria weights

Criterion	Relative importance	Weights, normalised to 100 (%)
Performance	4	17
Additional configurations	4	17
Manufacturing cost	3	13
Operational empty weight	3	13
Technical risk	2	9
Project risk	2	9
Development cost	2	9
Saleability	2	9
Deployment time	1	4

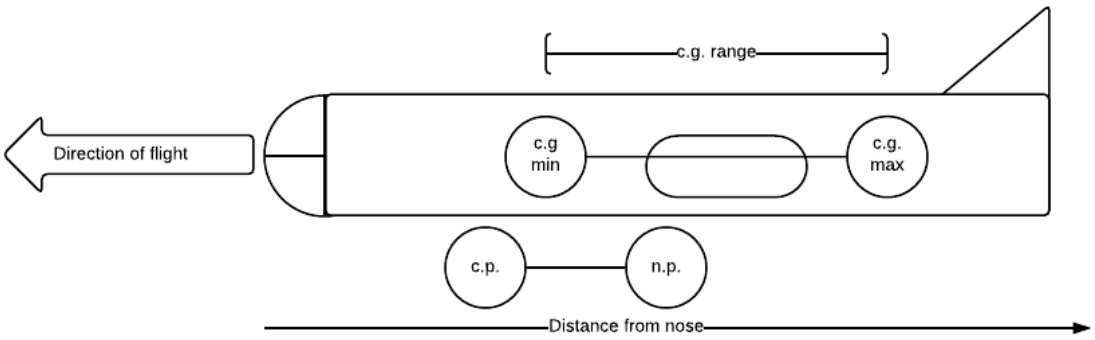

Figure 3.2: Indication of the control point, neutral point, and centre of gravity range of an aircraft

3.3.2 Stability and controllability analysis

In any aircraft designing process, analyses of stability and controllability are essential studies. Information about these properties is vital to predict the dynamic behaviour of the concept. Due to the inherent interdependences of many parameters, it is required to perform iterations to find an optimum combination of stability and control. Normally, there exists a unique point for which requirements on stability and controllability are most efficiently met. However, when designing a modular aircraft this is not the case, requiring a whole new standpoint on the concept of 'optimisation'. This subsection explains how all the concepts chosen cover the IDS discussed in section 2.6 by doing a stability and controllability analysis.
The quantities that determine an aircraft's dynamic stability and controllability are the location of the n.p. x_{np}, centre of pressure (c.p.) x_{cp} and c.g. x_{cg}. The following criteria have to be satisfied to have a stable and controllable aircraft [2].

1. The c.g. must lie in front of the n.p. with respect to the direction of flight for stability.
2. The c.g. must lie behind the c.p. with respect to the direction of flight for controllability.

See figure 3.2 for an interpretation of these criteria. The position of the c.g., n.p., and c.p. can be changed by changing the aircraft planform and the c.g. can be shifted as well by moving the subsystems within the aircraft. The aircraft can be be stable and controllable if part of the c.g. range fulfils the criteria mentioned above. Also, in accordance with Systems Engineering and Aircraft Design (SEAD) [2], it has been decided to use a stability margin (s.m.) of 0.05 Mean Aerodynamic Chord (MAC). This will allow some space for deviations without the aircraft immediately becoming unstable.

Though many parameters influence the locations of the c.g., n.p. and c.p., the ones that will vary most significantly due to modularity are determined to be leading edge sweep Λ_{LE}, taper ratio λ, aspect ratio

A and surface area S. On the other hand, the most effective aircraft parameters that can be used to tune the dynamic behaviour of the aircraft are fuselage length, wing position, tail length, payload location and payload mass.

The modularity parameters are regarded as four dimensions, whereby any combination of values of these parameters is a point in a 'four dimensional space'. The 'four dimensional content' enclosing all viable design options is the design space. It is evident that the volume of this space is determined by the locations of the control point and neutral point. Also, one should note that the modularity input parameters are not independent, for example: the effect of sweep on the n.p. location is amplified by high aspect ratios and damped by low taper ratios. Hence the shape of the design space is not a 'four dimensional cube' with straight edges. However, within the design space there ought to be a 'four dimensional content' that encloses content for which any value of any parameter yields a design that is both controllable and stable. This space allows the customer to set each modularity input parameter independently, as long as the ranges are considered. As explained in section 2.6 this space is called the IDS. Designs outside the IDS are possible as well, but require more elaborate assessments of stability and control.

The three concepts were optimised to be able to be stable and controllable with the parameters shown in table 3.5. This will remain the IDS for the rest of the project.

Table 3.5: Parameters of the Independent Design Space

-10	deg	$<$	Λ_{LE}	$<$	15	deg
0		$<$	λ	$<$	1	
5		$<$	A	$<$	15	
1.5	m^2	$<$	S	$<$	4.0	m^2

3.3.3 Additional configurations

With all concepts optimised for meeting the requirements of the IDS efficiently, there are other differences due to modularity that should be taken into account as well. In this section it will be explained what configurations beyond the IDS are possible, also additional non-quantifiable differences between the concepts will be pointed out.

Extreme design space

Beside the IDS the concepts can also be compared to an EDS. The design space is increased and the amount of points which can be accommodate by the concepts in this space are compared. In this way, if the client wants to test a wing which is not in the IDS, the amount of points which can be covered by the concept can be found. The EDS can be seen in table 3.6.

Table 3.6: Parameters in Extreme Design Space

-45	deg	$<$	Λ_{LE}	$<$	45	deg
0		$<$	λ	$<$	1	
5		$<$	A	$<$	30	
1.5	m^2	$<$	S	$<$	5.0	m^2

Additional possibilities

Except for the differing design spaces, the three concepts induce other differences to the design as well. The concepts will be assessed on the following three aspects:

- **Tuning dynamic behaviour.** Being able to move the wing as well as the payload allows the user to manipulate the dynamic behaviour of the aircraft more precisely than when only one of the two is variable. This will make it possible to create specific settings for controllability and stability.

- **Variable wing box size.** Flexibility in attachment locations for the wing box can easily accommodate various wing box sizes to be mounted to the fuselage as well.
- **Adaptability for box wing.** Specifically in the case of the box wing that is being developed, having flexibility in the attachment points of the main wing is an asset.

This list gives a good representation of differences between the concepts which are not easily quantifiable but can not be neglected in the trade-off. The assessment will be taken with respect to the fixed wing concept.

3.3.4 Initial sizing

Empirical relations are used to find the initial design point of the aircraft. Since the target MTOW is much lower than for conventional aircraft, empirical relations available from literature for mass fraction estimation are unreliable at best and invalid at worst. To find acceptably accurate estimations new empirical relations are determined from available data of reference aircraft. Then the OEW, fuel weight and payload weight fractions are estimated from the newly found empirical relations. This is followed by a more detailed OEW breakdown using empirical relations from literature since no data is available to calculate new relations. Then an initial drag polar is estimated. Finally initial design points for power and wing loading are determined.

Emperical relations

To find acceptably accurate estimations new empirical relations are determined from available data of reference aircraft. Eleven aircraft were selected and their parameter values are available in appendix B. The relations between parameters of interest are found by using a least squares fitting on the reference data. To find a relation for the Weight over Power ratio (WP) it was plotted against both the MTOW and the maximum speed of the reference aircraft. Unfortunately, almost no correlation can be found between those parameters. The cruise speed of the new aircraft must be higher than 55 m/s as defined in requirement M2RU-SYS-S02-01. One datapoint has a maximum speed at 56 m/s and a power loading of 0.06. This datapoint represents the RQ-7B Shadow. This power loading is used as an initial estimate. Plotting the empty weight fraction as a function of the MTOW resulted in a coefficient of determination close to one, hence the interpolation is a good fit and can be reliably used to estimate the empty weight fraction. After plotting the MTOW against the wing span and fuselage length it could be concluded that the wings will be oversized relative to the rest of the aircraft. The fuselage is expected to be between 3 and 4 metres in length.

Mass fractions

To find the aircraft mass fractions for the OEW, Payload Weight (PW), and Fuel Weight (FW) two approaches are taken. The OEW fraction is estimated from empirical data. For the expected MTOW of 75kg the empty mass fraction is found to be 0.6. As the MTOW increases the empty weight fraction is expected to decrease making this a conservative estimate. To account for the modularity of the aircraft an additional ten percent weight penalty is added to the OEW estimate. On top of this an additional ten percent is added as a contingency for weight gain during the design process. This results in an estimated empty weight fraction of 0.726. Then the FW fraction was calculated using the Breguet endurance equation for steady straight flight, resulting in a fuel fraction of 0.0119. The remaining 0.2621 is the PW fraction. Together with the payload requirement of 20 kg, the MTOW can be calculated.

Operational Empty Weight breakdown

The operational empty weight is broken down into subsystem weights using empirical relations from Raymer [3]. These relations have been derived for much larger aircraft and will likely be inaccurate for the current aircraft. No data is available regarding subsystem weights for small unmanned aircraft so they will have to suffice. For some subsystems an alternative estimation is used as the empirical relations gave entirely unrealistic results.

Drag polar

To get an idea on how the MUAV will perform on aerodynamics, an estimated drag polar is created. The plot is created by writing the drag coefficient as a function of the lift coefficient. Using the statistical data found in Raymer [3], a good approximation of the lift over drag ratio could be made. Assuming a cruising lift coefficient of around 0.3, the lift over drag ratio equals 15. This value is comparable to values given in Raymer for similar aircraft in similar conditions.

Wing and power loading

Finally, the required wing and power loading were determined using the stall and cruise speed requirements. Since the wings are relatively large, the wing loading remains low and the required lift coefficient is relatively low as well. To overcome the drag at the required 55 m/s cruise speed, an engine power of 11 kW is required.

3.3.5 Flight performance evaluation

The performance of each concept was evaluated using the stall speed, take-off distance, landing distance, climb rate, climb gradient and cruise speed. These characteristics were determined using equations from [3, 4, 5]. The difference in performance of aircraft is caused by different wing loadings $\left(\frac{W}{S}\right)$ and power loadings $\left(\frac{W}{P}\right)$. However, it is assumed that the same wings and engine (selected in section 3.3.4) are used. Therefore the difference between the different concepts is caused by the difference in MTOW.

3.3.6 Manufacturing costs

In order to come up with an estimation of the manufacturing cost, reference data is used. This reference data comes form a cost analysis study for commercial aircraft, which is conducted by Jacob Markish, a professor of Massachusetts Institute of Technology (MIT) [6]. This method is based on the mass of different parts of the aircraft, and an average cost is related to each kilogram of the different parts. Based on the sizing, the total manufacturing cost can be estimated.

This cost estimation assumes that the relation between manufacturing cost and mass is linear close to the data points of the reference aircraft. The UAV of this project does not fall in this range, so these values are assumed to not be valid in this case. However, it is also assumed that these linear approximations are still valid around any other design point. As design point the fixed wing concept is taken. This also means that giving an absolute value for the manufacturing cost is not something that should be done at this point, and therefore the manufacturing costs of the different concepts are normalised using an index. The fixed wing concept will score 100, and the other concepts will be scaled according to their performance.

3.3.7 Development costs

To make an estimation of the development costs a method from Roskam [7] based on statistical data was used. The difference between the three concepts are caused by a different MTOW and a difficulty judgement factor. The difficulty factor describes the functional complexity in terms of the probability of a successful design. The probability of success is defined by whether or not there is a working prototype already. The probability of success is split up in five steps. The first step is 'Proven flight design', which has the highest probability of success. Then 'Extrapolated from existing flight design', 'Based on existing non-flight engineering', 'Working laboratory model' and 'Feasible in theory' are defined from high probability of success to low probability of success with the lowest being 'Feasible in theory'. The difficulty factor can then be defined as a number between 1 and 2, where a difficulty factor of 1 is associated with 'Proven flight design' and a difficulty factor of 2 is associated with 'Feasible in theory'.

Again the MUAV is not in the range of the aircraft used for statistical data. Therefore the development costs are normalised using an index. The fixed wing concept will again be used as a reference with a score of 100.

3.3.8 Risks

In chapter 7 a more extensive description of the project and technical risks can be found. Here the difference between risks for different concepts is assessed. The difference in project risk originate from difference in complexity, resulting in an unfinished or unsuccessful product. The difference in technical risk originate from complexity as well. Besides that, more modularity, means more connections, which have a higher change of failure. Each concept is ranked with a low, medium, or high score.

3.3.9 Saleability

Besides the technological properties that will determine the performance of the MUAV, to make a credible business case less quantifiable factors have to be taken into account as well. Customers might have two reasons to incline more to one or another concept.

1. A potential buyer might have specific reasons to consider buying the MUAV which set requirements to the system that the team has not accounted for. One could think of an unaccounted research objective, but also total different applications such as land surveying. In such a situation more modularity will grant easier adaptability to the new environment.

2. Besides the conscious requirements a buyer would impose on the system, there are latent requirements as well. A customer would know this and is likely to be more inclined to favour the concept that leaves most freedom to design own modules for the aircraft. In short: the fact that there are more possibilities will simply enhance market prospects, regardless if these possibilities will ever be used.

The three concepts will be assessed on these aspects, yielding a low, medium or high qualification. The score of the saleability assessment shall be used as input for the final trade-off.

3.4 Concept evaluation

Using the methodology discussed in section 3.3 the three concepts generated in section 3.2 were evaluated. In this section the three concepts will be described in some more detail and their differences highlighted. Starting with the fixed wing concept in section 3.4.1, after that the movable wing concept in section 3.4.2 and finally the modular blocks concept in section 3.4.3. A summary of the results will be given in section 3.5.

3.4.1 Fixed wing

The first concept discussed is the fixed wing concept, of which the main distinguishing feature of this concept is that the longitudinal wing position is fixed. This means that even though the wing itself is modular, the centre wing box has a fixed location. Different wing designs can be tested at this position. Changing the wing configuration may lead to a shift in n.p., c.p., and c.g.. The c.g. can be varied by moving payload to be able to change stability and controllability margins for different wings. This concept has the most conventional layout and therefore probably the least complex. However, a large c.g. shift is required to ensure that the MUAV is stable and controllable for all test configurations. In many aspects this concept is used as a benchmark. In figure 3.3 the planform design for this concept can be seen.

3.4.2 Movable wing

The movable wing concept is a design with mostly fixed components while allowing small longitudinal adjustments in wing location on the fuselage. The concept also allows for interchangeable wings to accommodate different wing configurations just like the other two concepts. The movable wing concept is very similar to the fixed wing concept except one more degree of freedom in the design: the wing location on the wing box. This means that it can be stable and controllable for all test configurations while having a shorter fuselage than the fixed wing concept. Since the centre wing box will have multiple attachment

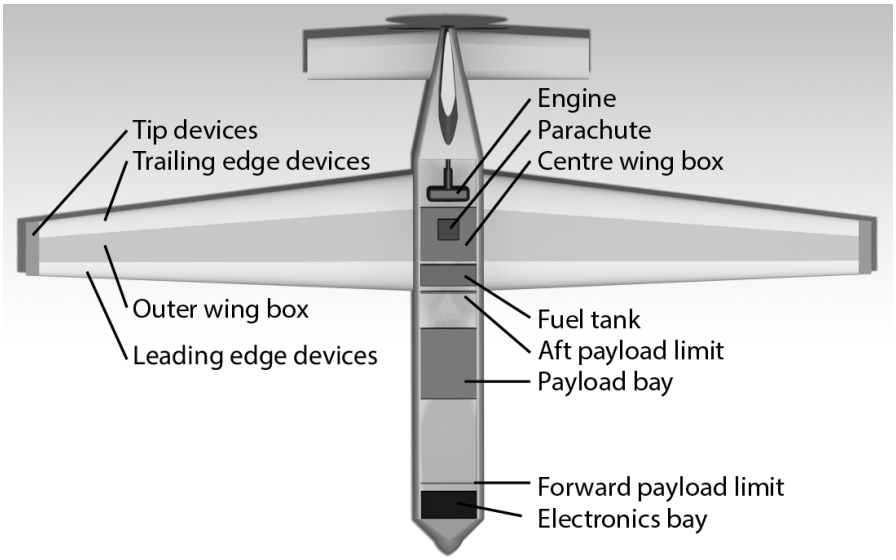

Figure 3.3: Planform layout of the fixed wing position concept

points, multiple wing box sizes can be mounted. Besides that, this concept gives the opportunity to tune the dynamic behaviour and is better suited to accommodate a boxed wing. Therefore this concept might be more appealing to potential buyers. Higher weight and complexity are the disadvantages of this concept. The planform design is shown in figure 3.4

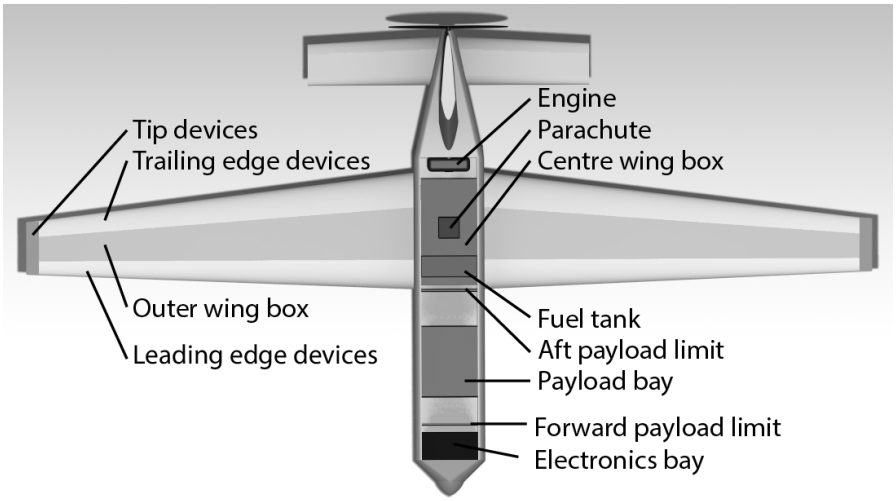

Figure 3.4: Planform layout of the movable wing location wing concept

3.4.3 Modular blocks

From all three concepts, this concept is the most daring one. This concept is based on splitting the UAV in multiple blocks that can be assembled in different orders. An artist impression of the concept in a possible configuration is shown in figure 3.5. This concept will give the user more freedom in choosing the position of the wing, the engine, the two payload compartments and the landing gear. The nose and the empennage

are fixed, as moving these parts to a different location of the UAV is not necessary. The freedom of choosing different configurations will have an effect on the stability of the aircraft, aerodynamics and on the propulsion. Several challenges need to be faced to make sure this concept will have a chance to succeed. The blocks need to be optimised to withstand all the different load cases, depending on the location of the block. Also the wiring needs to be investigated carefully, so that all blocks can be connected no matter what the configuration is. Therefore this concept has a high weight and complexity compared to the other two concepts. In return, this concept provides the most testing possibilities for the user.

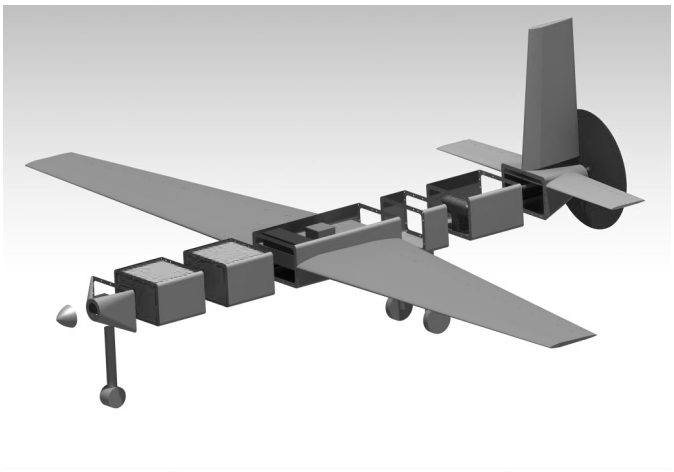

Figure 3.5: Artist impression of the modular fuselage blocks concept

3.5 Final trade-off

After analysing the three concepts the final trade-off can be performed. An overview of all the results is given as a table in section 3.5 and the concept choice is motivated in section 3.5.2.

3.5.1 Concepts overview

An overview of how the three concepts score on the different criteria can be seen in table 3.7. If a concept meets the requirements for the criterion (corresponding to a score of 5), its box is coloured green. If a concept does not meet the requirement, but is still in a the margin of correctable deficiencies (corresponding to a score of 3 or 4), its box is coloured yellow. If a concept exceeds the requirement by more than this margin (corresponding to a score of 1 or 2), its box is coloured red. All three concepts are designed such that they have a 100% target design space coverage. Taking this as a criterion would therefore not be useful. It is however included as a check, to emphasise that all concepts do meet this requirement.
From this table it can be seen that concept 3: modular fuselage blocks is not the best concept. The fixed wing and the movable wing concepts however score the same.

3.5.2 Concept choice

After close examination of the results from section 3.4.1 to 3.4.3, their graphical summary in section 3.5 and the final score of each concept a final decision could be made. Concept 3: modular fuselage blocks has been discarded, as it scores poorly on 4 criteria. From these criteria, the OEW and project risk are the most prohibiting, as the requirements are not met by far and these deficiencies are seen as not possible to overcome. The fixed wing concept and the movable wing concept have the same score and a winner cannot be chosen with only this trade-off. The main differences are the difference in OEW, the additional

Table 3.7: Final trade-off

Check		**Concept 1: Fixed wing**	**Concept 2: Moveable wing**	**Concept 3: Fuselage blocks**
Target configuration coverage		100%	100%	100%
Criteria	**Weight (%)**	**Concept 1: Fixed wing**	**Concept 2: Moveable wing**	**Concept 3: Fuselage blocks**
Performance	17	Stall speed: 16.73 m/s Cruise speed: 55.8 m/s Score: 5	Stall speed: 16.94 m/s Cruise speed: 55.7 m/s Score: 5	Stall speed: 18.02 m/s Cruise speed: 55.5 m/s Score: 5
Additional configurations	17	53.8% EDS coverage. Little design space for box wing. Score: 2	58.9% EDS coverage. Possibility for variable wing box size. Easier accommodation of box wing. Score: 4	82.6% EDS coverage. Great for accommodating different box wing designs. Score: 5
Manufacturing cost	13	100% Score: 5	105% Score: 4	112.5 % Score:3
Operational empty weight	13	67.5 kg. This is 12.5% higher than the requirement. Score: 3	70.6 kg. This is 17.5% higher than the requirement. Score: 2	81.5 kg. This is 36% higher than the requirement. Score: 1
Technical risk	9	Medium. Score: 4	Medium. Score: 4	Medium. Score: 3
Project risk	9	Medium. Score: 4	Medium. Score: 3	High. Score: 2
Develpoment cost	9	100% Score: 5	115% Score: 3	144% Score: 1
Saleability	9	Medium. Score: 3	High. Score: 5	High. Score: 5
Deployment time	4	75 minutes. Score: 5	80 minutes. Score: 5	130 minutes. Score: 2
Weighted scores		**3.9**	**3.9**	**3.3**

configurations and the saleability. The question now is, does the extra modularity and saleability of the movable wing concept weigh up against its weight- and cost penalty. This has been put up to a vote within the project team, and the decision was unanimous: the movable wing concept is chosen.

Chapter 4

Subsystem design

With the concept chosen in chapter 3, the next phase is the actual design of the MUAV. The following chapter will reflect on the design of the individual subsystems, and is followed by an evaluation of the whole concept in chapter 6. From the concept generation, a budget has been made for all different subsystems and the subsystems design is made. This design process is presented for all separate subsystems. First the wing is presented in section 4.1. This section is followed by the payload bay in section 4.3, the fuselage in section 4.2 and the empennage in section 4.4. The last part of the chapter consists of the smaller subsystems, first the propulsion and power subsystem in section 4.5, the electrical systems in section 4.6, the landing gear in section 4.7 and finally the parachute in section 4.8.

4.1 Wing design

In the following section the wing subsystem design is discussed. First the airfoil selection is discussed, followed be an analyses and design of the Leading edge, trailing edge, and tip interfaces. This is followed by the wing fuselage interface design in section 4.1.3. Finally the structural design of the default wing is treated in section 4.1.4.

4.1.1 Airfoil selection

Before the wing can be designed, a airfoil is need as the force distribution depends on the selected airfoil as well as the shape of the wing box. In the coming paragraphs a reflection shall be presented on the airfoil selection, leading up to the final selection of the airfoil in the last paragraph.

Driving parameters of the airfoil selection

Based on earlier research a shortlist of 6 airfoils is made that fit the given mission profile. As the default wing configuration of the MUAV is already used for testing other concepts, the choice is make to make a selection from conventional airfoils. These airfoils include 2 newer developed airfoils and 4 classical National Advisory Committee for Aeronautics (NACA) airfoils and are given in table 4.1.

To be able to select the proper airfoil, a trade-off table is been made. This table, including an overview of the driving parameters in the selection, is presented in table 4.2. Each of these parameters is given a weight specific for the mission of the MUAV and is assigned a score of 0, 0.5 or 1. The final selection process in table 4.3 shows the assignment of these scores and the conclusion that the NACA-02017 is the most favourable airfoil for the MUAV.

Table 4.1: Airfoil selection for the MUAV

Profile name	#
LS(1)-0417	1
MS(1)-0317	2
NACA-64119	3
NACA-05015	4
NACA-02017	5
NACA-1315	6

Table 4.2: Criteria for the airfoil design choice

Parameter	1	2	3	4	5	6
t/c (%)	17	17	19	15	17	15
C_l for α_0	0.5452	0.4111	0.135	0.079	0.06	0.124
C_{lmax}	1.8911	1.9342	1.502	1.462	1.588	1.495
α_{stall}	19	18.5	16	16	17	15
Stall characteristics	Gentle	Gentle	Moderate	Moderate	Gentle	Moderate
C_{dmin}	0.00503	0.00514	0.0068	0.00524	0.00541	0.00537
C_l of C_{dmin}	0.4202	0.1623	0.135	0.079	0.06	0.124
$(C_l/C_d)_{max}$	121	97	123.708	129.081	113.606	136.145
C_l of $(C_l/C_d)_{max}$	0.6677	1.306	0.976	0.802	0.674	0.846
$C_{m_{cruise}}$	-0.103	-0.0825	-0.026	-0.009	-0.004	-0.021

Performance of the NACA-02017 airfoil

In order to get a better understanding of the airfoil performance, an analysis is performed using Javafoil [1]. The data that is displayed in table 4.2 is related to the cruise conditions of the MUAV, meaning that the values obtained are related to a Reynolds number of $2,200,000$. At stall conditions the Reynolds number has a different value, namely $800,000$. To get a clear picture on how the airfoil will perform with respect to this Reynolds number, several plots has been created where the effects of different Reynolds number become clear. In figure 4.1a, the drag polar can be found. It can be seen that the design lift coefficient calculated early on, is located exactly in the middle of the drag bucket. This means that the design lift coefficient goes hand in hand with the minimal drag coefficient, which is very favourable. In figure 4.1b, the lift coefficient versus the angle of attack is presented from which it can be seen that the maximum lift coefficient in stall conditions is more than the minimum value specified.

4.1.2 Leading edge, trailing edge, and tip interfaces

In this subsection the attachment of various LE, TE, and tip concepts on the default wing box, which includes fairings and HLDs is discussed. First the load case is determined for the LE, TE, and tip devices. Once the load case is known, the aerodynamic forces on these devices can be calculated using approximation methods. Finally a few recommendations are given for further development.

Load cases for the leading edge, trailing edge, and tip devices

In order to determine the forces that are acting on the interface between the wing box and the LE and TE devices, two of the most critical structural load cases are defined. The first load case will simulate the MUAV at approach speed with the flaps fully deployed. The second load case will simulate the MUAV at diving speed with the flaps nested, while subjected to an ultimate load factor of 7.5. In both load cases, it is assumed that the heaviest and largest HLDs are used. This means that all the payload mass

[1] Javafoil latest version http://www.mh-aerotools.de/airfoils/javafoil.htm

Table 4.3: Criteria for the airfoil design choice

Parameter	1	2	3	4	5	6	Weight(%)	Remark
Thickness ratio	0.5	0.5	1	0	0.5	0	7.7	Highest is best
C_l for α_0	0	0	1	0.5	0.5	1	7.7	Close tot C_{ldes}
C_{lmax}	1	1	0.5	0.5	0.5	0.5	7.7	Highest is best
α_{stall}	1	1	0.5	0.5	0.5	0	7.7	Highest is best
Stall characteristics	1	1	0.5	0.5	1	0.5	7.7	Gentle, Moderate, abrupt
C_{dmin}	1	1	0	0	0	0	15.4	Lowest is best
C_l of C_{dmin}	0	0.5	1	0.5	0.5	1	7.7	As close as possible to C_{ldes}
$(C_l/C_d)_{max}$	0	0	0	0.5	0	1	7.7	Highest is best
C_l of $(C_l/C_d)_{max}$	1	0	0	0.5	1	0.5	7.7	Lowest is best
$C_{m_{cruise}}$	0	0	0.5	1	1	0.5	15.4	Closest to zero is best
Sum	5.5	5	5	4.5	5.5	5	7.7	Highest is best

is reserved for the HLDs (20 kg, 10 kg per wing), and that triple slotted Fowler flaps are attached to the TE. According to Niu [8], the LE will carry smaller and lighter devices and therefore only the forces on the TE are determined. The design of the TE interface will also be applied to the LE, resulting in a safe design for the LE.

In order to determine the forces acting on the winglets, two critical load cases are considered. The first load case simulates the MUAV subjected to an ultimate load factor of 7.5, while wingtip devices are attached on both wings with a maximum weight of 10 kg per wingtip device. The second load case simulates the MUAV in cruise conditions. For both cases, the winglet is assumed to be an extension of the wing, with no toe or cant angle. These angles are shown in figure 4.2. According to reference data [9, 10], the wingtip covers around 20 % of the wing span and the weight of the wingtip is around 7 % of the total structural weight of the wing. This results in a surface area of 0.36 m^2 and a weight of 1.05 kg. Using the familiar lift and drag equations, one can determine the forces and moments acting on the wingtip. Since the forces that are acting on the winglets are determined by means of reference data and assumptions, a contingency factor of 1.25 is used to correct for these simplifications/assumptions.

Forces acting on the HLD

The main forces acting on the HLDs are the aerodynamic forces, which can be summarised to one single force: the normal force. From the database of Engineering Sciences Data Unit (ESDU) [11], an empirical estimation method can be found that can be used to calculate the normal force on the flaps. This method is based on three measurement series, taking into account the flap chord ratio $\frac{c_f}{c}$, the deflection angle of the flaps δ_f and the normal load coefficient C_{N_f}. The latter can be defined per unit span, as follows:

$$C_{N_f} = \frac{N_t}{0.5 \cdot \rho \cdot V^2 \cdot c_f}. \tag{4.1}$$

c_f is the chord of the high lift device in nested position, which depend on the location of the HLD in spanwise direction. The normal load coefficient depends on the flap deflection, and an empirical relation between the coefficient and the deflection can be found in Niu [8]. According to Niu, the most efficient HLD (the triple slotted Fowler flap) will take around 30 % of the wing chord. These flaps will generate the most lift and are the heaviest, thus introducing the highest loads. Because the HLDs will be attached to the ribs of the wing box, the loads are going to be transferred to these ribs.

The normal force will cause a bending moment around the interface. The moment arm depends on whether the flaps are deployed. When the flaps are deployed the arm is a summation of the chord length of the HLD plus half of the extension distance, as it is assumed that the normal force will act on the centre of the extended (or nested) HLD. According to Niu [8], the maximum increase of the chord for an extended triple slotted Fowler flap equals 18 percent of the wing chord. When the flaps are nested, the arm is half of the chord length of the HLD.

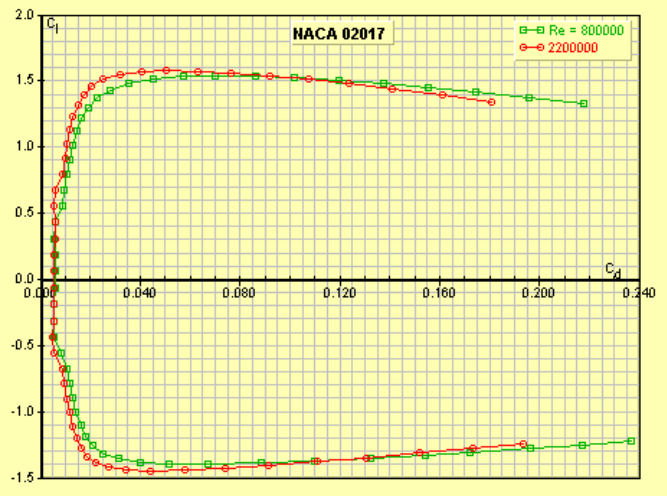

(a) C_L versus C_D

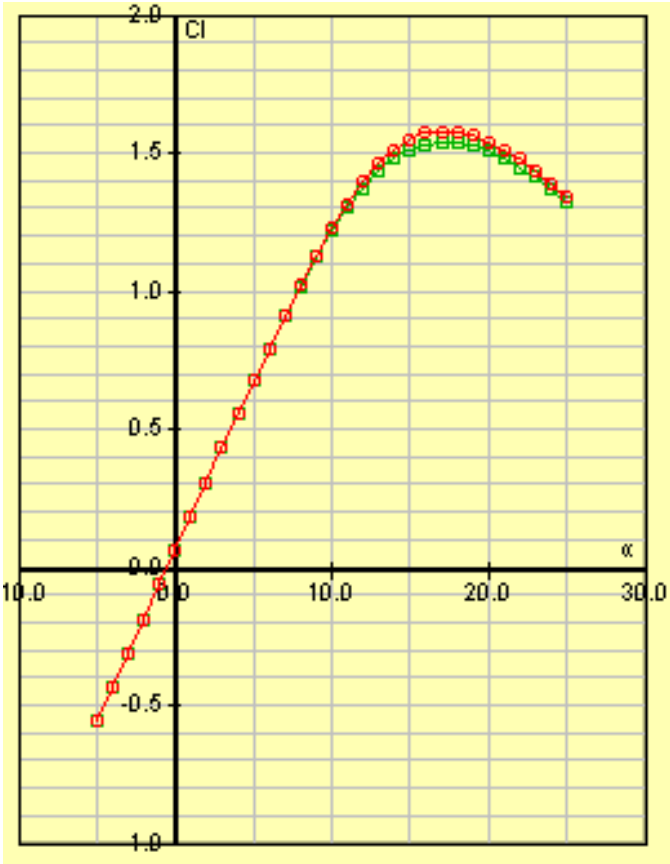

(b) C_L versus α

Figure 4.1: Polars figures for the NACA-02017 airfoil in 2D configuration

In table 4.4, the values for calculating the normal forces and bending moments for both load cases can be found. The results are located in table 4.5. It can be seen that load case 2 is the most critical one, and will therefore be used to design the interface.

Table 4.4: Values of variables for calculating the normal forces for the different load cases

Variable	Load case 1	Load case 2	Unit
ρ	1.225	1.225	kg/m^3
V	22	68.75	m/s
C_{N_f}	1.2	0.2	–
c_{wing}	0.6	0.6	m

Table 4.5: Forces and moments induced by the high lift devices per meter span

Load case	Normal force [N/m]	Bending moment [N · m/m]
1	213.4	53.8
2	347.4	87.5

Forces acting on the wingtip

In table 4.6 the results of the force analysis can be found. The contingency factor has been taken into account and it can be seen that the largest force is due to the weight with a load factor of 7.5 which is pointing in the negative z-direction. This force is causing a moment of 276 N · m per meter span around the x-axis. The drag is responsible for a force in the positive x-axis and causes a moment around the z-axis. When the cant angle reaches 90 degrees(see figure 4.2), a torsion is created around the y-axis. As can be seen in the table, the most critical load case is that when the winglet is subjected to a load factor of 7.5 and will therefore be the design target of the interface.

Table 4.6: Forces, moments and torsion on the winglets-wingbox interface

Contributor	Force [N]	Moment [N · m]	Torsion [N · m]
Lift	115.1	34.5	0
Drag	5.17	1.55	1.55
Weight	920	276	0

Leading edge, trailing edge, and tip interface results

The focus in the design of interface between the LE and TE devices and the wing box lays on the ease to remove the devices as well as the ability to transfer the loads to the wing box. With this in mind, the choice of design fell on bolts with coupling nuts. Coupling nuts can be seen as hollow bolts with screwing thread inside. An example can be found in figure 4.3 [2]. The final design of the interface is displayed in figure 4.4. To keep a laminar flow, the bolts have a sunken head and if necessary can be taped to flatten out the surface. The same design is used to connect the winglets to the wing box.

Recommendations

Simplifications and assumptions have been made to design the interface between the wing box and the LE and TE devices. Below a list is presented with recommendations for further research.

- The method used is based on empirical data, and does not take into account the Reynolds number and shape of the airfoil. To get a more accurate prediction on the normal forces, one should perform a Computational Fluid Dynamics (CFD) analysis to find the pressure distributions on the flaps.

[2] Nieuwlaat `http://www.nieuwlaat.nl/bevestigingsmaterialen-bout-c-45_83.html` Accessed on 13-1-2016

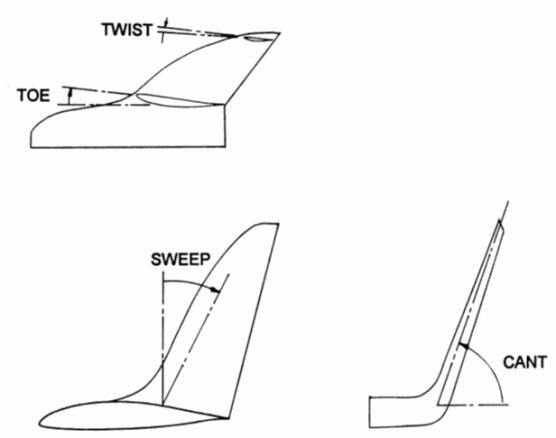

Figure 4.2: Geometric quantities to define the winglet [12]

Figure 4.3: Bolt with coupling nut

- The normal forces are a combination of static and dynamic loads, which are assumed to be acting in the same direction. A more accurate analysis should be performed to see if this is really the case.
- The forces acting on the TE have also been applied on the LE. A separate analysis of the forces acting on the LE should be conducted.

In order to get a more accurate tip interface design the following recommendations are given:

- The forces acting on the winglet are based on the lift and drag equations and are assumed to act at the centre of gravity of the winglet. A CFD analysis will give a proper distribution of the pressure which results in a better approximation of the forces acting on the winglet.
- The surface area and weight of the winglet are based on reference data and only applies to the simplest winglet, which is just an extension of the wing. One should take into account the many different wingtip devices that can be attached to the wing.
- Only two load cases are analysed, which can result in a under designed winglet-wingbox interface. Taken into account more load cases (for example a combination of the ultimate load factor with the lift generated during cruising) will result in a more accurate design of the interface.
- Depending on the device that is attached under the winglet, the drag will increase. This has been covered by the contingency factor, however a more extensive research needs to be performed in order to find a more accurate prediction on the drag.

These recommendations should be used for further development of the wing tip interface.

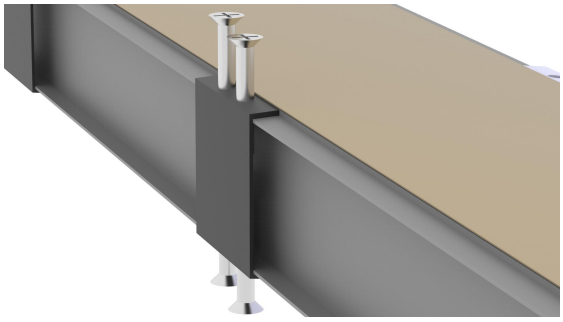

Figure 4.4: Final interface design of the wing box with the winglet, LE and TE

4.1.3 Wing-fuselage interface

The wing fuselage interface serves both to connect the wings to each other and to the fuselage, fulfilling the role of a centre wing box. It will be treated as part of the wing design. First the critical load case will be determined, followed by a discussion of the design strategy. Finally the resulting interface will be presented.

Wing-fuselage interface loads

The loads on the wing fuselage interface are higher than those on the default wing since it must accommodate all wing geometries of the IDS. The total lift, drag and load factors remain the same but higher wing spans mean larger bending moments will be generated at the root of the wings. The critical load cases are for the wing with the highest wing span, swept most forward, most aft and unswept. The unswept wing will generate the larges bending moments at the root, the swept wings will generate the largest torsional moments. The wing parameters used for the load determination are shown in table 4.7. The resultant lift load is assumed to act perpendicular to the wing surface and acts at 21% chord and 60% of the span of a single wing. The resulting critical loads can be found in table 4.8. For wing plan forms outside the IDS, especially those with a combination of high span and sweep, the maximum allowable load factor may no longer be five. For these plan forms the limit forces and moments should be evaluated and constraints should be placed on the manoeuvring load factors allowed during flight.

Table 4.7: Wing parameters for critical wing-fuselage interface loads.

Parameter	Value	Unit
Sweep	15, 0, -10	°
Aspect ratio	15	-
Surface area	4	m^2
Taper ratio	1	-

Wing-fuselage interface design strategy

Of the loads applied to the wing-fuselage interface the bending moment generated by the lift is by far the largest. This bending moment is introduced as close as possible to the fuselage centre line to reduce the amount of structure required to transfer the moment from one wing to the other. The shear loads caused by the lift and drag as well as any torsion are transferred to the fuselage. The torsion at the wing root is transferred to the wing-fuselage interface by differential bending of the two wing spars.

The wing fuselage interface is constructed from closed, thin-walled, rectangular beams made of aluminium 7075-T6. Relevant material properties can be found in table 4.10. The direct stress due to bending is evaluated by hand using the methods described in section 16.2.3 'Direct stress distribution due to bending' of [13]. Shear is evaluated using section 17.3 'Shear of closed section beams' of [13]. Buckling of

Table 4.8: Critical loads applied to the wing-fuselage interface by one wing.

Limit loads		
Fx	551	N
Fy	0	N
Fz	2291, -1374	N
Mx	5327, -3195	Nm
My	1180, -1113	Nm
Mz	-1281	Nm
Ultimate loads		
Fx	827	N
Fy	0	N
Fz	3436, -2062	N
Mx	7989, -4794	Nm
My	1770, -1670	Nm
Mz	-1922	Nm

the compressed skin sections of the beams is evaluated using the equation 9.7 of section 9.2 'Inelastic buckling of plates' from [13]. The von Mises stress is calculated for both the limit and ultimate load case. The limit von Mises stress is compared to the fatigue stress limit of the material and the ultimate von Mises stress is compared to the yield stress limit.

Wing-fuselage interface results

The wing-fuselage interface results can be found in table 4.9. An isometric view of the interface can be found in figure 4.5. The structure is fatigue limited since the fatigue stresses due to the limit loads are reached before yield stresses due to the ultimate loads. The buckling stresses are very high due to the large skin thickness and the short length of the beams.

For manufacturability the same profile has been used for the wing brackets as for the longitudinal beam sections. If the longitudinal beam sections are reduced to critical dimensions approximately 270 grams might be saved on the interface.

Since the structure is highly loaded and of relatively small dimensions st. Venant's principle regarding stress distributions may no longer apply and resultant stresses may be dominated by local stress effects. The structure should be evaluated using finite element methods to find the more accurate stress distributions.

Table 4.9: Wing fuselage interface results

Parameter	Value	Unit
Profile height	0.1105	m
Profile width	0.044	m
Top/bottom wall thickness	4.25	mm
Side wall thickness	2	mm
Minimum fatigue margin of safety	1	-
Minimum yield margin of safety	2.57	-
Maximum compressive stress	155	MPa
Buckling critical stress	470	MPa
Interface mass	2.6	kg

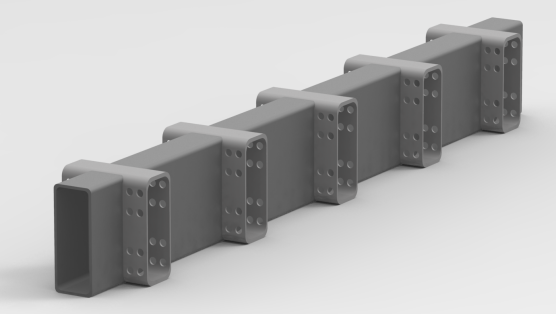

Figure 4.5: Isometric view of wing-fuselage interface

4.1.4 Default wing structure

To evaluate and optimise the performance of the wing structure a custom MATLAB script has been created. The wing box structure is idealised as a boom and web structure where the booms carry only direct stresses and the webs carry only shear stresses. The wing box is designed such that it can carry all loads by itself, no additional load carrying capability of the leading or trailing edge modules is required. First the primary and secondary assumptions are listed. This is followed by a short discussion on the critical load case. Then the program used to design and evaluate the wing box is discussed followed by the verification and validation of the program. Finally the resulting wing box design is presented.

Assumptions

The assumptions used to construct the model have been divided into primary assumptions, which have a major impact on the model, and secondary assumptions, which have only a minor impact on the model. The following primary assumptions are used to construct the model:

- Booms carry direct stresses only, webs/skins carry shear stresses only. The entire structure contributes both to the direct stress and shear stress carrying capability. To limit the impact of this assumption the cross sectional area of the skins is divided over the booms corresponding to the dominant load case.
- The parallel axis term is dominant in the moment of inertia calculation, the moment of inertia of the stringer profile is neglected. For an L stringer of 35mm cross-sectional area on the top plate, the profile moment of inertia is approximately 300 mm^4. The Parallel axis term associated with this stringer is approximately 3400 mm^4. This results in an under estimation of the moment of inertia by about 8.5%. This makes the structure conservative and 8.5% is an acceptable error at the current level of detail.
- The aerodynamic loads are invariant with regards to wing box deflection. Under load the wing box may deflect enough to affect the lift distribution over the span.

The following secondary assumptions are used to construct the model:

- Airfoil curvature is neglected in between booms, the skin is linearly interpolated between the boom locations.
- Localised stress concentrations are not taken into account. Fasteners have not been included in the model, the local stress distribution around them has therefore not been taken into account either. Inter-rivet buckling of the skin will also not be evaluated.
- All applied loads are carried by the wing box only. The wing must remain structurally intact regardless of the modules attached to the LE and TE. Any load taken up by these modules is an added benefit.

- A thickness of 1 mm is assumed for the ribs and no further calculations regarding the design of the ribs are made. The rib thickness is only used for the overall weight calculation. The ribs only contribute a small part to the overall weight, thus this assumption has a small effect.
- The wing box is assumed to be thin walled. The wall thicknesses are on the order of a single millimetre. This is small enough compared to the overall dimensions that the impact of the thin walled assumption is small.

Because of these assumptions the model is easier and faster to build, and faster to compute once it has been built. The errors introduced by these assumptions are acceptable for a first order model. More detailed modelling will have to be performed in later design stages to find more accurate results.

Loads

The loads applied to the model consist of the lift distributed over the span, the drag distributed over the span, the weight of the wing and any payload, aerodynamic loads due to LE and TE devices, and tip loads due to tip devices. Since the wing box and payload weight provides bending relief the most critical case is when the wing payload weight is set to zero at maximum MTOW. The applied tip loads are the maximum interface loads as specified in section 4.1.2. The aerodynamic loads of the LE and TE devices have been included in the distributed lift and drag forces. These loads are included whilst the wing payload weight has been set to zero, which is conservative and leads to a slightly over designed structure. The exact lift and drag distribution along the span has been extracted from XFLR5. The distribution is integrated along the span from the tip to the station location to find the lift and drag fraction loading the station cross section.

Design and evaluation

The calculations performed for a single wing box are shown in figure 4.6. The wing box geometry, material properties, and the internal moments and forces at all station locations are used as input. The stresses and safety margins are then evaluated at an arbitrary number of stations along the span of the wing. These stations are evaluated independently preventing the accumulation of numerical errors as the software proceeds along the span.

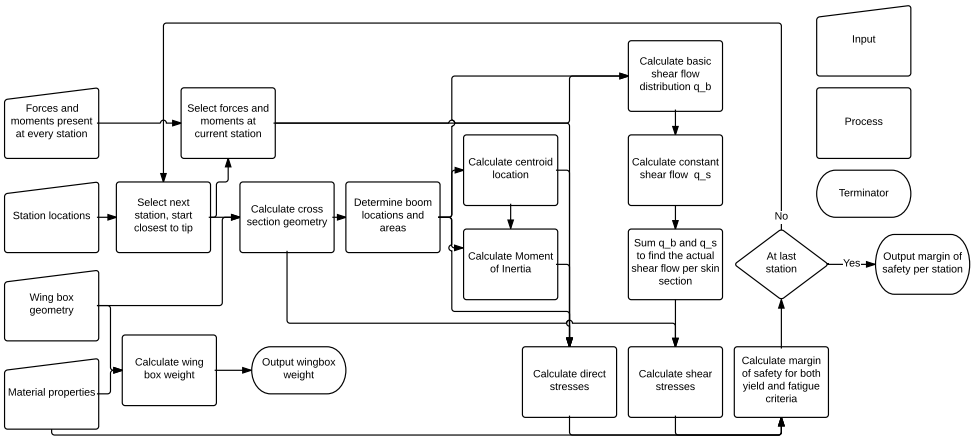

Figure 4.6: wing box design and evaluation program

The calculation begins by selecting the first station of the wing box. At this station a section is made and the local cross section geometry is determined. Booms are placed at all four corners of the wing box as well as at all stringer locations. The cross-sectional area of the booms is found by dividing the skin area over the booms and adding the cross-sectional area of the stiffeners at the boom location. Since the majority of the moment load consist of up/down bending moment the top and bottom skin areas are

divided such that half the skin area between two adjacent booms is added to one boom and half the area is added to the other boom. The spar web areas are divided over the booms at their top and bottom ends where 1/6 of the skin cross-sectional area is added to each as per section 20.2 'Idealisation of a panel' from [13].

After the boom areas and locations have been determined the centroid is calculated. About this centroid the area moments of inertia are calculated. For this calculation the parallel axis theorem is used to determine the contribution to the moments of inertia of the various booms. Since this term is dominant the moment of inertia contribution of the stringer profile is neglected. There is thus also no need to specify the exact shape of the stiffener, as long as the cross-sectional area is known. The bending moments present at the station can now be used to determine the direct stresses in the booms.

To determine the shear stresses in the skin, one skin panel is 'cut' and assigned zero shear flow. Then the applied shear loads and equation 20.11 from section 20.3.3 'Shear loading of closed section beams' of [13] are used to determine the shear flow distribution along the skins of the cross section. Since the skins carry no direct stresses the shear stress in between two booms is constant. Now that the shear flow distribution around the cross section is known the magnitude of the shear flows can be determined. The moments generated by a shear flow about the centroid are equal to the shear flow multiplied with two times the area enclosed by the vertices of the skin panel the shear flow acts on, and the centroid as per section A15.8 example problem 2 of [14]. The sum of all these moments generated by internal shear flow distribution plus the moment generated by the constant shear flow around the section must be equal and opposite to the moment generated by the external shear forces about the centroid plus the torsional moment applied by the structure on the tip side of the station. Solving this moment equilibrium gives the constant shear flow. Adding this to the shear flow distribution gives the actual shear flow in the skins. Dividing by the skin thickness gives the shear stress in each skin.

To find the margins of safety the resultant stresses are compared to two failure criteria. The stresses calculated using the ultimate loads are compared to the yield and shear strength of the material selected for the wing box. The stresses are also calculated for the limit load case which are then compared to the fatigue limit of the selected material for 10^6 cycles. To incorporate material variances the lowest specified fatigue stress limit is used for the selected material.

Now that the margins of safety have been calculated for this particular station the program continues to the next station until the root of the wing has been reached. The most critical margin of safety along the span is recorded and the loop is terminated. Next to the calculations described above the program also calculated the weight of the wing box using the specified geometry and material density to use as a performance metric.

The optimisation routine is shown in figure 4.7. The limit and ultimate load factors are used to calculate the internal forces and moments at every station along the span of the wing box. Geometrical parameters of interest are given a range of values and for all combinations the resulting geometry is set up. When this preparation is complete the routine shown in figure 4.6 and described before is used to evaluate the mass and margin of safety for every wing box geometry. The calculations are independently performed for every wing box configuration making this program suited for parallel processing, which has been implemented and resulted in significantly improved computation times. When the computation is complete the results are searched and the lowest mass wing box which meets the required strength is selected. To limit the total number of combinations the skin is first sized such that it can just support all shear loading. This skin thickness is then used for all subsequent stringer sizing.

The result is then evaluated manually to determine rib spacing and buckling. The rib spacing is determined by evaluating the panel instability using the equations from section 9.5 'Instability of stiffened panels ' of [13] and the buckling is evaluated for any compression members. Column buckling for the compressed panel as a whole is evaluated as well as buckling of the skin in between stiffeners, with four simply supported edge conditions, and for stringer buckling, with three simply supported edge conditions and one free edge condition. The lowest of these critical stresses is used to evaluate buckling under ultimate load. A thickness of 1 mm is assumed for the ribs and no further calculations regarding the design of the ribs are made since detailed rib design is outside of the scope of the current document.

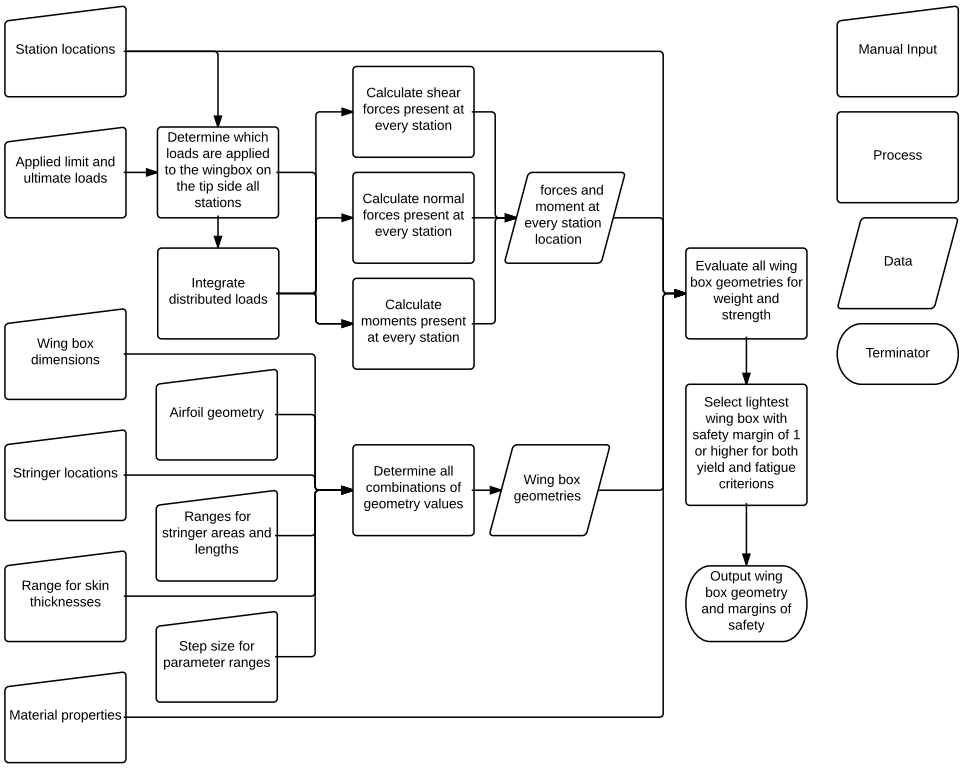

Figure 4.7: Wing box optimisation routine

4.1.5 Wing design verification and validation

The wing structural design has been performed using custom MATLAB scripts. All calculations performed in the scripts have been verified by comparing them to hand computations and discrepancies were corrected. The calculations have been grouped into functions which themselves have been verified. As much use as possible has been made of matrix calculations and generalised computational methods such that vectors of arbitrary length can be used as input. Two input vectors of differing length are used to verify that the function is correct for any vector length. A system level test has been performed for assembled program has also been verified by comparing the results to a manual calculation of the same input values. input loads have also been set to zero and it has been checked that the stresses in the wing box become zero. A small sensitivity analysis was performed by varying the applied loads and checking that the stresses in the structure varied accordingly. The structure geometry was also varied around the design point to check the sensitivity. The structure parameters were also set to zero one by one to check the influence on the moment of inertia and to check that none raised an error.
The program does not contain any iterative loops, all geometry combinations are evaluated and the lightest valid structure is selected. It therefore does not converge or diverge, and thus convergence does not have to be checked.
Since the verification has been completed successfully the model can be validated. For validation a test setup should be constructed to test the stresses in the structure resulting from applied distributed and concentrated loads. When the model predictions match the test results to an acceptable degree the model has been validated and can be used to design production parts. For the initial load determination a custom made script is used, of which the values are validated with known numerical software.

Results

The results of the wing box design can be found in table 4.10. Aluminium 7075-T6 has been selected for its high fatigue stress limit compared to other aluminium alloys and low cost compared to fibre composites. To account for extending the wing spars to within the fuselage the root of the wing box is set at the fuselage centre line rather than the fuselage side. The resulting wing box mass is 6.17 kg per wing.

Two stiffener sizes have been defined, type A and type B. Type A stiffeners are smaller in cross section, run the entire length of the wing box and serve to connect the spar webs to the wing skins. Type B stiffeners are larger in cross section and are used to reinforce the wing box structure where high bending moments must be resisted. All stiffeners start at the root and extend towards the tip. 2 type A stiffeners and 5 type B stiffeners are attached to the top and to the bottom skins of the wing box. A cross section can be found in figure 4.9 and the longitudinal layout can be found in figure 4.8.

The wing box structure is critical when it comes to fatigue, since the highest allowable fatigue stresses are reached under limit loading whilst the stresses due to ultimate loading remain well under the yield limit. To evaluate buckling L shapes of equivalent cross-sectional area are assumed for the two stiffener types. All buckling stresses are above the maximum compressive stress in the structure. The closest is the skin buckling stress where the skin in between two stringers buckles as a long, narrow plate. The panel column buckling criterion resulted in a maximum rib spacing of 350 mm at the root. The first rib is placed right up against the fuselage at 261 mm from the fuselage centre line, resulting in a high critical column buckling stress of 250 MPa.

Table 4.10: Wing box results, one wing box

Parameter	Value	Unit
Material	Aluminium 7075-T6	–
Material density	2810	kg/m^3
Material E modulus	71.7	GPa
Material yield stress limit	434	MPa
Material fatigue stress limit, 10^6 cycles	110	MPa
Stringer area type A	11	mm^2
Stringer area type B	35	mm^2
Stringer lengths type A	3000	mm
Stringer lengths type B	4x 1000, 4x 1500, 2x 2500	mm
Number of type A stringers	4	–
Number of type B stringers	10	–
Skin/web thickness	0.7	mm
Minimum yield safety margin	2.937	–
Minimum fatigue safety margin	1.068	–
Number of ribs trailing	6	–
Rib locations, from fuselage centreline	261, 620, 1040, 1500, 2010, 2680	mm
Rib thickness	1	mm
Maximum compressive stress, ultimate load	139.4	MPa
Critical panel column buckling stress	250	MPa
Critical skin buckling stress	144	MPa
Critical stiffener buckling stress	182	MPa
Stringer mass	1.84	kg
Skin/web mass	3.29	kg
Rib mass	1.03	kg
Wing box mass	6.17	kg

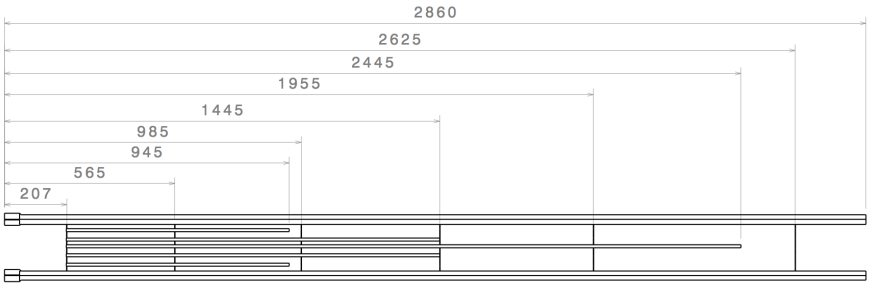

Figure 4.8: Top view of the final wing box layout.

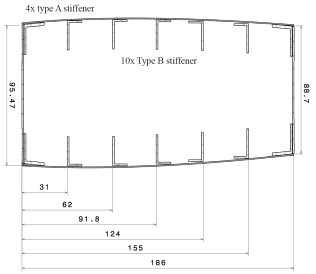

Figure 4.9: Cross section of the wing box layout with all stringers.

Leading edge, edge and tip fairings

Since all loads are carried by the wing box only the mass of the fairings has been calculated. Using the same skin thickness, rib number, rib locations and rib thickness as for the wings for manufacturability gives the weights shown in table 4.11. To account for the weight of the tip fairings the wing box used in the calculation has been extended all the way to the tip.

Table 4.11: fairing mass breakdown

Parameter	Value	Unit
Leading edge fairing skin	1.023	kg
Leading edge fairing ribs	0.140	kg
Leading edge fairing brackets	0.380	kg
Trailing edge fairing skin	2,158	kg
Trailing edge fairing ribs	0.200	kg
Trailing edge edge fairing brackets	0.360	kg
Fairing mass	4.261	kg

Conclusion and recommendations

The wing design is heavier than originally predicted. The original wing weight budget is 15 kg in total whereas the current design weighs 10.431 kg per wing for a total 20.9 kg. However in the first order weight estimation an additional 4.5 kg has been reserved separately for structural weight gain due to the modularity of the aircraft. This reduces the impact of the overweight wings. The wing box as is reaches the limits of manufacturability. The skin is incredibly thin at 0.7 mm and yet it still accounts for 62% of the wing weight. To save weight any of the following actions are recommended.

- Include tip payload bending relief. To find the most critical load case the bending relief due to any payload on the wings has been set to zero. However the maximum tip loads specified could only

be reached with some tip device in place. This would reduce the overall loading of the wing box and thus reduce the stresses present in the structure.

- Increase the fatigue stress limit. Due to material variability concerns the lowest specified fatigue stress limit of 110 MPa has been used to design the wing box. If the material can be demonstrated to be of acceptable consistency a fatigue limit up to 185 MPa may be used.
- Utilise composite laminate structures. The use of composites both provides inherently better specific stiffness and strength, and allows the use of thinner load bearing skin material when the material is sandwiched with a low density core. This would counter the manufacturability limitations currently encountered by the wing skin.

The following additional recommendations can also be made:

- Analyse the wing in more detail using finite element software to find localised stress concentrations.
- Evaluate the dynamic behaviour of the structure to prevent vibration problems in later design stages.

If these recommendations are used for further development, the MUAV will have a successful default wing.

4.2 Fuselage design

The fuselage is essentially the structure responsible for housing the various subsystems and carrying all the loads induced by these subsystems. This section describes the geometry of the fuselage as well as an initial estimate for the structural layout. The fuselage geometry is described in section 4.2.1, the different load cases are shown in section 4.2.2 and the structural geometry is discussed is section 4.2.3.

4.2.1 Fuselage geometry

The geometry of the fuselage can essentially be divided up into three sections. It consists of a nose cone, the main body and the aft body. The geometry of these sections is based upon several considerations. These considerations follow from payload, aerodynamic and stability requirements.

Nose cone

The nose cone of the fuselage is not housing any payload, its main function is to improve the aerodynamics of the fuselage. Having sudden changes in fuselage shape larger than 30 degrees will cause flow separation at the speeds the MUAV will be flying [3]. Furthermore it should smoothly merge into the main body. The geometry parameters of the nose cone can be found in table 4.12.

Main body

The main body of the fuselage is housing the majority of the subsystems. This means that the larger subsystems, like the payload bay and the engine should fit in here. As these subsystems are rectangular it is more convenient to go for a rectangular cross section of the fuselage as well. Additionally, as the fuselage is not pressurised, a circular cross section of the fuselage would not render any structural benefits either.

The length of the main body is mainly determined by the required length for the centre wing box, the engine and the payload bay. To be able to move the centre of gravity, the payload should be movable, requiring more space in the fuselage. The required shifting length originates from stability requirements.

For the modularity of the MUAV, it is desirable to have easy access to the payload bay and centre wing box. This means two fuselage doors should be present on top of the main body of the fuselage. All geometry parameters for the main body of the fuselage can be found in table 4.12.

Aft body

For the aft body of the fuselage, the driving requirements come from the stability department. The length of the aft body of the fuselage determines the tail length. Especially for directional stability reasons a large tail length is required.

For the aerodynamic requirements of the aft body, the same holds as for the nose cone that no angles larger than 30 degrees should be present to avoid flow separation. The engine shaft is mounted as far to the top of the fuselage as possible in order to give the propeller as much ground clearance as possible. Therefore the top of the aft body should remain straight. This way different propeller module sizes are accounted for during landing rotation. The one sided taper at the bottom of the aft body should start at the beginning of the aft body to avoid flow separation due to large angles.

To avoid disturbing the flow intake of the propeller, which is located directly behind the aft body, the aft body should taper in width as well. This taper can be two sided, but can only begin after the most aft location of the trailing edge of wings with high root chords. This is done to avoid a gap between the aft part of the wing and the fuselage. All geometry parameters of the aft body can be found in table 4.12 and a visual representation is shown in figure 4.10.

Table 4.12: Wing box results, one wing box

Parameter	Value	Unit
Nose cone length	400	mm
Nose cone angle	30	°
Payload bay shifting section length	1050	mm
Main body length	2100	mm
Main body width	520	mm
Main body height	310	mm
Aft body length	1500	mm
Aft body one sided taper ratio in height	0.68	–
Aft body two sided taper ratio in width	0.19	–
Start position two sided taper from nose	3000	mm
Total fuselage length	4000	mm

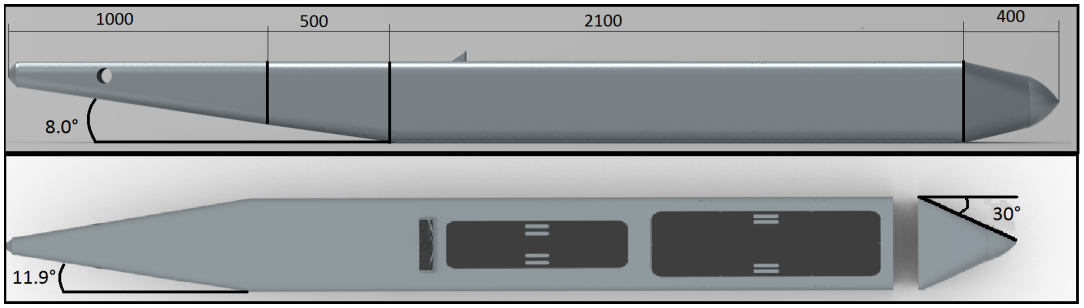

Figure 4.10: Top and side view of fuselage with dimensions

4.2.2 Fuselage loads

The loads on the fuselage mainly result from inertia forces from the weights of various components in the fuselage rather than from aerodynamic forces. Other major loads are resulting from the landing gear, tail and the main wing. The load analysis of the fuselage cannot be done without a structural analysis of the body, which involves a large amount of calculation. The fact that the loads on the fuselage depend on so many different components makes the load analysis highly complex. This complexity is further increased by the adjustable payload and wing positions. It is therefore decided, taking the limited time available

into account, to do a load analysis of a simplified nature suggested by Bruhn section A5.11 [14]. This process is described in the remainder of this section.

Weight balance table

The first step in the load analysis of the fuselage is making an initial drawing of the internal and external layout of the aircraft. The external layout drawing is based on the initial sizing in the conceptual design phase. The internal layout is based on the desired centre of gravity positions of the components in the fuselage and some estimations based on spatial visualisation and engineering sense.

The next step is to determine the distance of the components from the nose and the centre line of the fuselage. The positions and the weights found in the initial sizing provide the centre of gravity positions in x and z direction. For the load analysis of the fuselage the wing, and components attached to the wing, are removed from this table. At the wing position only the reaction forces will be used.

Panel point weight distribution

To get a relatively good estimation of the forces resulting from the weight of the components, the fuselage is divided into several stations. Then the weight balance table is used to locate the various subsystems and their weights between the stations.

All subsystems are considered as a point mass except for the fuselage itself. The centre of gravity of all the components is assumed to lie in the centre of their geometry. The fuselage weight is divided over the stations in such a way that the moment of the weights around the nose remains the same as it was originally. Furthermore the weights of the components are divided inversely linear to the distance of their neighbouring stations.

On top of that, the z location of the centre of gravity of the station is located with the use of the z positions and weights of the neighbouring subsystems from the weight balance table. With the z and x positions and weights of the station known the vertical and horizontal moments for each station can be determined.

Unit load factors in z and x direction

With the weight distributed over the stations, the loads due to a unit load factor can be calculated. With the total loads known the reaction forces at the wing attachments can be calculated with the moment equilibrium and the sum of the forces in z direction. Now all the applied loads are known, the shear forces and moments per station can be calculated.

The loads for a unit load factor in x direction can be found in an analogous way to the loads for a load factor in z direction. With the only exception that an additional reaction force is present in x direction. This reaction force, which represents the drag, is assumed to act at the front spar of the wing box.

Unit tail load

To asses the loads induced by a tail load from the vertical stabiliser a unit load of 100 N is applied at the horizontal stabiliser location. The reaction forces of the wing at the front and the aft should now produce the same couple moment as the tail load does around the front spar of the wing for static equilibrium. The shear forces and moments occurring throughout the fuselage length can now be found the same way as at the unit load calculation for the z load factor.

Torsion from roll acceleration

When the MUAV is performing a roll with a rotational acceleration around its body axis a torsion will occur due to the resistance against rotation from the mass moment of inertia around the x axis. To find the torque at every individual station the mass moment of inertia for each station is calculated using the panel point weight distribution for the weight of every system and assuming a uniform mass over the cross-section of every station. This is also done for the wing with a maximal wing span and surface area within the IDS. Now the torque is found by starting from the most aft part of the fuselage where

the total torque is applied by the tail to overcome the mass moment of inertia for the maximum angular acceleration specified by the empennage design of 1.09 rad/s^2. Then for the stations to the nose of the fuselage the torque is the maximal torque at the most aft part of the fuselage minus the opposite torque loads occurring in the stations leading up to the selected station.

Loads induced by the landing gear

For the loads induced by the landing gear on the fuselage structure, a levelled landing is considered for simplicity. The reaction forces on the fuselage are the maximum loads the landing gear is sized on. The maximum load factor is obtained by dividing the sum of the maximum landing gear loads divided by the gross weight of the MUAV. The shear loads and moments can be calculated by placing the two reaction forces for the unit load factor in z direction at the positions of the landing gear and using the unit load table for a load factor in z direction times the load factor in z direction during the landing.

Approximation for the loads on the fuselage in a boxed wing configuration

As the fuselage should also be able to carry the loads for a boxed wing configuration an estimation of the loads induced by the boxed wing is made. Normally the structure would be statically indeterminate, since the addition of a second wing results in four reaction forces. This would greatly increase the complexity of the calculations. To avoid this, the load on the aft wing is modelled to be the tail load. The total couple moment is assumed to be taken up by the front wing box.

Also an additional torque is induced on the aft body of the fuselage. This is the result of the sideways forces caused by the vertical structures connecting the front and aft wing. This provides a reaction force at the wing connection with the vertical stabiliser and at the centre wing box. The resulting force is opposite to the force of the rudder which tries to counteract the yawing motion. The vertical connector force, at the vertical stabiliser, and the rudder force do not act at the same point leading to a torque being introduced at this point. How this torque is induced is dependent on the empennage interface structure with the fuselage, for which no design is made. It is assumed that the torque is induced on the second station from the aft point of the fuselage which is at 50 cm. A visual representation of the forces inducing this torque can be found in figure 4.11.

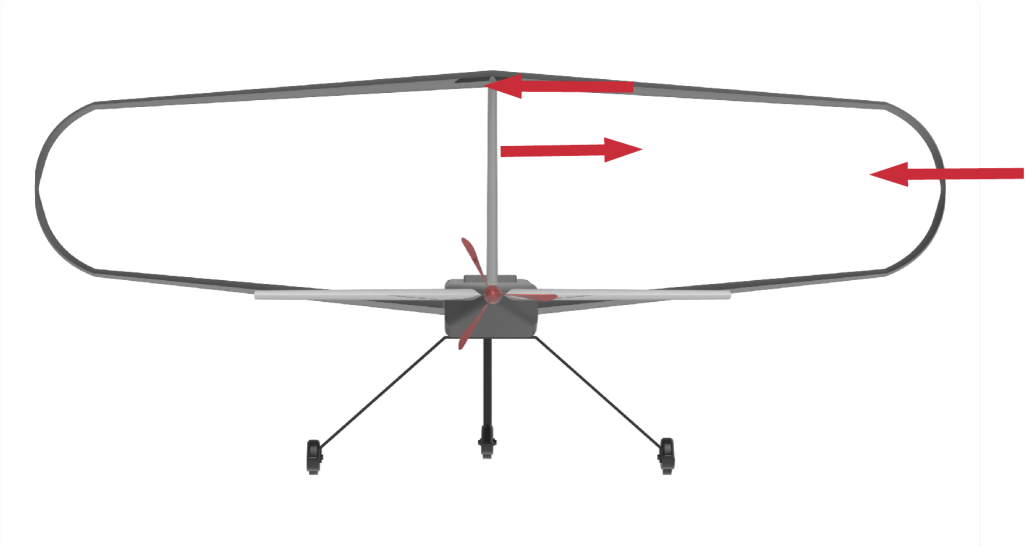

Figure 4.11: Visual representation of the forces inducing torque at the empennage

Load cases

To be able to make sure the highest loads for the fuselage are considered, the load cases deemed to give the highest loads are considered. For all these load cases the loads are computed. Furthermore, a moment and shear diagram is drawn up for every possible configuration at a certain load case.These can be found below.

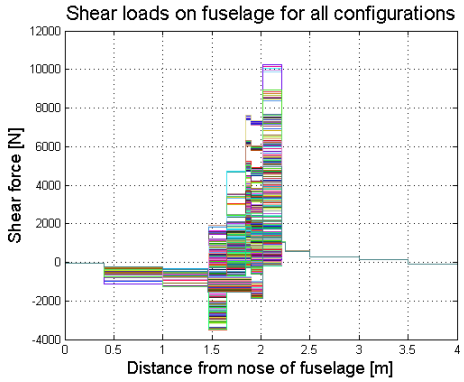

(a) Rolling pull up shear diagram

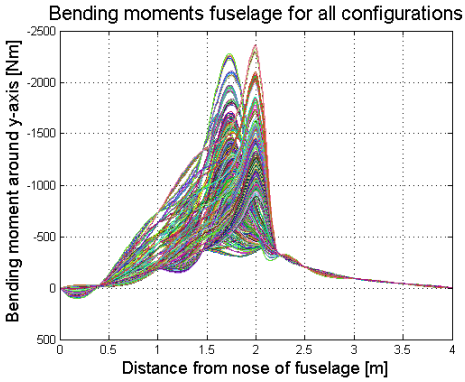

(b) rolling pull up moment diagram

Figure 4.12: Shear and moment diagrams rolling pull up

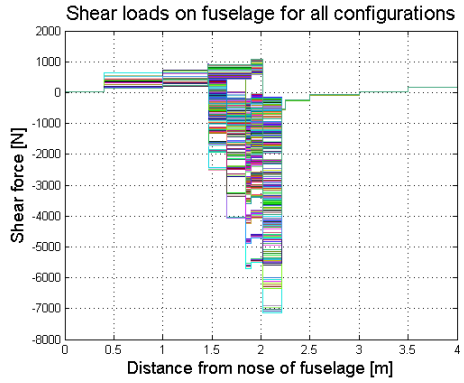

(a) Diving shear diagram

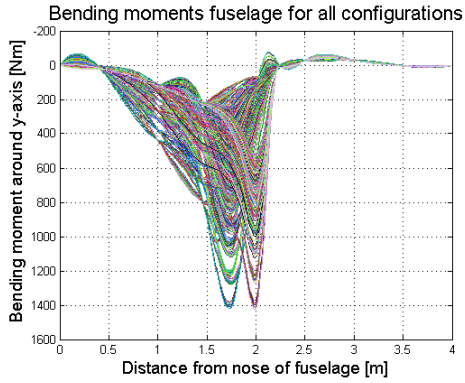

(b) Diving moment diagram

Figure 4.13: Shear and moment diagrams dive

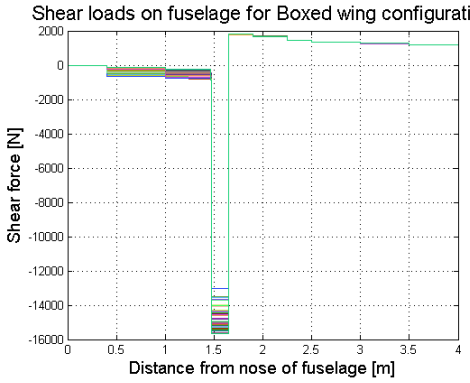

(a) Boxed wing shear diagram

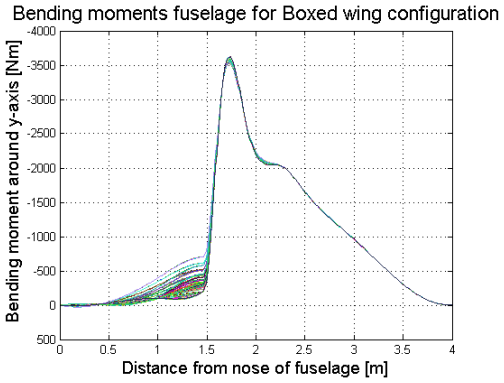

(b) Boxed wing moment diagram

Figure 4.14: Shear and moment diagrams boxed wing

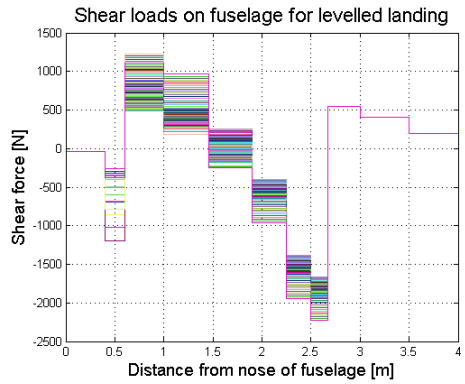

(a) Landing shear diagram

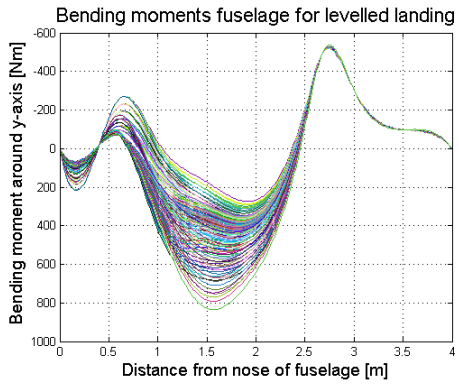

(b) Landing moment diagram

Figure 4.15: Shear and moment diagrams landing

The fuselage load program flow

The flowchart for the total load program for the fuselage can be seen in figure 4.16. From the flow chart it can be seen that the load calculation program is depending on a large number of variables. The panel point weight distribution is required for every Load case. The combination of unit load tables, depends on the desired load case. For example a rolling manoeuvre with a load factor 5 in z direction and a deceleration of -1.5 g, would result in a total load table made up of 5 times the moment and shear forces from the table for a unit load factor in z direction and -1.5 times the shear and moment loads from the table for a unit load factor in x direction. The total table with the loads and position of the station is then printed for every combination of input variables in a large matrix. From this matrix the maximum value for the loads at very station can be selected for every load case.

4.2.3 Structural geometry determination of the fuselage

The final selected geometry of the cross section at every station is determined by the shear flows and the safety margins at every station. With the moments and shear forces known from the load calculation program, it is now possible to calculate these shear flows. With these shear flows the structure can be optimised to be able to carry the required loads with a minimal structure weight.

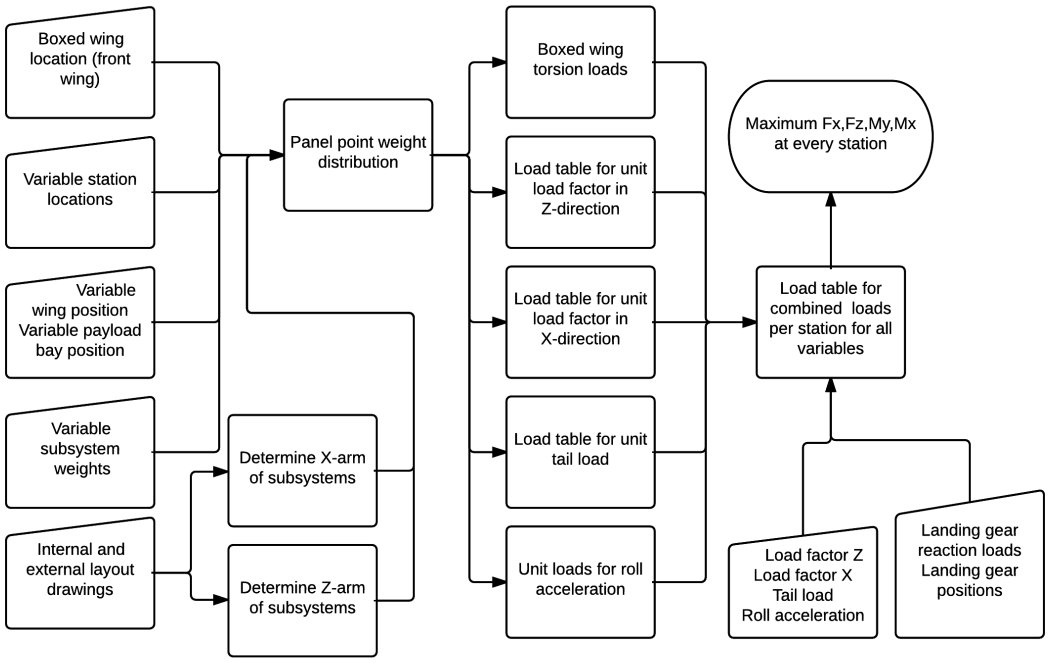

Figure 4.16: Flowchart for the load calculation program

Software program for the shear flow calculation in the fuselage

For the shear flow calculation in the fuselage, essentially the same program is used as for wing box shear stresses, with a few adjustments. This was done to save time and because the geometry of the cross section is similar. The flow diagram of this program can be found in figure 4.6 and the same assumptions stated in section 4.1.4 hold.

The only modules adjusted in the software program are the cross section geometry calculator and the shear flow calculator. The cross section geometry is adjusted to be able to incorporate a rectangular cross section rather than a trapezoidal cross section for the wing box. Furthermore the option to leave out the stringers on the top plate for the sections with the payload bay and centre wing box is included.

The shear flow calculator is only adjusted for the section with the payload bay where the fuselage door is not load bearing. In this section the cross section should be modelled as an open section rather than a closed section. The shear flow calculator is adjusted here in such a way that it does not include the partial sectoral area from the centroid to the boom positions for the top plate. By adjusting the shear flow calculation for closed sections in this way the method still holds.

The optimisation method for structure of the fuselage is done by hand rather than by an optimisation program. This is done because of the complexity such a system would behold, because of the differences in sign convention for the load cases as well as the non linearity of the load from the nose to the aft of the fuselage. The optimisation is done per section instead of per station to ensure the continuity of the stringers over the different sections of the fuselage. The way these sections are defined can be seen in figure 4.17

Results for the structure of the fuselage

This section presents the results for the cross section geometry of the different sections of the fuselage. This includes material choice, stringer pitches, stringer areas, fatigue safety margins and the masses of the different structural components. All results can be found in table 4.13. The results for the optimisation are based on the following four different load cases:

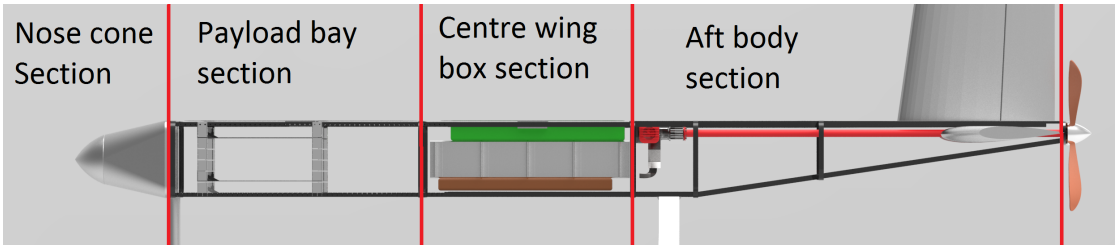

Figure 4.17: Fuselage divided up into sections

- Aircraft in roll with vertical load factor 5, horizontal load factor -1.5 and a tail load of -300 N
- Aircraft in dive with vertical load factor -3, horizontal load factor 1.5 and a tail load of 300 N
- Aircraft with boxed wing configuration
- Levelled landing

The results describe the optimised structural layout for the four different loading cases. For every section of the fuselage the stringer pitch as well as stringer area is given. Furthermore the lowest fatigue safety factor occurring for every load case is given. These are based on the limit loads for these flight and landing conditions. In the bottom part of table 4.12 the weight results of the fuselage are presented.

4.2.4 Fuselage design verification and validation

For the fuselage design essentially two software programs are used that are both written in MATLAB. These being the load calculator and the shear stress calculator used for the wing box structure. For the shear stress calculator the modules have already been verified, this verification is described in section 4.1.5. The adjusted weight module is checked by hand calculations and the adjusted geometry module is checked on consistency by printing the new values. For the Loads calculation program the correct division of the weight over the stations is is verified by hand calculations. The unit load tables and final load table is checked by hand calculation and constantly checked on consistency with the tables for the used method presented in Bruhn section A5.15. Also, the created shear and moment diagrams are checked for consistency.

To check whether the programme delivers consistent results or not, a sensitivity analysis is done as well. This sensitivity analysis is done using the rolling pull up load case as this one includes all models for the load calculations. The maximum direct and shear stresses are calculated for the reference situation. After that they are calculated with 10 percent added gross weight and with 10 percent subtracted gross weight. These results can be seen in figure 4.18a and figure 4.18b. From the results it can be seen that a 10 percent or decrease in gross weight leads to an approximately equivalent increased and decreased direct and shear stress. This means the model gives stable results for variation in gross weight.

The validation of the system should be done by applying limit loads as well as dynamic loads to the fuselage structure in a test setup and measuring the strain data and checking for failures.

Table 4.13: Fuselage structure results

Parameter	Value	Unit
Material properties		
Material	Aluminium 7075-T6	–
Material density	2810	kg/m^3
Material E modulus	71.7	GPa
Material yield stress limit	434	MPa
Material fatigue stress limit, 10^6 cycles	110	MPa
Nose cone section (no stringers)		
payload bay section		
Top stringer location	0.048, 0.952	% width
Top stringer areas	60, 60	mm^2
Bottom stringer locations	0.048, 0.33, 0.5, 0.66, 0.952	% width
Bottom stringer areas	55, 20, 15, 20, 55	mm^2
Centre wing box section		
Top stringer location	0.048, 0.952	% width
Top stringer areas	60, 60	mm^2
Bottom stringer locations	0.048, 0.17 0.33, 0.5, 0.66, 0.83 0.952	% width
Bottom stringer areas	55, 15, 20, 15, 20, 15, 55	mm^2
Aft body section		
Top stringer location	0.048, 0.33, 0.5, 0.66 , 0.952	% width
Top stringer areas	60, 15, 15, 15, 15, 60	mm^2
Bottom stringer locations	0.048, 0.33, 0.5, 0.66, 0.952	% width
Bottom stringer areas	55, 20, 15, 20, 55	mm^2
Total fuselage		
Minimum fatigue safety margin (rolling aircraft)	1.20	–
Minimum fatigue safety margin (diving aircraft)	2.81	–
Minimum fatigue safety margin (levelled landing)	1.137	–
Minimum fatigue safety margin (boxed wing)	1.123	–
Skin thickness	0.7	mm
Stringer mass	3.71	kg
Skin mass	10.79	kg
rib mass	1.92	kg
Fuselage mass	16.42	kg

Recommendations for further structural design

As mentioned before, an accurate structural analysis of the fuselage is highly complicated. The calculations provided here are of a simplified nature. To more accurately determine the required structural strength more loads should be taken into consideration, for example centrifugal forces of the components when the aircraft is pitching or yawing. Especially the yawing forces should be checked to make sure the fuselage can withstand the loads in y direction without side stiffeners. Other loads to consider are dynamic loads, an analysis of the bending stiffness and rotational stiffness of the aft part of the fuselage. Furthermore a more precise analysis of the centre of gravity of the individual component should be done.

For the time budget of this project optioning to use wing box stress analysis software seems like a viable method. However for more accurate calculations a dedicated software program should be developed for the fuselage. Lastly, a more precise load analysis should be done for a boxed wing configuration to

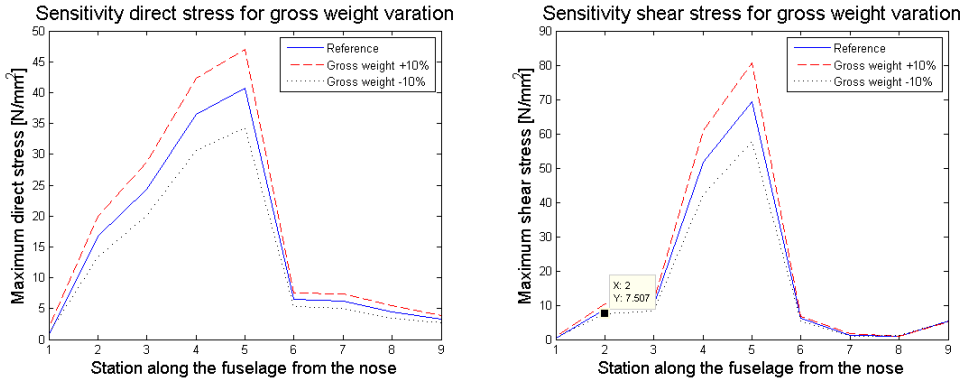

(a) Sensitivity analysis direct stress for variance in gross weight

(b) Sensitivity analysis shear stress for variance in gross weight

Figure 4.18: Sensitivity analysis

ensure the fuselage is able to carry the loads of such a construction.

4.3 Payload bay design

The payload bay is an important subsystem in the design of the MUAV and plays a key role in the ability to change the position of the centre of gravity. On top of that, it holds components of the user, which makes its accessibility and size important parameters. Therefore the choice is made to design the payload bay in more detail, which is discussed in this section. In subsection 4.3.1 a definition of the payload bay can be found, together with why it is needed and what it should do. Subsection 4.3.2 contains an explanation of the chosen design of the payload bay, and in subsection 4.3.3 the structure is analysed. In subsection 4.3.5 the payload possibilities are summarised.

4.3.1 Payload bay definition and functions

Aircraft carry payload, the goods that are needed to fulfil its mission. In this case the payload that has to be taken aboard can vary greatly from SHLDs to sensors and data acquisition systems and part of this payload will be stored in a specified location inside the fuselage called the payload bay. This means that the payload bay shall be large enough to provide space for various possible payload configurations. The movements of this payload during flight shall be constrained as an in-flight c.g. shift will have detrimental consequences. The payload bay also has to be movable to make sure the MUAV is stable in the chosen aircraft configuration.

4.3.2 Payload bay design

The chosen design of the payload bay is based on the 19-inch rack standard. This standard is often used in computer cases, server racks and audio applications. It allows for placement of modules with variable height and depth. It is chosen to use four columns, one on each corner of the payload bay, with guidance slits in each of them to support the forces in vertical direction. The maximum amount of units (44.45 mm of height) that can be used is six, of which the bottom one will be used for the electronic systems that always have to be present in the MUAV. They will have to be mounted with bolts on plates that can fit in the payload bay, which means they have a plate width of 463 mm. The length of the plate is variable but can be 500 mm at maximum. A front plate is needed to connect the plate with the columns. The size of this front plate is 482.6 mm in width and 44.45 mm in height per unit. The thickness of the plates is dependent on the amount of payload that is placed on them and will be calculated in subsection 4.3.3.

The plates will have to be custom made for a specific application, as holes need to be made for the bolts connecting the payload to the plate.

The columns to which the plates will be connected will be made out of aluminium sheets that are bent into shape. The holes and slits can be cut out prior to this. The geometry and dimensions can be seen in figure 4.19. These columns are connected to stringers on the top of the fuselage with M4 bolts. On the bottom they will fall into slits made in the bottom stringers, which will loosely constrain them and will take forces if the deflections get too large. The lateral distance between the stringers on the top shall be 452 mm and between the bottom stringers 470 mm. The holes and slits in these stringers are spaced such that the longitudinal location of the payload bay can be changed in 20 mm increments. A Catia[3] render of the payload bay can be seen in figure 4.20.

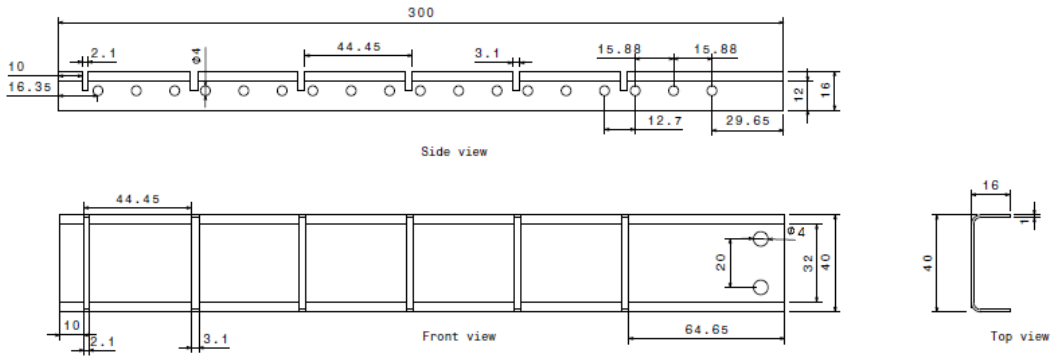

Figure 4.19: Column front, side and top view

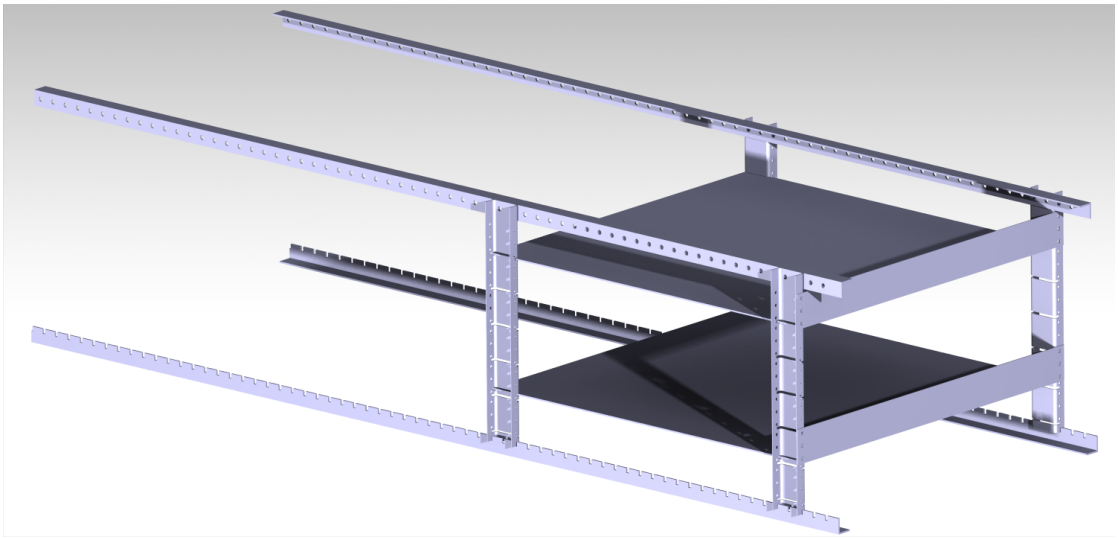

Figure 4.20: Catia render of one possible configuration payload bay in forward position

4.3.3 Structural analysis of the payload bay

To verify whether the payload bay will stay intact during the entire mission (with an ultimate load factor of 7.5), a structural analysis has to be performed. The parts of the payload bay that are most likely to fail

[3]CATIA V5R21

during operations are the bolts that connect the columns to the top stringers due to shear, the bolts that connect the mounting plate to the columns due to tension and bending of the plates under the weight of the payload.

Bolts connecting columns to stringers in shear

For the load case for the bolts that connect the columns to the stringer it is taken that 15 kg of payload is placed in the highest unit and that the MUAV experiences a 7.5 ultimate load factor in vertical direction. Assuming that the load is evenly divided over all four columns, each bolt (8 in total) receives 138 N in shear force. These bolts are used in a single shear configuration and will be loaded repeatedly, so as material strength the fatigue strength shall be used, leading to a conservative estimate as the ultimate load factor will not often be achieved. The bolts used here are M4 12.9, made from high alloy steel, which means that the fatigue strength is 128.5 MPa in tension.[4] For shear, roughly 60% of this value can be used, so 77 MPa.[5] The average shear stress in a bolt is calculated to be 11 MPa, which is well below the maximum allowable shear stress. The diameter of the bolt is however not taken any smaller as this would get impractical to handle.

Bolts connecting mounting plate to columns in tension

The load case for the bolts that connect the mounting plate to the columns is taken to be 15 kg of payload on a single mounting plate, with again an ultimate load of 7.5 but this time in longitudinal direction. This would simulate a full frontal crash. It is also assumed that of the 6 bolts in total, only 4 are used. This results in a normal force on each bolt of 289 N. An M4 12.9 bolt can bear a tensile force of 1118 N, so this is again well below the maximum allowable force. For practicality reasons the bolt diameter is not taken any smaller.

Bending of mounting plate under payload weight

The load case for the bending of the mounting plate consists of a variable weight and an ultimate load factor of 7.5 in vertical direction. The weight is assumed to be evenly distributed over the plate. Since bending of thin plates is different than bending of beams, the theory of NACA technical note no. 846 is used [15]. Here the pressure due to the weight of the payload is made dimensionless, and this non-dimensional pressure is then related to a non-dimensional deflection at the centre of the plate and a non-dimensional stress at four different locations on the plate. The results have been found using Excel and can be found in table 4.14. These have been calculated with the assumption that half of the volume of the plate is removed for making space for mounting the payload and reducing unnecessary material to save weight. To account for this the calculated deflection is doubled. The maximum deflection that is allowed is taken as 5 mm. It should be noted that the plate has three free edges and one beam-supported edge. It is however assumed that the plate is simply supported on all four corners, and the stiffening effect of the front plate is not taken into account. The method used is meant for rectangular plates under uniform load, simply supported on all four corners. From table 4.14 it is concluded that the minimum useful plate thickness is 2 mm and that the maximum plate thickness is 3 mm, as it is deemed unreasonable to mount more than 9 kg on a single plate. If smaller deflections are needed, a thicker plate can be used.

4.3.4 Payload bay design verification and validation

For the design of the payload bay a simple numerical tool has been written in MS excel. This tool calculates the dimensionless pressure on a thin plate and relates this to a deflection using statistical relations as found in NACA technical note 846 [15]. This excel file has been verified by performing hand calculations on three chosen input values to check the corresponding deflections. The results were identical to the values found using the excel tool.

[4] General Mechanical Properties. `http://www.fullermetric.com/technical/information/tech_mechanical_properties.aspx` Accessed: 6-1-2016

[5] Bolted Joint Design. `https://www.fastenal.com/content/feds/pdf/Article%20-%20Bolted%20Joint%20Design.pdf` Accessed: 6-1-2016

Table 4.14: Values of mounting plates with different thicknesses

t (mm)	$m_{payload}$ (kg)	m_{plate} (kg)	Relative weight (%)	σ (MPa)
2	3	0.7	23.3	6.6
2.5	5.5	0.88	16.0	7.8
3	9	1.05	11.7	8.8
3.5	13.5	1.23	9.1	9.7

4.3.5 Payload results and recommendations

From this section it can be concluded that the weight of the payload bay is dependent on the amount of plates that are inserted. The maximum weight that can be attained is 5.5 kg, although it is unrealistic that this configuration will be used. A realistic configuration that can hold 20 kg of payload weighs 3.0 kg. The centre of gravity of the payload bay including payload can be shifted from 650 mm from the nose to 1150 mm from the nose. The front limit of the payload bay is 400 mm from the nose, and the aft limit is 1400 mm from the nose, complying with the requirements. The payload bay location can be changed when the door on top of the fuselage is opened and the payload plates can be mounted when the nosecone is detached.

It is recommended that the deflection of the plates under the loads of the payload are calculated using Finite Elements Method (FEM), since the method used is simplified to a large extent. This would lead to more accurate estimations of necessary plate thicknesses, cutout possibilities and weight estimations.

4.4 Empennage design

In this section a detailed design for the empennage is presented. The two major tasks of this subsystem are to provide stability and control over the behaviour of the aircraft. This section is divided into 5 subsections. In the first subsection the effects of modularity on the design are stated and respectively the input and output of the mathematical model that will be developed are introduced. Secondly, the empennage design for static stability is analysed and the horizontal and vertical tail size are found. Thirdly, the dynamic longitudinal stability is analysed for these tail sizes. In the fourth subsection the controllability is analysed and the elevator, aileron and rudder size is calculated. Lastly, concluding this subsection an overview of the empennage is given and recommendations are stated.

4.4.1 Effects of modularity on stability and control

The modularity of the aircraft plays a key role in the design process of the empennage. Contrary to a normal aircraft, this design has to be optimised for a range of wing planforms instead of a single design point. The four most influential wing planform parameters are leading edge sweep Λ_{LE}, taper ratio λ, aspect ratio A and surface area S. Interviews with aeronautical experts of DUT made clear that these parameters themselves are no likely subjects of studies, however it is valuable to be able to vary them to a limited extent to accommodate freedom when designing a new wing. Therefore a design space has been defined for which any combination of the four planform parameters yields a stable and controllable design. This space is dubbed the IDS, its dimension can be found in table 3.5. The reader should notice that this approach has substantiated the previously vague concept of modularity into a four dimensional mathematical space. Discretisation of the design space has been performed by establishing ten values for each of the modularity parameters, yielding 10,000 data points which represents a unique configuration. Hence the team is able to optimise the design: for each requirement on stability and control the least favourable configuration(s) will be determined. A design that fulfils the requirement for that design point will automatically fulfil the requirement for the entire IDS. This will unavoidably imply that all control surfaces and actuators will be over-sized for the non critical configurations of the IDS.

Also the reader should notice that many planforms lying outside the IDS are viable as well, though not unconditionally. Before a non-IDS configuration is used, a flight dynamics assessment needs to be

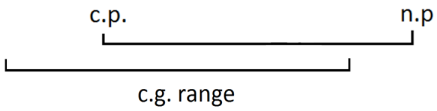

Figure 4.21: Indication of the control point, neutral point, and centre of gravity range of an aircraft

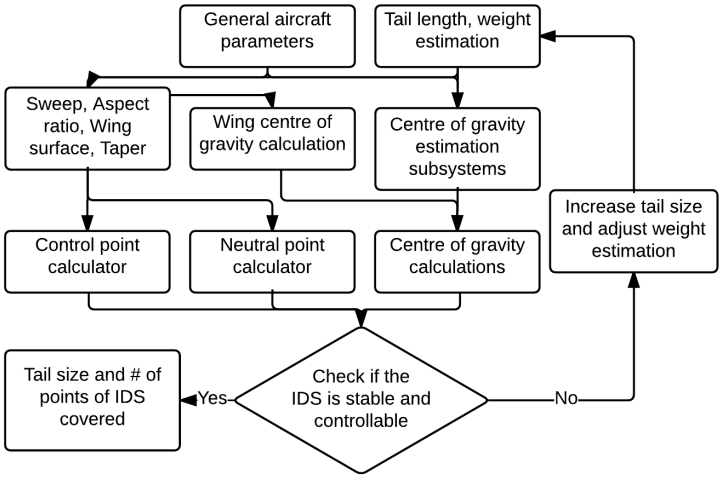

Figure 4.22: Numerical solution flow chart for stability analysis

performed.

4.4.2 Empennage design for static stability

The static stability of the MUAV can be divided into the longitudinal, lateral and directional stability. First the static longitudinal stability is assessed and second the lateral and directional stability.

Horizontal tail design for longitudinal static stability

The requirements for static longitudinal stability and controllability can be seen in subsection 3.3.2. In figure 4.21 an interpretation of these criteria is shown. A MATLAB program was created to calculate the location of the n.p., c.p. and c.g. to check whether or not the aircraft is stable and controllable for different wing parameters. The variable wing parameters are the sweep, taper, aspect ratio and surface area. It was decided that the complete IDS as seen in table 3.5 had to be fully static longitudinal stable and controllable. For this IDS the n.p. and c.p. where calculated using the equation 4.2 and 4.3 [2] where especially the tail length, aerodynamic centre and root chord change accordingly for different wing parameters.

$$x_{np} = x_{ac} + \frac{C_{N_{h_\alpha}}}{C_{N_\alpha}}\left(1 - \frac{d\varepsilon}{d\alpha}\right)\left(\frac{V_h}{V}\right)^2 \frac{S_h l_h}{S\bar{c}} \quad (4.2) \qquad x_{cp} = x_{ac} - \frac{C_{m_{ac}}}{C_{L_{A-h}}} + \frac{C_{L_h}}{C_{L_{A-h}}}\frac{S_h l_h}{S\bar{c}}\left(\frac{V_h}{V}\right)^2 \quad (4.3)$$

The numerical solution flow diagram of the MATLAB code can be seen in figure 4.22. The output is the horizontal tail size needed to have a longitudinally stable and controllable aircraft for the complete IDS. During the detailed design the weights of the subsystems had to be updated regularly and it had to be checked if the horizontal tail size was still able to cover the IDS. This optimisation resulted in a minimum tail surface of 1m^2.

Horizontal tail geometry

Now that the surface area is known the other horizontal tail parameters can be calculated. First the airfoil will be selected followed by the aspect ratio, taper, root and tip chord. Because of the different wing parameters the tail should generate both positive and negative lift and therefore a symmetric airfoil is chosen. Furthermore the tail should not stall before the main wing stalls and must be clean of the compressibility effect [16]. In order to do so the tail should be thinner than the main wing. The NACA 0016 airfoil meets these requirements and is therefore selected. According to the thin airfoil theory the 2D lift curve slope is estimated to be 2π [5]. Next the aspect ratio was determined. This is one of the most important parameters which is responsible for the change in lift coefficient from 2D to 3D. For an initial guess the aspect ratio is determined as $2/3$ of the aspect ratio of the default wing [16]. Taking the aspect ratio of the default wing configuration of 10 the horizontal surface aspect ratio will be set to 6.67.

The lifting line theory was used in order to find a taper which results in a maximum lift coefficient of the horizontal tail [5]. The wing is divided into N segments and the lift of each segment is calculated separately. The average of the segments will be the total lift coefficient. An optimisation was performed and a taper of 0.75 was found to be optimal. Lastly, the tip and root chord can be calculated by solving the equations in subsection 6.7.10 of [16]. Resulting in $C_{h_{tip}}$ of 0.33m, $C_{h_{root}}$ of 0.44m and a span of 2.58m. Trailing edge sweep is not desirable because the propeller is directly behind the empennage, therefore because of the taper the leading edge sweep will be 4.9°.

Horizontal tail design for lateral static stability

The MUAV will be symmetric in yz-axis. This means that for the static lateral stability the aircraft is neutrally stable.

Vertical tail design for directional static stability

Directional stability is required for, as the word suggest, maintaining direction without having to constantly adjust the rudder. A key parameter for this property is the vertical tail volume V_v in equation 4.4 (with higher values making the aircraft more stable) and according to Sadraey [16] a value of 0.04 yields desirable behaviour for the default configuration. It is important to notice that 0.04 is not a discrete transition to instability, it merely is a value that corresponds to commonly desirable properties. Hence values of V_v slightly lower than 0.04 do not mean the aircraft is unstable. The reader can observe that the modularity parameters influence the vertical tail volume.

$$V_v = \frac{S_v(S,A,\Lambda,\lambda,x_{cg}) \cdot l_v(S,A,\Lambda,\lambda,x_{cg})}{Sb(S,A)} \tag{4.4}$$

Figure 4.23 gives an overview of the relation between the fuselage length l_{fus}, tail size S_v and the percentage of the IDS for which $V_v > 0.04$. Trading between a longer fuselage and a larger tail surface, the maximum length of the fuselage is set on 4 m. Still longer fuselages will become more and more mass inefficient in increasing the IDS coverage percentage. The tail surface area is determined to be 0.63 m^2, a value that is rather high compared to reference aircraft. One will observe that this will yield an IDS coverage of 97%.

Figure 4.24 provides insight in the reasons why the team has settled with only 97% IDS coverage. The figure displays the occurrence of values of sweep, taper, surface and aspect ratio in the 3% outside the IDS. Each range of these parameter (see table 3.5) has been divided into ten values. These are displayed on the x-axis. It can be observed that mainly the wing area and (to a lesser extent) aspect ratio determine the vertical tail volume, since the parameters are equally distributed over the range. Therefore the verical tail volume van be assumed to be independent of the taper ratio and sweep angle, reducing the IDS to a two dimensional plane. This implies that the default wing configuration is in the outer large surface area, high aspect ratio plane of the design space.

Optimising for the default configuration more or less means covering the entire IDS (up to 97%). Only the upper 3% ultra high aspect ratio and surface area configurations will have vertical tail volume coëfficients lower than 0.04 for $S_v = 0.6$. The team supposes that this plane of the design space is not

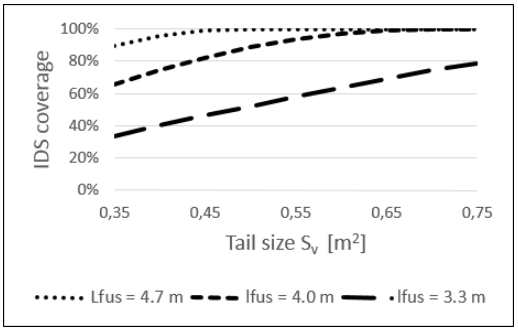

Figure 4.23: Percentage of IDS stable as function of the vertical tail surface.

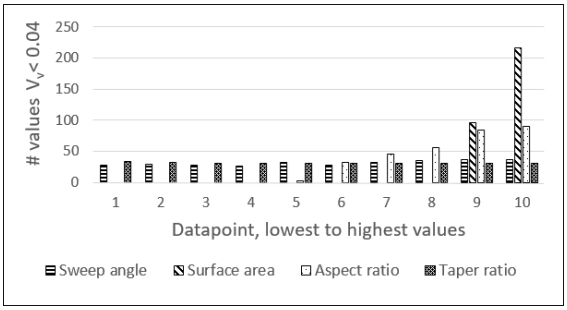

Figure 4.24: Wing planform parameter distribution of the 3% of the IDS for which V_v¡0.04 and $S_v = 0.6\text{m}^2$.

most vital to the merit of the MUAV and that the increasingly inefficient enlarging of the IDS coverage with greater tail surfaces does not weigh up to the gain beyond this point. As suggested by a TU Delft higher dimension expert, corners become increasingly sharp with higher dimensions hence making it more difficult to an entire cube. In this case it is likely that the 3% in fact is stable, only *less* stable than desired for optimum behaviour. Further research on the stability of this 3% is recommended.

Having set the vertical tail surface area, the planform needs to be determined. The propeller restricts the trailing edge sweep to zero. To maximise tail length l_v, the aspect ratio should be maximised while a taper ratio of 1 is ideal. Based on reference aircraft, an aspect ratio of 2 (same ratio as 4 for a horizontal wing) is used. Higher values will yield higher bending loads while the gain in tail length decreases. Also, a limited taper ratio of 0.75 is proposed for the sake of good looks to increase saleability (sweeping a vertical tail just for this reason actually is common practice for low-speed propellor aircraft). A thin airfoil is chosen to avoid compressibility [16] : NACA0010. Future studies to the vertical tail are recommended to include (inter alia) weight optimisations for the tail length and surface area trade-off, and detailed analyses of the planform and airfoil.

4.4.3 Empennage design for dynamic stability

In the conceptual design phase the main analysis of the IDS was performed using the static longitudinal stability and controllability. Now the dynamic longitudinal stability will be analysed for the IDS. A MATLAB program is made which can be used by the costumer to check if their particular wing is dynamically longitudinal stable.

The main contributor to the dynamic longitudinal stability is the moment coefficient with respect to pitching velocity, namely C_{m_q}[17]. In the requirements it is found that for most aircraft the value of C_{m_q} is between -5 and -40 1/rad [16] and therefore it is assumed that the configuration of the IDS is dynamically stable if C_{m_q} is between these values. C_{m_q} is estimated using equation 4.5 [17].

$$\mathrm{C_{m_q}} = -(1.1)C_{N_{h\alpha}} \left(\frac{V_h}{V}\right)^2 \frac{S_h l_h^2}{S\bar{c}^2} \tag{4.5}$$

Different tail surface areas were compared and can be seen in figure 4.25. It can be seen that a tail surface area of 1 m^2, as selected during the static stability analysis, results in 89% coverage of the IDS.

Longitudinal stability derivatives

Now there is known that 89% is dynamically stable a phugoid analysis can be made using a state-space model. In order to do so the following stability derivatives have to be calculated: C_{X_u}, C_{Z_u}, C_{m_u}, C_{X_α}, C_{Z_α}, C_{m_α}, C_{Z_0}, $C_{m_{\delta_e}}$, $C_{Z_{\delta_e}}$, K_Y^2 and μ_c. To calculate the derivatives the following assumptions were made:

1. The aircraft is in gliding flight [17].

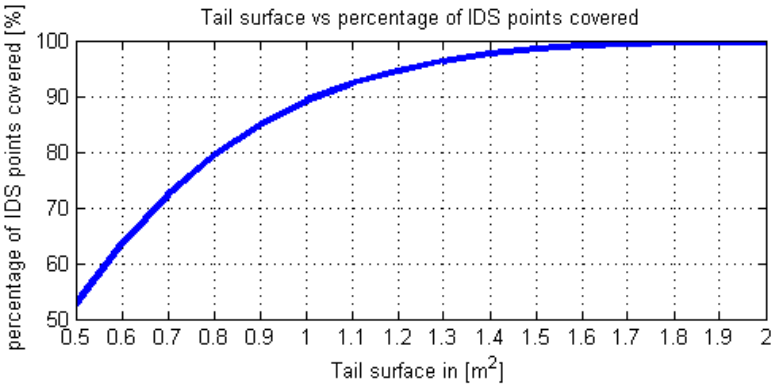

Figure 4.25: Tail surface versus percentage of IDS points covered

2. The considered angles of attack are small, so it is assumed that $C_{N_{h\alpha}} = C_{L_{h\alpha}}$ and $C_{N\alpha} = C_{L\alpha}$.

3. Velocity ratio $\frac{V_h}{V}$ is assumed to be equal to $\sqrt{0.85}$, since the tail is fuselage mounted. However, it is quite likely that the velocity ratio is not constant but in fact a function of wing planform parameters. Unfortunately, there are no accurate estimates available, hence the value of $\sqrt{0.85}$ proposed by SEAD [2] is used.

4. The initial condition is steady horizontal flight in cruise [17].

C_{X_u}, C_{Z_u}, C_{m_u} and C_{Z_0} can be calculated using equations 4.6, 4.7, 4.8 and 4.9.

$$C_{X_u} = -2C_D \quad (4.6) \qquad C_{Z_u} = -2C_L \quad (4.7) \qquad C_{m_u} = 0 \quad (4.8) \qquad C_{Z_0} = 0 \quad (4.9)$$

C_{X_α} and C_{Z_α} can be calculated using equations 4.10 and 4.11. C_{m_α} has already been calculated in section 4.4.2. The derivatives $C_{Z_{\delta_e}}$ and $C_{m_{\delta_e}}$ can be calculated using equations 4.12 and 4.13.

$$C_{X_\alpha} = C_L\left(1 - \frac{2C_{L\alpha}}{\pi A e}\right) \quad (4.10) \qquad C_{Z_\alpha} = -C_{L\alpha} \quad (4.11)$$

$$C_{Z_{\delta_e}} = -C_{N_{h_{\delta_e}}}\left(\frac{V_h}{V}\right)^2 \frac{S_h}{S} \quad (4.12) \qquad C_{m_{\delta_e}} = -C_{N_{h_{\delta_e}}}\left(\frac{V_h}{V}\right)^2 \frac{S_h l_h}{S\bar{c}} \quad (4.13)$$

μ_c and K_Y^2 are not derivatives but moments and products of inertia for symmetric motion. These can be caluclated using equation 4.14 and 4.15 although a more reliable estimation can be obtained experimentally.

$$\mu_c = \frac{m}{\rho S \bar{c}} \quad (4.14) \qquad K_Y^2 = \frac{I_{yy}}{m\bar{c}^2} \quad (4.15)$$

It has to be noted that the stability derivatives are calculated without the effects of the propeller, aeroelasticity and compressibility of air. The complete derivation of the stability derivatives can be found in chapter 7 of [17].

Phugoid symmetric motion

In order to calculate the symmetric aircraft motions as a response to a given disturbance the equations of motions are needed. The linear model for symmetric aircraft motions can be found in equation 4.16 [17].

$$\begin{bmatrix} (C_{X_u} - 2\mu_c)D_c & C_{X_a} & C_{Z_0} & C_{X_q} \\ C_{z_u} & C_{z_\alpha}(C_{Z_{\dot{\alpha}}} - 2\mu_c)D_c & -C_{X_0} & C_{Z_q} + 2\mu_c \\ 0 & 0 & -D_c & 1 \\ C_{m_u} & C_{m_\alpha} + C_{m_{\dot{\alpha}}}D_c & 0 & C_{m_q} - 2\mu_c K_{yy}{}^2 D_c \end{bmatrix} \cdot \begin{bmatrix} \hat{u} \\ \alpha \\ \theta \\ \frac{q\bar{c}}{V} \end{bmatrix} = \begin{bmatrix} -C_{X_\delta} \\ -C_{Z_\delta} \\ 0 \\ -C_{m_\delta} \end{bmatrix} \cdot \delta_e \quad (4.16)$$

All parameters in this equation are dimensionless. D_c is a differential operator and can be written as $D_c = \frac{\bar{c}}{V}\frac{d}{dt}$. $\hat{u}$ is the dimensionless airspeed, $\hat{u} = \frac{u}{V}$ with V as cruise speed of the aircraft. Instead of

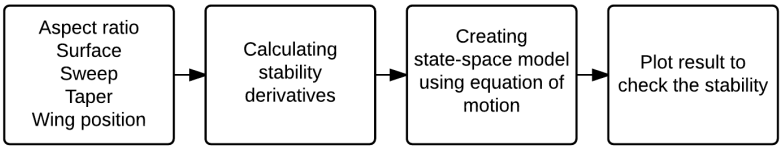

Figure 4.26: Flow diagram of the numerical model for analysing the longitudinal stability.

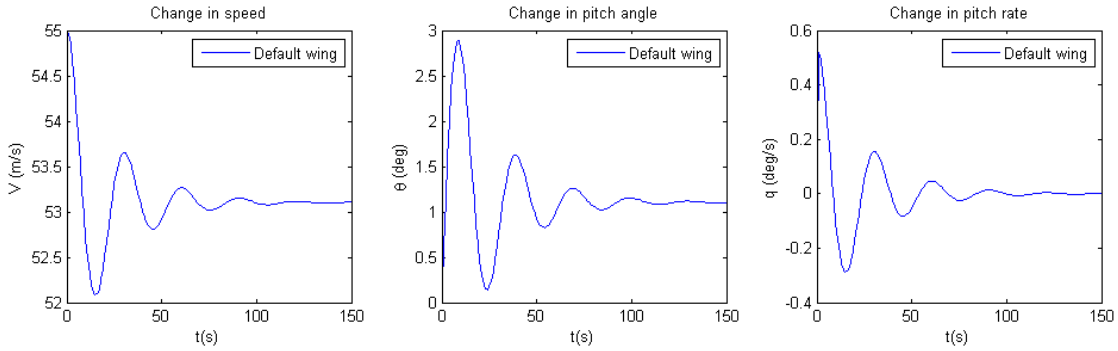

Figure 4.27: Phugoid response curves for a step elevator deflection ($\Delta\delta_e = -0.002$rad)

the relative airspeed $\hat{u}$, this equations can be rewritten using the absolute deviation u from the nominal airspeed. In this case $\frac{q\bar{c}}{V}$ will be the normal angular pitch rate q. For the phugoid and short period motions equation 4.16 can be reduced to equation 4.17 using the following assumptions:

1. $\dot{\alpha}$ and $\dot{q}$ are assumed to be 0.
2. The initial steady flight condition is assumed to be level. This implies that in the equation of motions, $C_{X_0} = 0$ and γ is constant.

$$\begin{bmatrix} C_{X_u} - 2\mu_c D_c & C_{X_\alpha} & C_{Z_0} & 0 \\ C_{z_u} & C_{z_\alpha} & 0 & 2\mu_c \\ 0 & 0 & -D_c & 1 \\ C_{m_u} & C_{m_\alpha} & 0 & C_{m_q} \end{bmatrix} \cdot \begin{bmatrix} \hat{u} \\ \alpha \\ \theta \\ \frac{q\bar{c}}{V} \end{bmatrix} = \bar{0} \tag{4.17}$$

Now a state-space model is created using MATLAB and the output of the system gives the dynamic stability results of the phugoid motion for different wing configurations. In figure 4.26 the flow diagram of the total program can be seen. Where the wing parameters are used as input and the resulting outputs are the stability plots.

For the default wing the dynamic stability was analysed using the program. As a step input the elevator was deflected -0.002rad. The results of this calculation can be seen in figure 4.27. It can be seen that the aircraft for this wing position is longitudinal dynamically stable. For further analysis the characteristics of this motion where calculated and the results can be seen in table 4.15. The eigenvalues where calculated using the eig.m script in matlab. From the eigenvalues the period (P), the time to half the amplitude ($T_{1/2}$), the undamped natural frequency (ω_0) and the damping ratio (ζ) can be calculated.

Table 4.15: Characteristics of the phugoid motion for the default wing

	λ_c	P	$T_{1/2}$	ω_0	ζ
Phugoid default wing	-0.0408 ± 0.2080i	30.2034s	16.9780s	0.2120rad/s	0.1925

The eigenvalues of this motion are complex and the real part is negative, this means that the aircraft behaves as a damped oscillator. This results in a damping ratio smaller than 1.

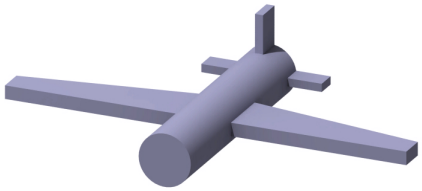

Figure 4.28: Simplified lay-out used for I_m calculations.

4.4.4 Empennage design for controllability

Controllability describes the extent to which the attitude of the aircraft can be manipulated using flight controls. The requirements on controllability can be found in table 4.16, each of the requirements has been tested for the least favourable design point in the IDS. In each of these cases the task of the control surface is to produce or counteract a moment with an aerodynamic force. One can observe that all requirements impose values on the angular acceleration. Mass moment of inertia I_m is calculated by integrating the square of distance r to mass m, figure 4.28 shows the simplifications made for calculating I_m. The reader should notice that the I_m is a function all modularity input parameters. The aerodynamic force L is described by a very familiar equation in which ρ is the air density, V the velocity, S the surface area and C_{L_i} the aerodynamic coëfficient.

Table 4.16: Empennage requirements

Parent	ID	Controllability Requirements	Type	Verification
M2RU-SYS-S01-12	T1	**Three-axis control of the vehicle shall be provided by the empennage**	Function	
	T1.1	The elevator must be powerful enough to rotate the aircraft about the main gear and lift the nose with an angular pitch acceleration $\ddot{\theta}$ of 15 deg/s^2. This requirement shall be satisfied when the aircraft has 80 percent of take-off speed $0.8 \cdot V_{TO}$.	Performance	Testing
	T1.2	During climb, cruise and descent the time to achieve a bank angle of 45 [deg] and zero angular velocity shall be at most 1.7 [s] following full deflection from the aileron.	Performance	Testing
	T1.3	During take- off and landing the time to achieve a bank angle of 30 [deg] zero angular velocity shall be at most 1.7 [s] following full deflection from the aileron.	Performance	Testing
	T1.4	A 90 degree cross-component of wind velocity, demonstrated to be safe for taxiing, takeoff, and landing must be established and must be not less than $0.2 \cdot V_{SO}$.	Performance	Testing
	T1.5	The aircraft must be able to recover from a one-turn spin on no less than 3 seconds.	Performance	Testing

Elevator design for pitch control

Requirement T1.1 governs the design of the elevator. The UAV has a full movable tail, so the elevator is equal to the horizontal stabiliser. To solve the equations for horizontal stabiliser size S_h, the mass moment of inertia around the main landing gear I_{mg} should be determined. Furthermore, to make sure the requirement is met in any configuration, we assume that the aircraft is in the 'worst' configuration for this requirement. The following assumptions have been made:

1. A symmetrical wing is installed so $L_{(\alpha=0)} = 0$.
2. The weight is equal to MTOW.
3. The centre of gravity lies furthest forward with respect to the main landing gear.
4. Drag acts through the centre of gravity.

Equating the moments generated by the weight and the elevator deflection to the required angular acceleration yields an equation that can be solved for horizontal elevator size S_h. The result is a required horizontal tail size of 0.72m^2

Aileron design for roll control

Since the UAV should be fully controllable using the empennage only, the ailerons are in fact the same control surfaces as the elevators. A moment is introduced in the structure by opposite deflections of the ailerons, the arms associated with the forces are the y-coordinates of the aerodynamic centres of each aileron. Therefore taper ratio λ_h influences the moment heavily. The moment of inertia around the x-axis I_{mxx} resists movement and is in this analysis the only parameter dependent on the four wing planform parameters. The following assumptions are made:

1. Changes in apparent angles of attack of the wings due to rotational velocity p are negligible.
2. Angular accelerations are constant.
3. The wing has a maximum taper ratio, wingspan, surface area and aspect ratio.

The required angular acceleration for T1.2 and T1.3 can be calculated from the required bank angle. Both requirements prove to be non-critical with maximum required surface areas S_h of respectively 0.17m^2 and 0.28m^2. In fact, the values are low enough to not even impose requirements on taper ratio λ_h.

Rudder design for yaw control

The last control surface that should be designed is the rudder, providing yaw control. Requirements T1.4 and T1.5 are both evaluated after which the rudder will be sized for the most critical one. The following assumptions are made [16]:

1. The aerodynamic force the cross wind exerts on the aircraft can be decomposed into a component acting through the aerodynamic centre of the rudder and a component acting through the centre of gravity of the aircraft.
2. The angle of attack during spin is 40 degrees.
3. The typical maximum rotational speed of an uncontrolled spin is between 120 and 240 deg/s. Stopping in three seconds therefore implies a maximum angular acceleration of -80 deg/s^2.
4. The aerodynamic efficiency parameter η is assumed to be equal to 0.97 [18].

Since the spin is not a symmetrical motion, equation 4.18 calculates required moment N_{SR}. Applying this equation to each configuration in the IDS will allow the most critical configuration to be found. Deflection curve $C_{n_{\delta r}}$ quantifies the change of the rudder lift coefficient with the rudder deflection and is dependent on the vertical tail lift slope $C_{L_{\alpha_V}}$, vertical tail volume V_V, aerodynamic efficiency η, control surface to lifting surface ratio τ_R, rudder chord b_R and vertical tail chord b_v. It is clear that the ratio of the last two should be maximised.

$$N_{SR} = \left(\frac{I_{mxx} I_{mzz} - I_{mxz}^2}{I_{mxx}} \right) \ddot{\Theta} \qquad (4.18)$$

$$C_{n_{\delta r}} = -C_{L_{\alpha_V}} V_V \eta \tau_R \frac{b_R}{b_V} \qquad (4.19)$$

The approach is as follows: the rudder area will be set at $0.25 S_v$ after which the required rudder deflection for meeting the requirements will be calculated. A typical maximum allowable deflection is 30 degrees. Evaluating T1.4 yields a required deflection of 34 degrees; the requirement is not met. Also, the moment introduced by the crosswind of T1.5 is less than the moment to recover from spin, therefore T1.4 is most critical. Deciding to meet T1.4 at 25 degrees deflection (thus leaving 5 degrees margin) produces a required rudder size of 0.34 S_v when the rudder/vertical tail span ratio is set to 1.

Table 4.17: Damping ratio of different wing positions compared to the middle position of the wing

	ζ	*%change*
Wing most front position	0.1978	−2.75
Wing middle position	0.1925	0
Wing most aft position	0.1885	2.08

[t]

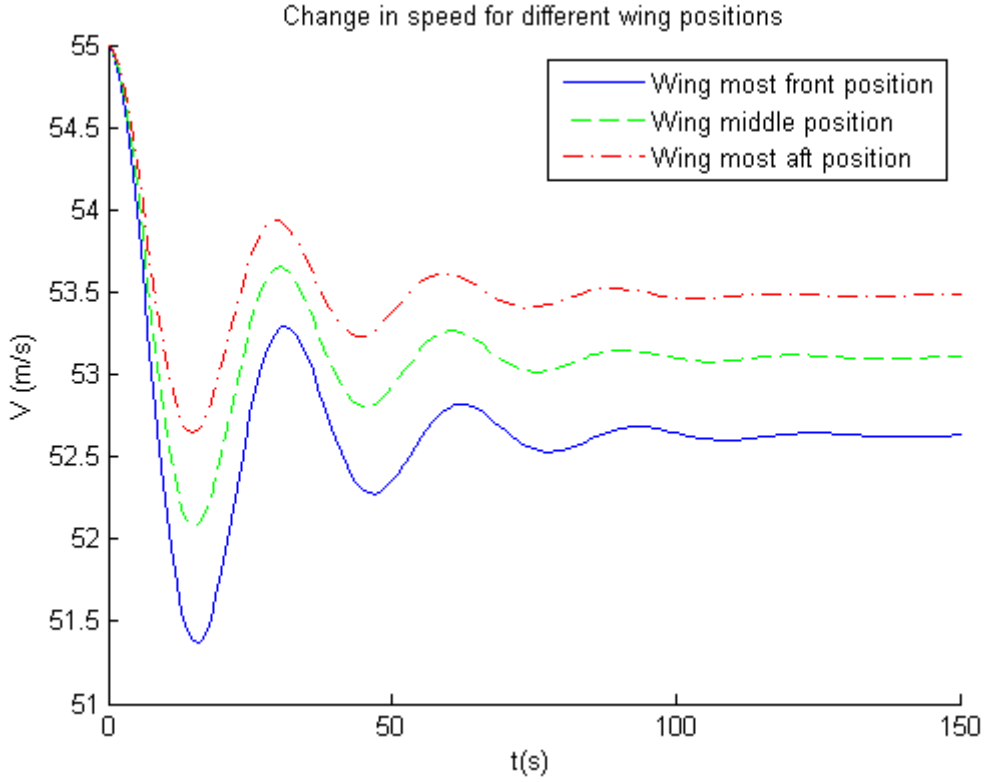

Figure 4.29: Sensitivity analysis of the empannage by checking different wing positions

It should be remarked that it is questionable whether spin recovery is relevant at all, given the current maximum altitude of 100 m. It is rather likely that there is not enough time to recover, forcing the operator or autopilot to deploy the parachute in stead of trying to recapture control. However, it is not ruled out that the MUAV will be certified to fly at higher altitudes in the future, making spin recovery possible.

4.4.5 Empennage design verification and validation

The empennage is designed using multiple numerical models. Which have been divided into scripts and functions. Both were checked and verified individually by hand the same way as the wing design. After this the complete model was compared and calculated by hand and found to be correct. One part of the verification is also the sensitivity analysis. For the empennage it was checked what the effect is of the different wing positions of the default wing. Only the change in speed was checked and can be seen in figure 4.29. It can be seen that a shorter tail length results in a more damped motion. In table 4.17 it can be seen that the change in the damping ratio between the middle wing position and front and aft position is approximately the same. This means that the program is stable for a change of the wing position.

In order to validate the models test flights have to be performed. First a prototype of the default wing has to be checked and verified. Next two other wings have to be tested, this way the model with

variable wing parameters can be validated. To validate the stability derivatives in order to asses the dynamic stability wind tunnel experiments have to be performed. One can also use a CFD analysis for the derivatives which can be cheaper than test flights. To validate the control surfaces test flights with multiple critical wing configurations can be used where the aircraft has to perform certain manoeuvres which validates the control requirements. The validation of the control surfaces can as well be performed using CFD. When all these requirements are met the full empennage is validated.

4.4.6 Empennage design summary and recommendations

Table 4.18 provides an overview of the values of surface area S, leading edge sweep angle Λ_{LE}, aspect ratio A, taper ratio λ, root chord c_r, dihedral angle Γ, wing span b, root chord leading edge position x_{LE} and maximum load F_{max} for both the horizontal and vertical tail. These values will be used as input for further studies, in particular the structural design of the airframe and the sizing of the actuators.

Table 4.18: Overview of the design parameters and the maximum loads on the stabilisers.

	S	Λ_{LE}	A	λ	c_r	Γ	b	x_{LE}	F_{max}
Horizontal tail	1.00 m	4.9 deg	6.67	0.75	0.44 m	0 deg	2.58 m	3.54 m	193 N
Vertical tail	0.63 m	8.1 deg	2.00	0.75	0.55 m	NA	1.10 m	3.45 m	38 N

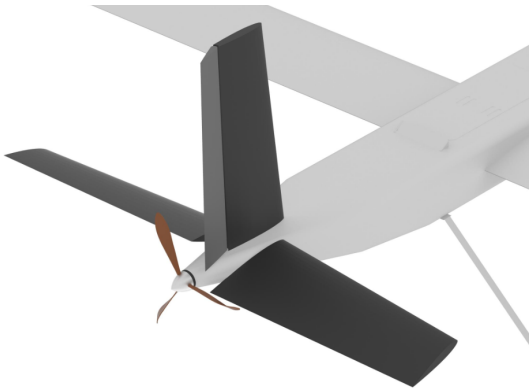

Figure 4.30: Final layout of the empennage.

In figure 4.30 the final layout can be seen. In this figure one can see the full moving horizontal tail and the size of the rudder. For future more elaborate empennage design the following recommendations can be taken into account:

- In the stability analysis the airfoil of the wings is assumed to be the same NACA profile for all parameters. This can be changed by the customer and results in a different C_L. For future studies this can be taken into account and can result in an increase of the IDS.
- As seen in this section only the longitudinal dynamic behaviour is analysed because the stability derivatives of the asymmetric motion are not very reliable [17] when calculated mathematically and therefore wind tunnel experiments have to be performed to obtain the stability derivatives.
- During the conceptual design it was decided to have a fixed empennage, however if a modular empennage is introduced the IDS can be further increased. Especially if there is also a variable tail length.
- For a more complete analysis, wing dihedral and twist can be added. These will especially have an effect on the dynamic stability.

- In this design the wing is seen as a constant shape, however it can be incorporated into the numerical solution to have a wing that consists of multiple partitions where each partition can have a different shape. Especially for the box wing analysis this is very useful.
- It is recommended to research the stability of the 3% of the IDS with $V_V < 0.04$.
- A mass optimisation of the trade-off between tail length en surface area will result in a lighter design.
- More elaborate studies to the planform and airfoil of the vertical rudder will yield higher weight efficiency.

As can be seen the empennage design is influenced to a large extent by the modularity. The scope of this project limited the ability to analyse all variable parameters. The effect of including all recommendations might increase or limited the IDS. This is left for future studies.

4.5 Propulsion and power system design

The main requirements of the propulsion and power system are providing at least 11 kW of propulsive power and an additional 1.2 kW of electrical power. As discussed in section 3.2.4 a combustion engine will be used for propulsion. Which engine is used and what the other components of the propulsion system are is discussed in section 4.5.1. The electrical power generation will be discussed in section 4.5.2.

4.5.1 Propulsion system

To get initial engine dimensions, a suitable engine was already selected in the conceptual design phase. In this phase, the selected engine would provide the required power. The best power to weight ratio can be achieved by using a two stroke engine [19]. This kind of engines is used often in UAVs and model aircraft, therefore quite a lot of them are available off-the-shelf. The engine that was selected is named 3W-170 XiB2 TS CS[6]. The specifications of this engine can be seen in table 4.19. It can be seen that the selected engine is slightly more powerful than required. However, it is not bigger or heavier than an 11 kW engine.

Table 4.19: Specifications of the 3W-170 XiB2 TS CS

Specification	Value
Power	14.48 kW
Speed range	1100-8500 rpm
Weight	4.1 kg
Length x width x height	225 x 302 x 233 mm
Frontal area	360 cm^2
Price	1,851.00 euro

The manufacturer recommends a couple of propeller sizes to use with this engine. Since the propeller is mounted on the back of the aircraft, it has a large influence on the landing gear size. Therefore the propeller with the smallest diameter (3-bladed 28 inch) is chosen here. This propeller size will thus limit the size of new propellers that the customer might want to test.

For the stability of the MUAV it is favourable to position the engine as much to the front as possible. Therefore the engine is located right behind the centre wing box. Since the propeller should be behind the empennage, a rather long shaft of about 1.5 m is needed. To make sure the propeller will not move

[6] 3W-170 XiB2 TS CS - Product page, `http://www.3w-modellmotoren.com/katalog/motoren-alle-motoren-84/3w-170-xib2-ts-cs.html`, Accessed: 2015-12-01

around to much and the shaft does not buckle, the shaft will pass through a thrust bearing right before it leaves the fuselage.

A bladder tank will be used to store the fuel. To supply the fuel to the engine a technique often found in model aircraft is used: the pressure is fed into the air bubble in the top of the tank forcing the fuel to flow through the fuel line to the engine.

The engine is air-cooled. To make sure sufficient air flows over it, an air inlet is placed on the top of the fuselage, directly behind the centre wing box. The exit is placed close to the back of the fuselage. Therefore, the low pressure in front of the propeller enhances the airflow through the cooling duct.

4.5.2 Electrical power generation

Since the propulsion system works with a combustion engine, the electrical power for the avionics and payload should be generated separately. This can be achieved by converting the kinetic energy of the engine into electric energy, taking separate batteries or using the energy from the engine's exhaust.

The last option can be executed in two ways: guiding the exhaust flow through a turbine which is attached to a generator[7] or by using a thermoelectric generator[8]. Both technologies have a positive effect on the overall efficiency of the power generation system. However, they are both still in an experimental phase and not commercially available. Therefore this option is not yet suitable for this project.

The kinetic energy of the engine can be converted by mounting an alternator on the shaft, this works in the same way a dynamo does on a bicycle. This electricity flows to a Power Distribution Unit (PDU) that converts it to the voltage range(s) needed. Since the power generated depends on the number of revolutions the engine makes, an energy buffer is required to make sure that enough power is available. On top of that, the aircraft should stay controllable when the engine stops working. Therefore a battery is needed to feed the actuators and control system.

From a designers point of view, the most straightforward solution is using batteries. However, this imposes problems for the user. Between flights the batteries should be replaced/charged next to the refuelling. On top of that, the fuel tank offers the possibility to bring more fuel for longer endurance, in that case more batteries should be brought as well. Therefore the alternator option is considered to be the more user-friendly option. Finally, the alternator option is lighter, but more expensive. However, the user-friendliness is considered to be more important in this case. Therefore, the alternator is selected to provide the electrical energy to the subsystems.

As mentioned earlier, it is preferred to use off-the-shelf components. However, correspondence with the manufacturer Sullivan UV[9] showed that these systems are always modified or custom designed. Therefore the weight and cost of the alternator and PDU were estimated based on data provided by Sullivan UV. This data, together with all the other propulsion and power system components, can be seen in table 4.20. In this table the function, component name, their weight and cost is shown. The weight is 1.2 kg more than the initial estimate.

4.5.3 Propulsion and power design verification and validation

For the propulsion and power systems, off-the-shelf components were used as much as possible. For these components the main parameters are published by the manufacturer. However, this could not be done for all components. The fuel system and PDU are almost always custom made. To estimate their weight and cost, the characteristics of multiple models of one big manufacturer were interpolated to find the characteristics at the required design point.

[7] Porsche 919-Racecar Engineering, `http://www.racecar-engineering.com/cars/porsche-919/`, Accessed: 15-12-2015

[8] A design to generate UAV electrical power in-flight, `http://www.eetimes.com/document.asp?doc_id=1279690`, Accessed: 15-12-2015

[9] Sullivan Unmanned Vehicle product overview, `http://www.sullivanuv.com/products/`, Accessed: 7-1-2016

Table 4.20: Overview of propulsion and power system components

Fuction	Component name	Weight (kg)	Cost (€)
Engine	3W 170XiB2 CS TS	4.16	1954
Propeller	Xoar PJI 38x12 + spinner	0.496	130
Shaft	Incl. SKF 51106 bearing	0.416	10
Fuel system	Based on ATL bladder	0.5	200
Alternator	Sullivan S676-400U-01	0.67	1437
PDU	Based on Sullivan products	1.5	3200
Back-up battery	Zippy 7S 4000 mAh	0.705	48
Total		8.5	6979

4.6 Electrical system design

In this section the design of the electric subsystem is discussed. The electrical system manages the data handling, on board control, actuation and communication of the MUAV. This section will start off with a short functional analysis of the electrical system in subsection 4.6.1 after which suitable off-the-shelf components will be selected in subsection 4.6.2. The electrical system data handling and communication will then be shown in a diagram and will be discussed in subsection 4.6.3. The section concludes with a short analysis on the mass, cost, and power in subsection 4.6.4.

4.6.1 Electrical system functional analysis

The electrical system functions stem from the subsystem requirements shown in table 4.21, these are treated more elaborately in the requirement specification [1]. A choice of component functions can be set up from these requirements, which will later be used to determine specific electrical components. In short; the electrical system has to measure certain flight parameters, communicate with a ground station, and control the MUAV. Table 4.22 shows the component categories resulting from the subsystem requirements. The component numbering shown in the table will be used in the next subsection to verify whether the component selection fulfils the functional needs of the subsystem.

Table 4.21: Electrical subsystem functional requirements

ID	Functional requirement
E1	The electrical subsystem shall not exceed its mass and cost budgets
SYS-S01-12 E2	It shall be possible to measure data corresponding to the aircraft motion
SYS-S01-17 E3	It shall be possible to measure structural data of the wing
SYS-S01-09 E4	It shall be possible to acquire the aircraft trim data
SYS-S01-09 E5	It shall be possible to retrieve the aircraft flight data
SYS-S01-09 E6	The flight data shall be sent to the flight computer
SYS-S01-09 E7	The aircraft shall be able to communicate data with a ground station
SYS-S01-09 E8	The control system shall be able to process inputs
SYS-S01-09 E9	The control system shall control the aircraft motions
SYS-S01-09 E10	The control system shall be able to operate on auto pilot
SYS-S01-09 E11	It shall be possible to operate the control system manually

4.6.2 Electrical subsystem component selection

The component selection has been optimised to be compatible with the whole subsystem and to comply with the requirements. All the component function needs stated in table 4.22 have to be satisfied for the desired electrical system. Table 4.23 shows the electrical component selection along with the functions

Table 4.22: General electrical component functions needed for the electrical system

Number	Component function needed	Number	Component function needed
1	Acceleration measurement units	8	Data storage unit
2	Rotational measurement units	9	Data retrieval port
3	Airspeed measurement unit	10	Programmable flight computer
4	Altitude measurement unit	11	Data processor
5	Strain measurement unit	12	Receiving antenna
6	Shape measurement unit	13	Transmitting antenna
7	Deflection measurement unit	14	Actuators

that are fulfilled by each component. The table shows that all the functional needs are satisfied with this component selection. More information on the components can be found in the footnotes. [10] [11] [12] [13] [14] [15] [16] [17]

Table 4.23: Component selection along with the function numbers that are fulfilled by each component

Component name	Brief description	Functions
Arduino Mega	Microcontroller with open source flight controller software	10,11
Arduino Yun	Small microcontroller with several universal connector ports	8,9
Arduino micro	Small microcontroller useful for small scale calcultions	11
Arduino 101	Small microcontroller with an Inertial Measurement Unit (IMU) included	1,2,11
Pixhawk Airspeed Sensor	Digital airspeed meter recommended for Arduino	3,4
HBM - RY9x strain gauge	Strain gauges for analysing biaxial strain with unknown principal strain directions	5,6
SparkFun Venus GPS	GPS receiver for autopilot functioning recommended for Arduino	10
Duplex R11 EPC EX	On board full duplex receiver	12,13
DC-16	Ground station transmitter and control system	12,13
SanDisk Micro SDHC 32 GB	Sufficient storage capacity for flight data	8,9
Hitec HSR-5990TG	Titanium Gear Robot Servo for landing gear brakes and vertical stabiliser	7,14
Seiko ssps-105	High torque servo for horizontal stabilisers	7,14

The next subsection will show a data and communication flow diagram indicating the specific role of each electrical component as well as the data that is being communicated between components.

[10] Arduino components `https://www.arduino.cc/` Accessed on 5-1-2016

[11] Ardupilot open source flight control script `http://dev.ardupilot.com/wiki/license-gplv3/` Accessed on 6-1-2016

[12] Pixhawk airspeed sensor `https://store.3drobotics.com/products/pixhawk-airspeed-sensor-kit` Accessed on 7-1-2016

[13] Strain gauges `http://www.nvms.com.au/wp-content/uploads/2014/07/Y-Series-Product-Catalogue.pdf` Accessed on 6-1-2016

[14] Communication system `http://www.jetimodel.com/en/katalog/Transmitters/@produkt/DC-16/` and `http://www.jetimodel.com/en/katalog/Duplex-2-4-EX/Receivers-EX/@produkt/Duplex-R11-EPC-EX/` Accessed on 6-1-2016

[15] Data storage `http://www.dataio.nl/sandisk-32gb-sdhc-ultra-class-10-30mbs/` Accessed on 7-1-2016

[16] Rudder and brake servos `http://www.servodatabase.com/servo/hitec/hsr-5990tg` Accessed on 7-1-2016

[17] Elevon servos `http://www.tonegawaseiko.co.jp/pro/e_pro02.html` Accessed on 12-1-2016

4.6.3 Data and communication handling

There is a lot of data transfer and communication going on inside the electrical system. A data handling and communication flow diagram was made to give an idea of how the data will be processed and communicated. This diagram is shown in figure 4.31 with indications on what roles are performed by which components. A distinction was made between sensors, actuators, data processors, flight computer, and communication equipment.

4.6.4 Electrical system budgets

With the selection of the electrical components the mass, power, and cost budget were monitored. These parameters have been documented in table 4.24. Some of the crucial components have redundancy to account for component failure. With all the components and their electrical requirements known, an electrical block diagram was made and is shown in figure 4.32. This diagram gives an overview of how the power is distributed.
The PDU output voltages are chosen to be 5, 7.4 and 24 V. 5 V is the operating voltage of the Arduinos. A voltage range of 6-7.4 V is often required for off-the-shelf actuators and can be used by the rudder and landing gear actuators. Finally, 24 V is chosen since the actuators for the horizontal tail need it, besides that this is voltage which is very common in electronics and therefore useful for the payload bay. To accommodate modules, 7.4 and 24 V connections are available at the wings. On top of that, all voltages are available in the payload bay.

Table 4.24: Mass, cost, power, and input voltage for the electrical components

Component	Amount (redundant)	Mass [kg]	Cost [€]	Power [W]	Voltage [V]
Arduino Mega	2 (1)	0.070	70.00	15	6-20
Arduino Micro	5 (1 for airspeed)	0.065	90.00	12	5
Arduino Yun	2 (1)	0.064	104.00	6	5
Arduino 101	3 (1 for backup data)	0.15	87.00	4	5
Pixhawk airspeed sensor	2(1)	0.10	100.00	0.02	5
SparkFun Venus GPS	2 (1)	0.05	94.60	0.13	5
RY9x	8	0.01	332.00	0.3	2
R11 EPC EX/DC-16	2/1 (1 redundant receiver)	0.015	1,300.00	0.3	3.2-8.4
Hitec HSR-5990TG	3	0.204	345.00	115.44	6.0-7.4
Seiko ssps-105	2	1.56	800.00	216	24
SanDisk Micro 32 GB	2 (1)	0.02	26	≈0	-
Electrical wiring		2	180.00	≈0	-
Total	-	4.308	3,361.00	364.06	-

4.6.5 Electrical system design verification and validation

The electrical system consists of off-the-shelf components which have been verified thoroughly. Each component's functionality and performance was researched to ensure that the requirements were met. Initial wiring diagrams have been set up which were used to verify component interactions and validate the subsystem interaction overall. These diagrams can be used in later design phases to verify the wiring of the electrical system. Lastly the cost, weight, and power consumption were inventoried to check if they fell within the budget. The electrical subsystem performs all the required functions reliably exceeding the minimum performance expectations. More information on the required performance can be obtained from the requirement specification [1]. With these procedures the electrical subsystem has been sufficiently verified for this design phase. These activities should continue and get more elaborate further in the design phase. Validation can be performed with on-ground tests as well as with physical model tests. This can be done by connecting the electrical system components to a simulation set up with simulated sensors and actuators with which the mission environment of the MUAV can be simulated.

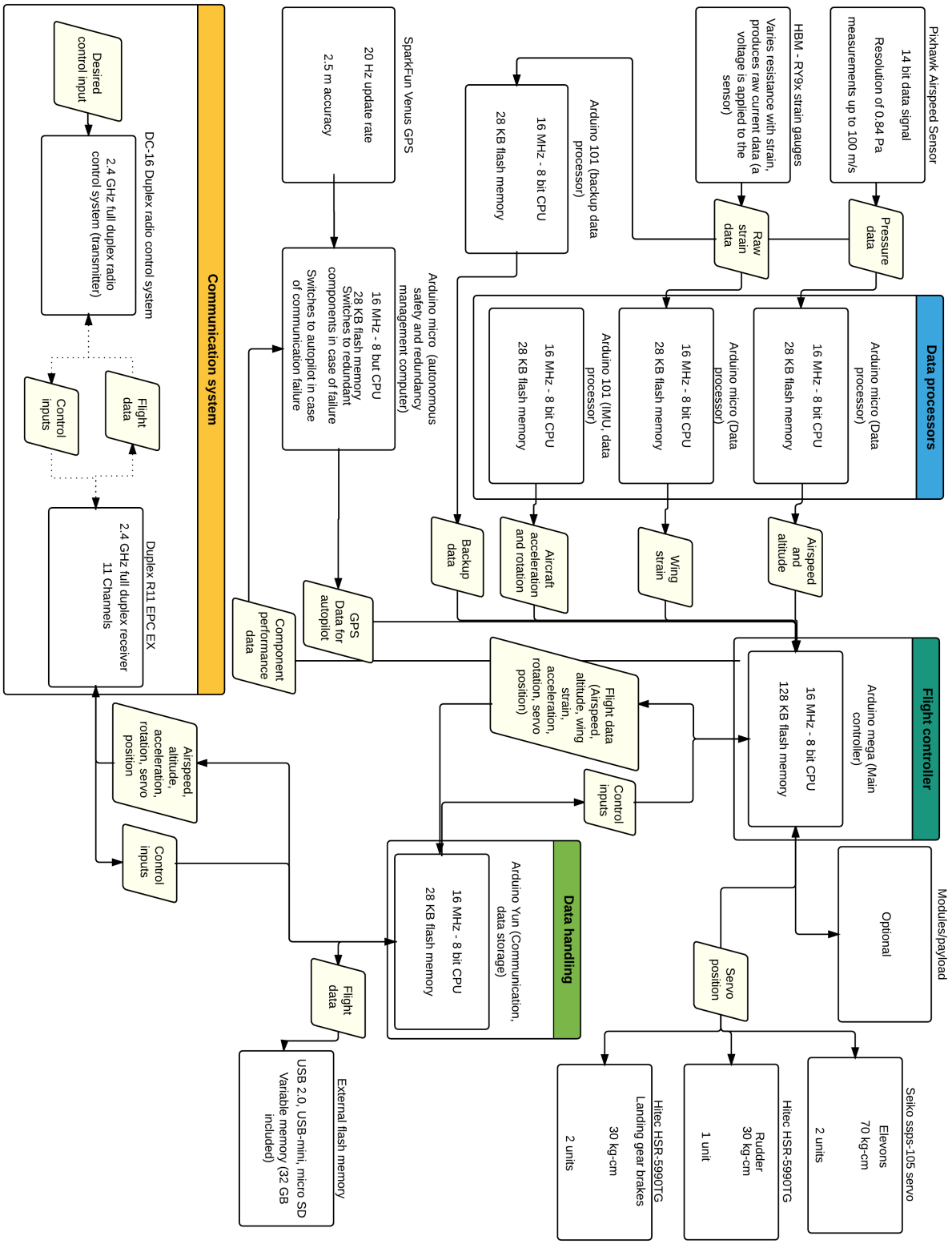

Figure 4.31: Data handling and communication flow diagram

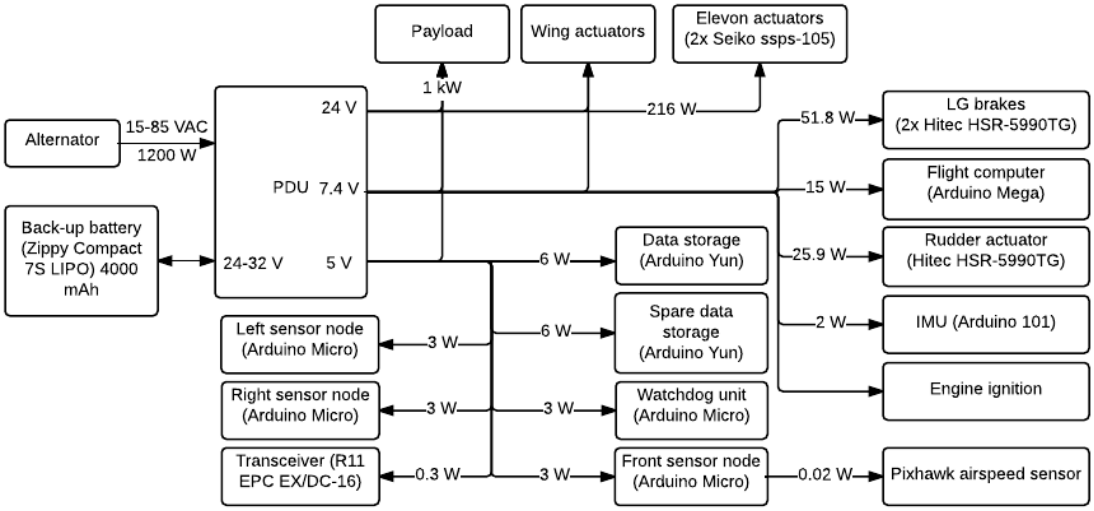

Figure 4.32: Electrical block diagram

4.6.6 Recommendations for further electrical system design

At this point of the design process the electrical system design is still not finished. This will be addressed to give a starting point for further subsystem design in the list below:

- The components have been selected, but details on where they should be placed, how they should be attached, and how they should be wired is still missing. This can be laid out in detail in the next design phase.
- A flight control scheme has been selected but it has not been optimised for the MUAV nor has it been verified. All the computers need to be properly programmed and verified further in the subsystem design.
- Finally the interaction between the electrical subsystem and other subsystems has not been analysed thoroughly yet, which should also be done in detail.

4.7 Landing gear design

In this section the design of the landing gear subsystem is discussed. In the first subsection the definition of the landing gear subsystems is given and the functions that the landing gear has to fulfil are defined. This is followed by the landing gear type trade-off and the sizing in subsection 4.7.2. In the third subsection the landing gear layout is discussed and in the fourth subsection the verification and validation methods are given. Finally in the last subsection recommendations for future landing gear design is discussed.

4.7.1 Subsystem definition and functions

The landing gear is the subsystem which take care of the landing and take-off phases of the MUAV mission. Without this subsystem the MUAV is not able to take-off and land on its own. The landing gear consists of struts, tires, shock absorbers, wheel brakes, electrical cables and data wires for the control system. It is the part of the MUAV that is attached to the bottom of the fuselage. The functions of this subsystem are:

- To provide lateral and longitudinal stability on the ground;

- To provide ground control on (wet) grass land;
- To absorb (kinetic) energy on the ground;
- To carry static and dynamic loads during landing, take-off and taxi;
- To provide ground clearance.

To check whether or not the landing gear is able to fulfil all these functions, requirements are made. These requirements together with the constraints on the landing gear subsystem are defined in the Requirement Specification [1].

4.7.2 Landing gear type and sizing

For the selection of landing gear types, two important decisions have to be made: [20]

1. Fixed (non-retractable) or retractable landing gear
2. Use of a tricycle, bicycle, tailwheel or unconventional gear

To make the first decision the pros and cons of the fixed and retractable landing gears are given in table 4.25. According to Roskam [20], aircraft with a cruise speed less than 278 km/h will be able to afford the aerodynamic drag penalty caused by non-retractable landing gears. Therefore non-retractable landing gears are selected because of lower weight, complexity and cost. After the first drag calculations this assumption will be checked and based on the performance of the overall aircraft the landing gear might have to be re-designed with retractable landing gear, if that is within the cost and weight budget.

Table 4.25: Pros and cons of fixed versus retractable landing gears [20]

	Fixed	Retractable
Aerodynamic drag	High	Minimal
Weight	Low	High
Complexity and cost	Low	High
Maintenance cost	Insignificant	Significant

The second decision is more obvious, as the use of a propeller at the rear makes the tailwheel configuration inconvenient. The bicycle is less stable than the tricycle. There is also no need to use unconventional landing gear types. Therefore a non-retractable tricycle landing gear type will be designed for the MUAV to save time and money.

After deciding the type of main landing gear the size has to be determined for the following components: the struts, the shock absorbers and the tires. The size of the tires is determined by the weight of the aircraft. The main tires typically carry about 90% of this weight. Nose tires carry the rest of the static load but experience higher dynamic loads. For the tricycle arrangement for the main landing gear and nose landing gear a single tire per strut will be used. For taking-off from unpaved runway the diameter of the tires and width should be increased about 30%. The maximum static load on the main landing gear includes an additional 25% to the loads to allow for growth of the aircraft design. [3]

The size of the shock absorbers is determined by the type and the load factor. There are four different shock absorption systems which can be used on the MUAV: spring system, flexible elements, steel disc spring or oleo-pneumatic. For the nose landing gear the Oleo-pneumatic shock absorber is the most efficient but costs more and weighs more than the other options. Less efficient shock absorbers will result in more stroke length and thus a longer total strut length. A longer strut length will generate more drag in flight which is undesirable. For the main landing gear struts flexible elements are the obvious choice for light weight aircraft. The flexible elements weighs less and are easier to design than the other absorption systems. As a flexible element shock absorber a cantilever spring leaf system is chosen for the main landing gear. However after one or more design iterations, a different shock absorber may be chosen if

that is more desirable. In table 4.26 these decisions are recorded as input parameters for the landing gear design.

The size of the struts is determined by the location of the landing gear and the layout of the vehicle. The vehicle should have enough ground clearance as to not damage the structure, it should not tip-over or turn-over. In table 4.26 these parameters serve as guidelines for the design.

Furthermore a braking system is chosen to control the speed of the MUAV on the ground. The braking system is a disc braking system which consists of a servo, spring and braking pad. The disc brakes are attached to the two main landing gear wheels.

Table 4.26: Input parameters for design of the landing gear

Decision			Guidelines		
Parameter description	Value	Unit	Parameter description	Value	Unit
Ground clearance	0.15	m	Min tipover angle	15	deg
Landing gear struts	2	-	Max tipover angle	25	deg
Landing gear load factor (ultimate)	7.5	-	Max turnover angle	63	deg
Safety factor	1.5	-	Allowable landing gear load for single strut (unprepared surfaces)	5	kN
Flight Performance			**Lay-out**		
Parameter description	Value	Unit	Parameter description	Value	Unit
Take-off speed	24	m/s	X-position c.g. Most aft	2.45	m
Landing speed	20	m/s	Y-position c.g. Most aft	0	m
Max Take-off angle	17	deg	Z-position c.g. Most aft	0	m
Sink speed	5	m/s	X-position propeller	4	m
Braking efficiency	0.25	g	Y-position propeller	0	m
			Z-position propeller	0.105	m
			Propeller diameter	0.71	m
			Fuselage width	0.53	m
			Fuselage height	0.31	m
			Fuselage length	4	m
Material characteristics			**Constraints**		
Parameter description	Value	Unit	Parameter description	Value	Unit
Al 7075-T6 density	2800	kg/m^3	Maximum take-off weight	880	N
Al 7075-T6 Young's modulus	72	GPa	Maximum mass	4.5	kg
Al 7075-T6 tensile yield strength	580	GPa	Maximum cost	5000	€
Al 7075-T6 fatigue yield strength	130	GPa	Maximum power	100	W

4.7.3 Landing gear lay-out

The landing gear lay-out is determined by calculations of the static and dynamic loads on the nose and main landing gear (section 11.3 in Raymer [3]) as well as the landing gear load factor, the ground clearance, the tip-over and turn-over angle criteria (setion 11.2 in Raymer [3]), flight performance parameters, c.g. location, propeller location, propeller diameter, material characteristics and design constrains. In table 4.26 all the input parameters to these calculations are given. Furthermore the bending stresses (section 16.1 in Megson [13]) and buckling (section 8.1 in Megson [13]) have been checked against the fatigue stress of Al 7075-T6 . The calculations have been done in MATLAB and the MATLAB script is validated by hand calculations. To reduce the aerodynamic drag introduced by the wheels carbon fibre wheel covers with a more aerodynamic shape are used. The landing gear parameters are given in table 4.27 and can be seen in the figures of section 6.1.

In table 4.27 cost, mass and power estimations are given. The cost estimation is based on the material costs of Al 7075-T6, tires, carbon fibre wheel covers, wheels and off-the-shelf brake costs and the oleo-

pneumatic shock absorber on the nose. The oleo-pneumatic shock absorber and the wheels have to be custom designed, there are no ready made off-the-shelf alternatives. The total estimated cost of 2000 euro is within the cost budget allocated to the landing gear which is 2500 euro. The mass estimation is based on the material weight of Al 7075-T6 and the mass of the tires, carbon fibre wheel covers, wheels, brakes and oleo-pneumatic shock absorber. The allocated mass to the landing gear was 4.5 kg thus with the current mass estimation of 4.38 kg this is within budget. The power estimation is based on the servos that are used for the braking systems on the main landing gear wheels. There was 100 W reserved for the landing gear thus the landing gear is designed within the power budget.

Table 4.27: Output parameter of the landing gear design

Locations			Dimensions		
Parameter description	Value	Units	Parameter description	Value	Units
X-position Nose LG wheel	0.6	m	Max strut Height (incl. Shock absorber) from fuselage to wheel axis	1.171	m
Y-position Nose LG wheel	0	m	Max Stroke (Main and Nose)	0.517	m
X-position Main LG wheels	2.667	m	Tire outer diameter	0.2	m
Y-position Main LG wheels	± 1.0532	m	Tire outer width	0.05	m
Constraints (estimation)			Outer diameter nose shock absorber	79	mm
Parameter description	Value	Units	Diameter nose strut	61	mm
Total mass	4.38	kg	Thickness nose strut	1	mm
Total material cost	2000	€	Thickness main strut (height/width cross-section)	1-2	mm
Total power used	75.48	W	Width main strut (cross-section)	80	mm
Nose LG mass	1.01	kg	Height main strut (cross-section)	15.4	m
Main LG mass	3.37	kg	Max length nose strut	1.176	m
Loads			Max length main strut	1.411	m
Parameter description	Value	Units			
Nose LG strut static load	301	N			
Main LG strut static load	739	N			
Nose LG dynamic Load	659	N			
Max load Nose LG strut	960	N			

4.7.4 Landing gear design verification and validation

For the landing gear a simple software model was used: a custom MATLAB script. This model is verified by step-by-step hand calculations and a sensitivity analysis. Thus making sure that the simulated model represents the physical model. The validation can only be done when the actual landing gear is build and tested. To validate the design of the landing gear a test setup has to be made to check if the loads and stresses within the structure are in close enough proximity to the ones predicted by the model.

The sensitivity analysis of the landing gear consist of two major parameter:

1. The effect of an increase of the maximum take-off mass on the mass of the landing gear
2. The effect of an increase in shock absorber efficiency of the main landing gear on the length of landing gear

The first parameter can be approximated as 25 kg increase in take-off mass causes an 1 kg increase in landing gear mass. As can be seen from figure 4.33. The fraction of the landing gear to the total mass of the vehicle decreases with increasing mass of the vehicle. This is a linearisation at the design points and not valid for an increase in take-off mass of more than 50% of the original mass. For the second parameter, as can be seen in figure 4.34, with an increase in shock absorber efficiency a smaller strut

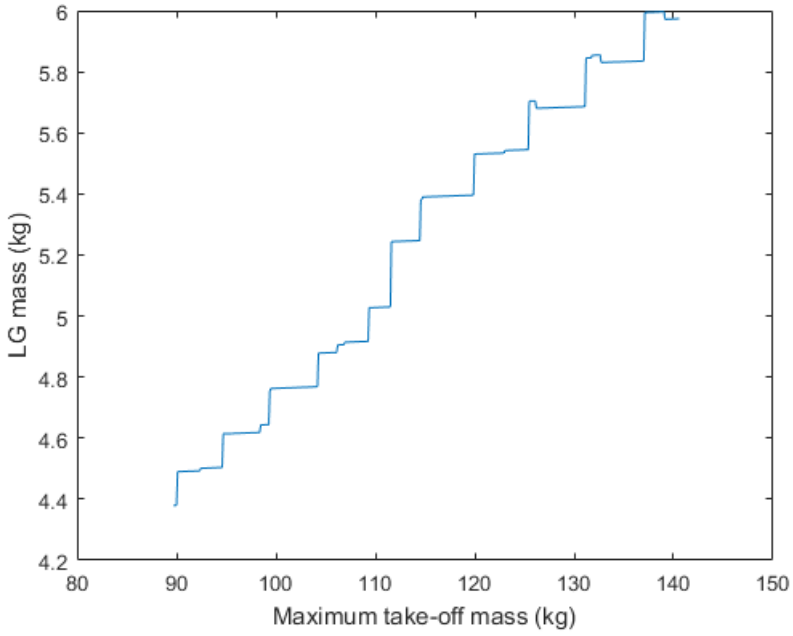

Figure 4.33: Maximum take-off mass increase versus landing gear mass

height is needed as the stroke needed decreases. In figure 4.33 a non-continuous increase can be seen, this can be explained by the discrete nature of the calculations and the iterations done within the script and the variation of step size within the loops used. The curve in figure 4.34 is directly related to the equation of stroke length used in the script [3].

It can thus be concluded that the design of the landing gear is robust enough to cope with any weight increase of the MUAV and that if the efficiency of the shock absorber used for the main landing gear is increased a shorter strut length is required.

4.7.5 Landing gear recommendations

The landing gear design was done in the limited time available, more time and research is needed for a better and more detailed design of this subsystem. In the following list the recommendations are given:

- The parameters found in table 4.27 are based on theoretical data. To verify if the landing gear can indeed withstand the loads introduced during the entire mission of the MUAV and meet all the requirements related to the landing gear further research and testing is needed.
- The oleo-pneumatic shock absorber on the nose has to be increased by going to a levered gear to be able to have sufficient length for the shock absorber. Also the main landing gear length can be decreased by going to oleo-pneumatic shock absorbers, however if the weight penalty is too high this might not be possible.
- The wheel size can be decreased but more research is needed to check whether or not the required rolling coefficient while braking can still be achieved with smaller braking pads. Decreasing the wheel size will lower the weight of the landing gear.
- A different material might be more suitable for the landing gear but more research is needed.
- Jet engines or propeller placement on the front of the vehicle can possibly decrease the landing gear height and thus decrease the drag caused by the landing gear.

These recommendations have to be taken into account for further development of the MUAV.

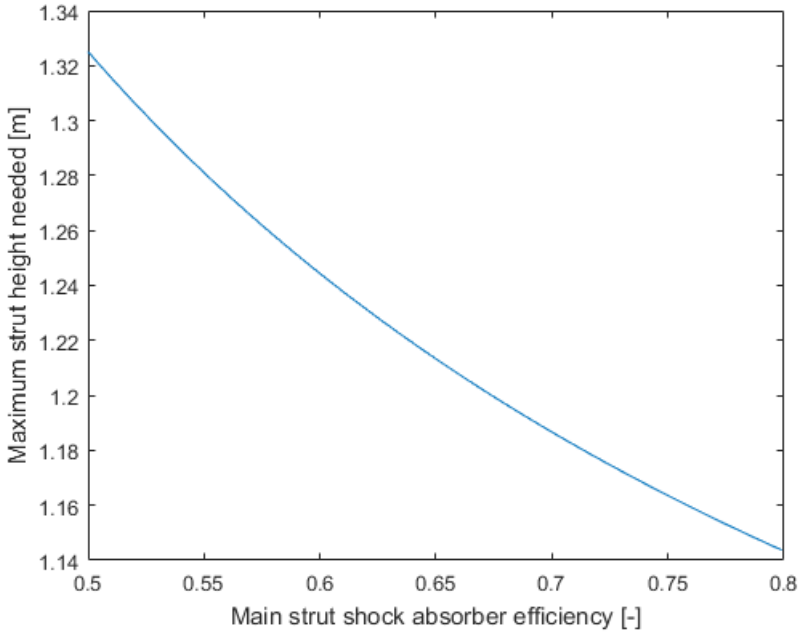

Figure 4.34: Main landing gear shock absorber efficiency versus maximum strut height required

4.8 Parachute design

To minimise damage after an in-flight failure, the MUAV will be equipped with a parachute. For smaller UAVs off-the-shelf systems are available, but for the size of the MUAV they are normally custom made. This is usually done by specialised manufacturers. In section 4.8.1 a custom parachute will be sized using basic equations and existing parachutes from different manufacturers. Besides the design of the parachute itself its location should be determined, to make sure it lands on the landing gear in all configurations. This will be discussed in section 4.8.2.

4.8.1 Sizing

The parachute characteristics that are of interest for the design are: weight, cost, volume and the opening force. Those were determined using the basic equations found in a paper published by the Butler Parachute Systems Group [21]. This method determines the size of the parachute based on the MTOW and the maximum rate Rate of Descent. With the size known the weight, volume, and opening force can be found.

The landing gear is designed for a sink rate of 5 m/s. Since the UAV should land on the landing gear during a parachute landing as well, this is taken as the Rate of Descent. Given the MTOW and a parachute drag coefficient of 1.2, this results in a parachute area of 45 m^2. Using data from the paper and other manufacturers (Skygraphics AG[18], Aero Telemetry[19] and Uçman Havacılık[20]) the weight, volume and cost were estimated. For the volume it is assumed that it should be possible to repack the parachute by hand, so it can be done at the test site. Due to the relatively high speeds the UAV is capable of flying, the parachute should be reefed, to make sure the opening force does not exceed the 5G load the structures are designed for. The reefed percentage is the percentage of the parachute area that is opened directly

[18] ProtectUAV - Configuration, `http://protectuav.com/2.html`, Accessed: 08-01-2016

[19] High Speed Flight Termination Parachutes - Aero Telemetry, `http://www.aerotelemetry.com/our-products/recovery-parachute-systems/high-speed-flight-termination-parachutes`, Accessed: 08-01-2016

[20] Uçman Havacılık - IHA-1 PARACHUTE SYSTEM, `http://www.ucman.com.tr/index2.php?Id=63`, Accessed: 08-01-2016

when the parachute is activated. While the vehicle slows down the parachute gradually opens further. All parachute parameters are summarised in table 4.28.

A Rate of Descent of 5 m/s is low compared to other emergency parachute systems. Therefore, the parachute is relatively big and heavy. The initial estimate of 1 kg is not met.

Table 4.28: Parachute parameters

Parameter	Value
Parachute area	45 m^2
Reefed percentage	15%
Weight	2.9 kg
Volume	7 l
Cost	€2000

4.8.2 Location

When the parachute is deployed the aircraft will always balance in such a way that the c.g. is right below the parachute attachment point. This means that the vehicle will remain horizontal in case the parachute is mounted directly above the c.g. when the aircraft is standing on the ground. This is how it is done in most other fixed wing UAVs. However, in case of the MUAV the c.g. location differs per configuration. When the c.g. is not precisely below the parachute mounting point, the vehicle will be hanging under an angle. This could be solved by having a movable parachute. However, this makes life harder for both the users and the designers. Therefore it was decided to place the parachute at a fixed location that is best for minimising damage in all configurations. To determine this location the most aft and forward c.g. locations from the stability analysis were considered. In case the parachute is deployed because a part was lost, the c.g. location is very hard to predict. Therefore this is not taken into account.

The maximum angle under which the MUAV will still land on its landing gear is determined by the position of the landing gear. In the front a maximum angle of 62 degrees. In the rear the propeller is the limiting factor. However, the propeller is a off-the-shelf part of about 50 euros. Therefore it was decided that the propeller will not be taken into account. An important remark on this, is that the propeller should fail before the shaft does, since the shaft is way harder to replace.

Taking these constraints into account the attachment point of the parachute was placed on 1.94 m from the nose. When not used, the parachute is placed behind that point, on top of the centre wing box.

4.8.3 Parachute design verification and validation

Normally, parachutes of the required size are custom made. Since designing a complete parachute system was considered outside the scope of this project. Therefore the main parameters of the parachute were determined using basic equations. The outcomes were verified using data of existing parachutes from four different manufacturers.

Chapter 5

Module design

As the MUAV is designed for modularity, it is capable of handling many different new concepts. The aircraft industry experiences a never ending urge for increased efficiency and performance. Two of the most promising concepts are SHLD and the boxed wing concept. As the main mission goal of the MUAV is the testing of these kind of concepts it is worthwhile to discover the possible integration of these concepts. On top of that they push the limits of the modular design. In the following sections, these two concepts will be used as a test case to show the possibilities of the modular platform. First the boxed wing will be treated in section 5.1, followed by SHLD in section 5.2.

5.1 Boxed wing design

One of the new promising concepts is the boxed wing, also called the PrandtlPlane concept which is named after Ludwig Prandtl [22]. The PrandtlPlane is an innovative and exciting new wing configuration for the aircraft of the future. In this section a first design of the boxed wing will be presented. First the fundamentals behind the design of the boxed wing are discussed in section 5.1.1. With this information the actual design can be made which is presented in section 5.1.2. Because the boxed wing is fundamentally different from a conventional wing, the effects of the boxed wing on the MUAV is treated 5.1.3.

5.1.1 Boxed wing fundamentals

The main purpose of a boxed wing design is the minimisation of induced drag. Unlike for conventional aircraft, there is little information available for boxed wing concepts which makes the design more challenging. In this section a preliminary geometrical design, with an initial load estimation on the MUAV will be developed. Although the design of a boxed wing opens a whole new register of possible configurations, the design for this boxed wing will only cover the most conventional configuration possible. Furthermore, due to the fact that the net lift over two wings should be equal it is assumed that the total the wing for the reference plane is split in to the two wings of the boxed wing. Also, the horizontal tail is not taken into account until the stability assessment.

In this section a summary of important considerations in the design of a boxed wing design are given. An overview of all parameters can be found in table 5.1.

Geometry definitions: Aspect ratio and Stagger

The main feature of the boxed wing is the reduction of the induced drag:

$$C_{D,i} = \frac{C_L^2}{\pi \cdot A \cdot e}. \tag{5.1}$$

Therefore the aspect ratio A and the efficiency factor e are essential in the design of the boxed wing. The optimisation can be done both for A and e, however the approach chosen is to set the aspect ratio and

optimise for the corresponding span efficiency factor. This is done because there is some minimal data on the induced drag for boxed wing that can be used in estimating the efficiency factor. On top of that, the wings were assumed identical so that applying the equation for aspect ratio to one of the isolated wings, the aspect ratio is twice as high as for the whole combination.

The horizontal distance between both wings is referred to as stagger. As most parameters, the stagger (h) is also going to be normalised to the wingspan (b), which leads to the ratio: h/b.

Optimal lift distribution for the boxed wing

In research literature there is still some controversy on the other conditions for optimal lift. However for this design the most conventional train of thought is used, which states that lift must be equal on both wings for an optimal design [22]. In situations where stability requires a different moment, solutions like taper and twist can change the properties of both wings keeping the lift generated over the two wings roughly the same. As will be discussed later, the stability does not seem to be of critical importance to this boxed wing design. On top of that, introducing special wing parameters creates interference problems that lie beyond the scope of this design. Therefore the most conventional solution is chosen: equally sized wings.

Induced drag

In order to analyse the induced drag reduction by the boxed wing configuration, the following ratio is considered [23]:

$$\frac{D_{i,box}}{D_{i,ref}} = \frac{0.44 + 0.9594 \cdot (h/b)}{0.44 + 2.2019 \cdot (h/b)} \tag{5.2}$$

Where $D_{i,box}$ is the induced drag of the wing box and $D_{i,ref}$ is the induced drag of the reference wing. As $D_i = \frac{L^2}{q \cdot \pi \cdot b^2 \cdot e}$, the ratio of drag is equal to the ratio of efficiency factors:

$$\frac{D_{i,box}}{D_{i,ref}} = \frac{e_{i,ref}}{e_{i,box}} \tag{5.3}$$

Optimising for h/b it can be seen that the h/b value must be as large as possible to decrease the induced drag. As our boxed wing configuration has the same wingspan as for the conventional plane, the wingspan is relatively large compared to the other parameters of the aircraft. This is especially true for the h/b ratio, which makes the boxed wing far less effective as it could potentially be. Even so, as $h/b = 0.1667$, the induced drag reduction is theoretically about 25%.

Structural weight

To be able to withstand the bending moments the wing box needs a thicker skin which will increase the structural weight of the wing box. A correlation for this can be found in [24] and is given by:

$$\frac{m_w}{m_{MZF}} = 6.67 \cdot 10^{-3} \cdot b_S^{0.75} \cdot \left(1 + \sqrt{\frac{b_{ref}}{b_S}}\right) \cdot n_{ult}^{0.55} \cdot \left(\frac{b_S/t_r}{m_{MZF}/S_W}\right)^{0.3} \tag{5.4}$$

The only problem is that, as for most of the equations, this equation applies to cantilever wings so it can not be used straight away. However, when evaluating the different parameters some better conclusions can be drawn. To do so the boxed wing will be evaluated by approximating it with a conventional wing with similar parameters. In that case, the total wing area is the same as its corresponding wing area. Furthermore the wingspan is equal as well, which leaves only the airfoil thickness at the root:

$$\frac{m_{w,box}}{m_{w,ref}} = \left(\frac{t_{r,ref}}{t_{t,box}}\right)^{0.3} = 2^{0.3} \approx 1.23 \tag{5.5}$$

The value for t stems from the fact that the chord length of the boxed wing is only half compared to the reference wing, so that the relative thickness is also half. The result from this equation is that the weight

of the wing box structure is about 23% higher. It is important to note that due to the lower moments on the wing, the increase in wing weight is normally partly compensated by a decrease in fuselage weight.

5.1.2 Design parameters of the boxed wing

Apart from the most important parameters mentioned above, there are more parameters that describe the properties of a boxed wing. A complete overview is presented in table 5.1.

Table 5.1: Parameter comparison: boxed wing versus conventional wing

Parameter	Boxed wing	Reference wing
Span [m]	6	6
Area [m^2]	3.6	3.6
Aspect ratio [-]	10	10
Root chord length [m]	0.41	0.83
Taper ratio [-]	0.28	0.45
Sweep (ϕ_{25}) [deg]	18	0
Dihedral [deg]	6	0
Span efficiency [-]	0.57	0.76
Glide ratio [-]	16.98	14.77
Wing weight [kg]	18.98	15.43

5.1.3 Effects of the boxed wing on the modular platform

Because of the configuration being so different from the ordinary configuration, the effects of applying a boxed wing to the modular platform need to be investigated. In this subsection the two most important changes will be discussed. First, the boxed wing needs to be connected to the rear of the fuselage. As stated earlier, the stagger needs to be as large as possible. This requirement means that the aft wing needs to be connected to the top of the vertical stabiliser on the empennage. These effects will be discussed first, followed by the effects of the boxed wing on the stability and controllability, which changes drastically due to the large lifting surface behind the c.g. of the MUAV.

Effects of the boxed wing on the structure of the vertical tail

As the aft wing is attached to the top of the vertical stabiliser, the vertical stabiliser and fuselage need to be able to withstand the applied loads. In the following paragraphs the most important loads are discussed.

The point loads on the top of the vertical stabiliser are due to the loads on the wings. For this initial evaluation it is assumed that all loads are half the loads of the reference wing. First the loads of the vertical connectors are discussed. Under the maximum bank angle, the sideways loads are found to be 54.5 N. Assuming a 2 mm thick wing box structure, the total deflection is 0.03 mm and can therefore be neglected. The other directional forces are due to the drag and the lift and create an equally ever small deflection.

A more challenging situation occurs when considering the bending and torsional moment that occur on the vertical fin. As the boxed wing configuration is statically undetermined, there are many parameters of influence on the design. As in the wing box design is shown, the wing box structure is capable of handling the bending loads. As the wing box for now is assumed continuous, the bending moments are all carried by the wing box structure of the aft wing. The conventional configuration however, is not capable of bearing the torsional loads under the given flight conditions. Under the current manoeuvring conditions, the angle of rotation in the XY-plane is around 10°. As the wing-fuselage interface for the front wing is designed for the loads generated by the conventional wing, the front wing can be stiffened so that it caries more loads, this can relieve the loading on the tail. Another option is to make the flight envelope smaller. For the current design, the maximum load factor when all loads can stil be handles is around three.

Figure 5.1: Stability analysis planform

Effects of the boxed wing on the stability

To asses the effects of the boxed wing on the stability the method explained in section 4.4 is used. To be able to incorporate the design in the stability analysis the assumption is made that the aft wing is appended on the front wing. This can be done because the aerodynamic consequences in longitudinal direction are roughly the same. A sketch of the assumed planform is given in figure 5.1.

In figure 5.2 the result of this analysis is displayed. From this figure it can be concluded that the boxed wing configuration is stable, but that the difference between the most aft centre of gravity and the control point is around 10 cm. One of the solutions to this problem is altering the sweep parameters, as for this concept the assumption of equal sweep angles for the front and the aft wing is used. To make this configuration controllable these values should be adjusted. The actual generation of these values is beyond the scope of this project.

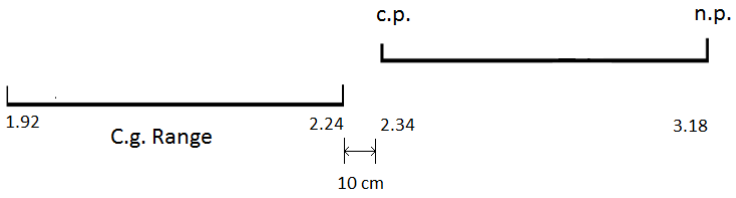

Figure 5.2: Stability and controllability analysis boxed wing

5.1.4 Boxed wing design verification and validation

The boxed wing concept is difficult to validate as there are almost no working examples available for the boxed wing concept, especially not when UAVs are concerned. To be able to validate the use of certain equations, they have been validated against the values for normal wing configurations. In the case of enough information to doubt the values for conventional wings, it is mentioned in the text. As for the calculations done to asses the loads on the vertical tail, these were all verified by the use of a conventional calculator, and have also been verified for similar loads on conventional aircraft.

5.1.5 Conclusion and recommendations on future studies

According to the theory from previous subsections, the boxed wing configuration could prove to be a major breakthrough in the aircraft design due to the significant decrease in induced drag. Recent research

seems to support this theory. However, much is still unknown about the interaction between the two wings as all most research approaches cover one large and one much smaller wing. On top of that, there has not been a design yet, for which the efficiency of the boxed wing weighs up against the added structural weigh. Though, with the current evolution of composite materials that design is getting closer.

Considering the modular platform it can be concluded that the MUAV is reasonably fit for the application of the boxed wing concept. The fact that the wing is moveable, and therefore the distance between front and aft wing can be increased, contributes to the fact that it is probably stable in normal cruise conditions and almost controllable. On top of that, the MUAV has a relatively large vertical fin so that the vertical distance h, is large. The problem is; for multiple reasons this design is based on the conventional wing as designed in the development of the MUAV. This results in having a very large wingspan, so that most of the effects are cancelled as they depend on a large value of h/b. Finally it can be said that the design of the tail is not optimised for carrying the loads of the boxed wing, if one would want the ability of having a boxed wing, the tail should be redesigned.

In the design of the boxed wing there are three main challenges for which there is not enough information available. These challenges are of great interest to future boxed wing designs and research with the MUAV. The first challenge lies in assessing the interaction between the front wing and the aft wing. It is supposed that the effects of the front wing on the aft wing is significant, although the extend of this effect is not clear. The second challenge is the behaviour of the tail plane which is directly below the large aft wing. And finally the structural effects of the application of the boxed wing. How do the earlier mentioned challenges effect the loads on the wing, and where can one defer from a conventional design to decrease the relative weight of both the wing and the fuselage.

5.2 SHLD design

As holds for the boxed wing, the SHLD are state of the art innovations that test the limit of the MUAVs application. In this section an elaboration will be given on the design of the SHLD, which starts with a short summary of the state of this design process in subsection 5.2.1. Subsequently the SHLD module will be designed with more detail in subsections 5.2.2 - 5.2.4. This entails the choice of skin material, deformation shape, actuation mechanism, and dimensions of the structure. This design process concludes with subsection 5.2.5 showing an overview of the SHLD module with an assembly rendering.

5.2.1 Current SHLD state

SHLDs have been a promising topic of research for the past decades, with a lot of innovations surfacing over the recent years. The concept of SHLD design revolves around creating a wing-HLD combination without edges or crevices, improving aerodynamic characteristics and reducing fuel consumption. SHLD also produce less noise than conventional HLD which makes them attractive for airports near residential areas.

There are numerous existing SHLD concepts which have been researched in earlier design phases of this project; These mainly revolved around their way of actuation. Investigated actuation concepts were: eccentric beam actuation, pre-stressed cables, fluidic actuators, selective deformable structures, and kinematic mechanisms. One of these concepts has been chosen to be designed as a module: the eccentric beam actuated SHLD. This mechanism works by rotating an eccentric beam inside a flexible structure to achieve more camber in the TE. A functional representation of this concept can be seen in figure 5.3. The concept was selected based on design feasibility, ease of use, and attractiveness. The next subsection will look into the first design step of the SHLD, the skin and shape selection.

5.2.2 Skin and shape selection: combining flexibility with structural integrity

The skin has to be able to deal with aeroelastic effects while also being elastic enough to be deformed by the actuation system. Skin material has been researched extensively which lead to the conclusion that

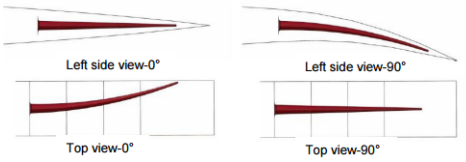

Figure 5.3: Eccentuator applied as TE flap [25]

composite materials are the most promising materials for SHLD. References like SADE [26] and DLR [1] show that Glass Fiber Reinforced Polymer (GFRP) and aluminium are the most suited composite material for SHLD. Aluminium is the preferred skin material as a high yield strain is needed for this design.

The skin shape will be modelled to the airfoil of the standard wing (NACA 02017) so it fits to the wing. When actuated the eccentric beams will rotate such that the TE tip deflection is increased from 0° to 25°. This will have a significant effect during take-off since the MUAV has a relatively low wing loading. The shape of the TE in cruise and high lift configuration and the effect of the deflection on lift performance can be seen in figure 5.4.

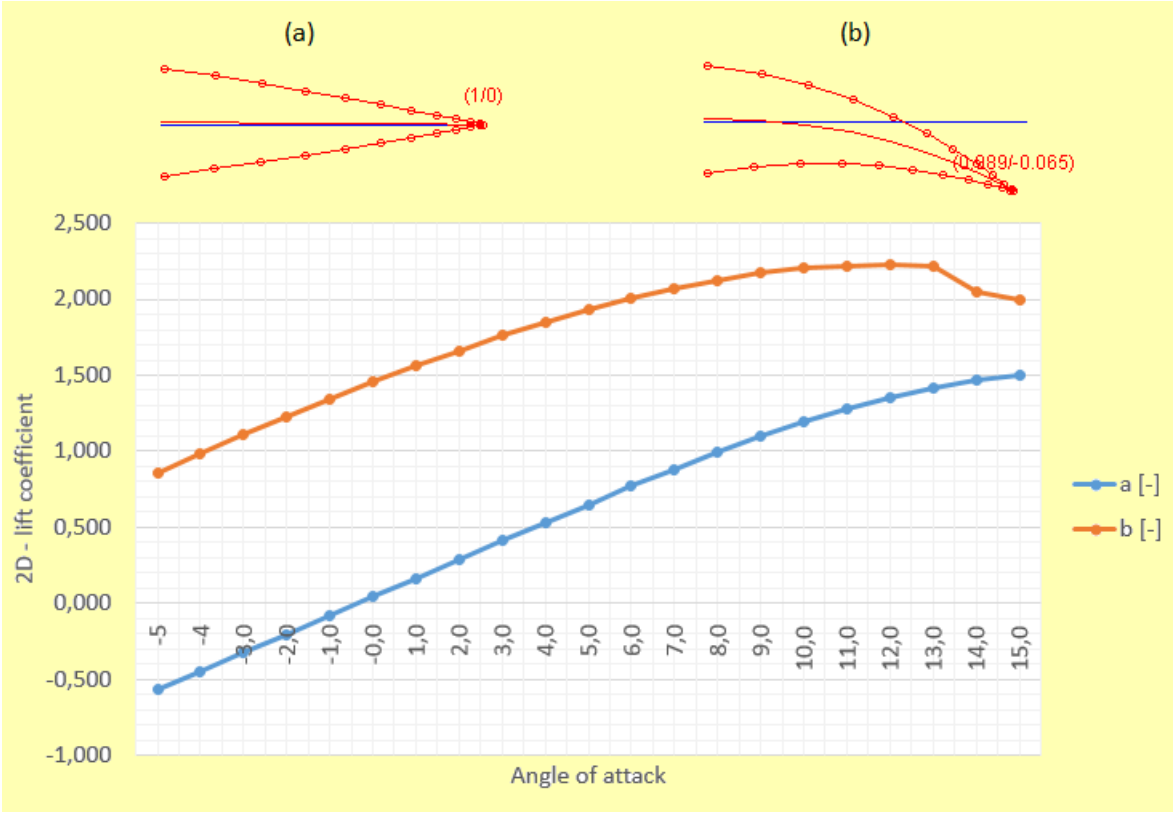

Figure 5.4: Trailing edge SHLD shape and airfoil lift performance. (a) Cruise, high lift deviceundeflected: no rotation of the actuators, no deflection. (b) High lift device deployed: 90° rotation of the actuators, maximum flap deflection.

The skin thickness will be 0.3mm which allows for actuation and sufficient stiffness against aerodynamic loads. This is thinner than the wing box skin but the SHLD skin will carry lower loads since there are load carrying beams inside. For weight calculation purposes a skin density of 2700kg/m^3 has been

[1] `http://www.dlr.de/fa/en/Portaldata/17/Resources/dokumente/2012/CE_Droop_Nose.pdf` accessed on 11-1-2016

selected [2]. A V-shaped stringer will be attached to the skin at the LE tip to provide additional stiffness against aerodynamic loads.

5.2.3 Actuation to achieve a morphing trailing edge

The eccentric beam actuation system needs to be designed. This system consists of an eccentric circular beam that is rotated by an actuator. A linear actuator will be connected to a gear mechanism to rotate the eccentric beams. The beams will be rotated to reach the desired TE deflection, up to a maximum of 25° tip deflection. A Techdrive LMR02-RL2-c50-CC24V Linear actuator [3] will be used to actuate the mechanism, this motor provides sufficient force to rotate the beams and deform the skin while still fitting in the wing. The actuation mechanism and rotary beams are designed to fit within the airfoil, a rendering of this can be seen in figure 5.5.

5.2.4 Structural sizing as a module

The SHLD module has to fit to the trailing edge module attachment point, therefore the attachment structure will be designed. The actuation mechanism also needs to fit to this structure, as it will keep the rotary beams in place. This means the structure needs to conform to the wingbox height at the attachment point as well as brace the rotary beams at their root. A rendering of this structure can be seen in figure 5.5. The next section will conclude the SHLD design with a complete assembly, a weight and power check, and a cost estimation.

5.2.5 Final SHLD Design

With all the components modelled, a final assembly and exploded view of the complete SHLD module is shown in figures 5.5 and 5.6. The total weight and power consumption of the SHLD module have been calculated and are shown in table 5.2. The SHLD module fits to the TE module interface and falls within the mass and power budget, which makes the module fully compatible with the MUAV. The SHLD design is not optimised and more detail should be put into flow analysis, load predictions, and deformation calculations in future design phases to reach an optimal structure and actuation mechanism.

To get an indication on what a costumer would have to spend to build a HLD module, the manufacturing cost of this device is estimated. The manufacturing cost breakdown is shown in table 5.3. The raw material cost of the linear gears are negligible and have been taken into account in the labour cost.

Table 5.2: SHLD Weight and power parameters (including fairings) compared to the wing module budget

Parameter	Weight [kg]	Power consumption [W]
SHLD value	12.94	312
Wing module budget	20	1000

Table 5.3: SHLD manufacturing cost breakdown

Component	Price [€]
Actuators	920
Skin	80
Eccentric beams	400
Labour	1400
Total	2800

[2] `http://www.engineeringtoolbox.com/density-solids-d_1265.html` Accessed on 13-1-2016

[3] `http://www.techdrives.co.uk/Multimedia/Linear%20Actuators/data-sheet-lmr01-03.pdf` Accessed on 13-1-2016

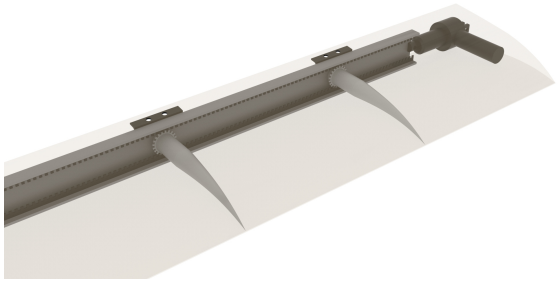

Figure 5.5: Isometric view of a rendering of the initial SHLD design in deflected state

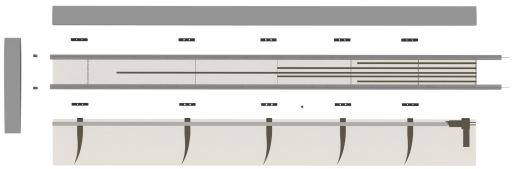

Figure 5.6: Top down exploded view of the initial SHLD design in undeflected state including LE and wingtip fairings

5.2.6 SHLD design verification and validation

The SHLD module has been designed mostly using available literature and the wing box design. The initial design was made using a chosen concept and fitting it to the TE module interface with an existing mechanism that fell within the mass and power budget. The sources that were used were thoroughly checked on their validity by tracing the references and stakeholders. The sources were supported by numerous technological universities and institutes across the world including the DUT which verifies the SHLD design for this phase. Validation should take place at later stages of this design phase as there is currently not much data available on the design.

Chapter 6

Design evaluation

In this chapter a design evaluation is presented. This is started by showing the complete design using some renderings and technical drawings in section 6.1. In section 6.2 an evaluation of the subsystems as well as technical resource budget allocation tables are shown. The flight and aerodynamic characteristics are analysed in sections 6.3 and 6.4. The stability of the design point is discussed in section 6.5. Finally a compliance matrix is presented in section 6.6 together with a feasibility analysis of the requirements that are not met.

6.1 Design overview

In this section an overview of the platform with the default wing and its sizes is given. This is done by using renderings of the full platform and some subsystems, as well as technical drawings.

6.1.1 Renderings

To give a good impression of the final design, a rendering without the fuselage skin is shown in figure 6.1. A side view of the same situation can be seen in figure 6.2.

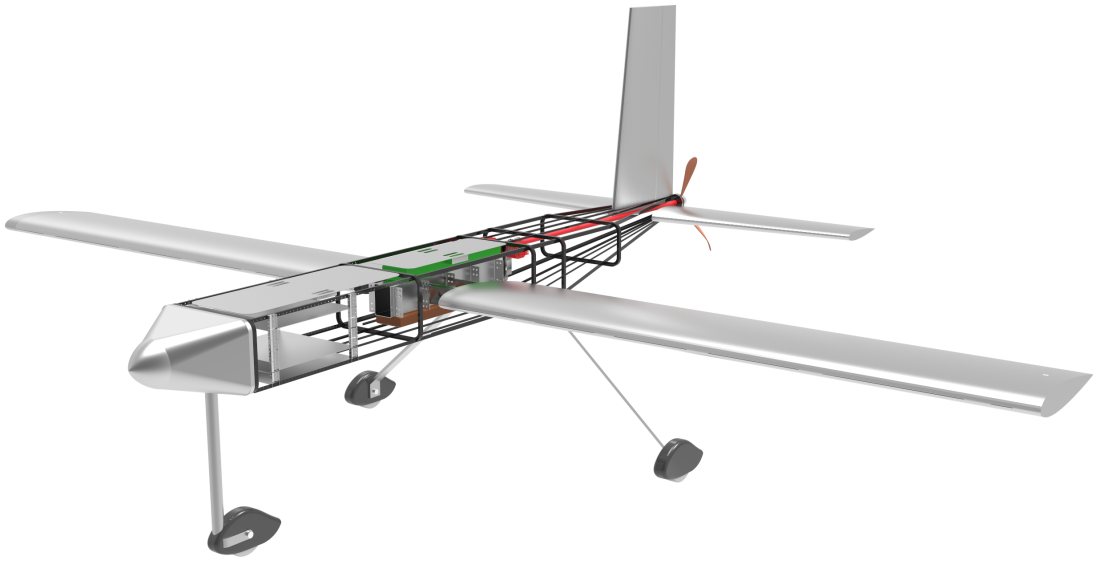

Figure 6.1: Rendering of the final design without fuselage skin

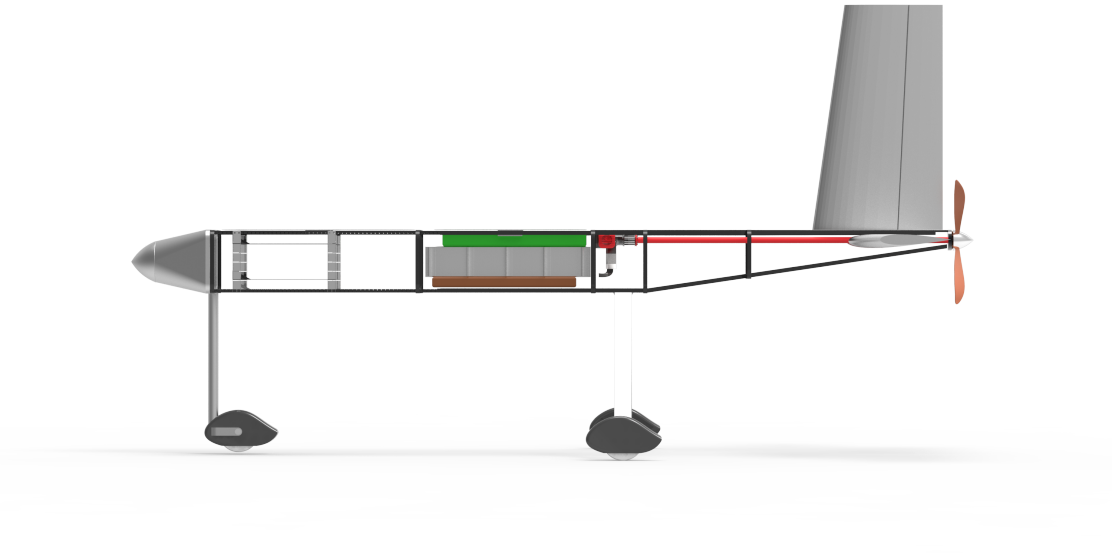

Figure 6.2: Rendering of the final design without fuselage skin, side view

In these pictures an overview of the entire design can be seen, along with the location of the major subsystems. In the front, just behind the nose cone the payload bay is visible. In between the wings the centre wingbox, fuel tank and parachute can be found. Directly behind that the engine can be seen, as well as the shaft driving the propeller. It can be seen that the available space in the fuselage is fully used (since the payload bay shall be able to move), except for the part behind the engine. It is difficult to make more use of this extra space, as the aircraft's centre of gravity shall not shift backwards because this would limit the IDS.

6.1.2 Technical drawings

In order to put the size of the MUAV in the right perspective, technical drawings including sizes are presented for the side view in figure 6.3, for the front view in figure 6.4 and for the top view in figure 6.5.

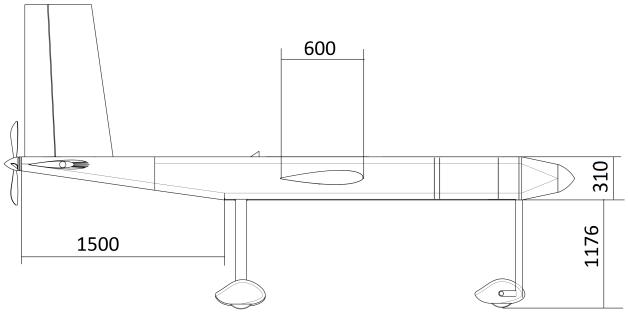

Figure 6.3: Platform side view. Dimensions in mm.

From these figures the sizes of the main subsystems and the exterior can be seen. The size is large enough to enable production and testing of complex subsystems such as SHLD, while still being small enough to be easily transported and light enough to allow for easy handling.

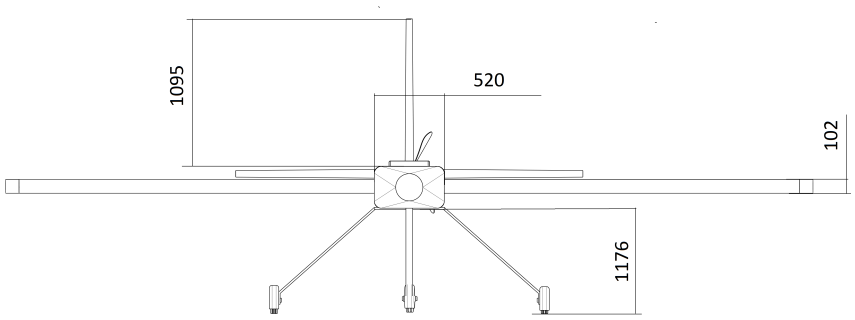

Figure 6.4: Platform front view. Dimensions in mm.

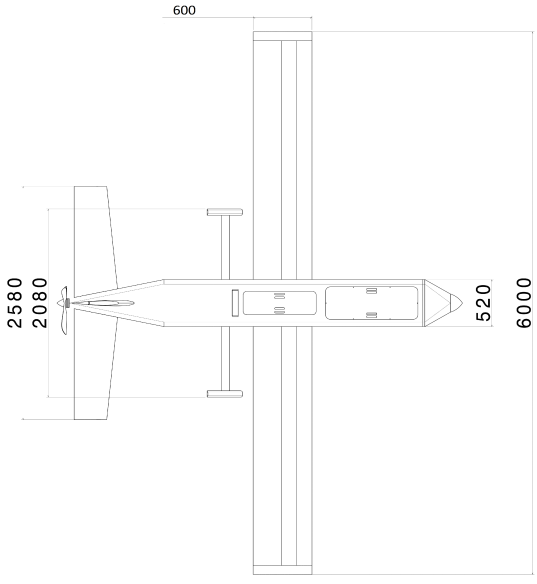

Figure 6.5: Platform top view. Dimensions in mm.

6.2 Subsystem evaluation and resource budget allocation

In this section the evaluation of the subsystems can be found together with a technical resource budget allocation. First the evaluation is presented, and the section will be concluded with tables showing the breakdowns of the cost, weight and power budgets.

6.2.1 Subsystem evaluation

Due to time restrictions, the level of depth for designing the subsystems differ from each other. As the design focuses on modularity, the subsystems that have a direct influence on this aspect shall have a greater depth of detail than the subsystems that are less related with modularity. The level of detail depends on the parameters of that subsystem that is related to modularity. For example the empennage is detailed designed with respect to stability and control, while the structure is not designed at all. The structure of the wing however, has been designed with more detail due to the fact that the fairings and winglets are modular, meaning that the structure of the wing should be able to be subjected to many load cases. The subsystems that have been designed with more detail are the wing, the empennage , the fuselage, and the payload bay. The other subsystems are mainly designed with the help of off-the-shelf products. A brief evaluation of each of the subsystems can be found below.

- **Fuselage design**
  The design of the fuselage mainly is detailed with respect to the structure of the fuselage as it should withstand loads that are coming from the nose, the empennage, landing gear, and wing. The level of depth goes to the determination of the spacing between the stringers and their cross-sectional areas.

- **Payload bay design**
  The most important function of the payload bay is to accommodate for the payload, meaning it should be able to carry weights up to 20 kg. The focus lay therefore on the structure of the payload bay, which is designed to accommodate several payloads with a combined weight of 20 kg or a single unit with a mass of 20 kg. The payload bay is directly related to the modularity of the MUAV, as the payload should be able to change position for changing the centre of gravity. This means that the payload should be removable, and is therefore designed with bolt connections.

- **Wing design**
  The main design target of the wing are the interfaces between the fairings and wing box, as well as the interface between the winglets and wing box. This is due to the modularity of the LE, TE and tip devices. Due to this variety of devices that can be attached to the wing, the wing box should be able to withstand many different forces. The wing box is therefore designed in more detail with respect to the ribs, spars, and top and bottom skins as well as the spacing between the above mentioned aspects. The centre wing box is designed with a high level of detail, as it should be able to carry many different load cases due to the fact that the wings are modular. With respect to aerodynamics, the main design target was to make sure the MUAV is able to take-off and land without any high lift devices.

- **Empennage design**
  The empennage is mainly designed to supply stability and controllability for a wide range of different wing configurations. This means that the structural design of the empennage has largely been neglected while the performance of the empennage has been designed in detail.

- **Propulsion and power system design**
  Because the propulsion and power systems are not directly related to the modularity of the MUAV, this subsystem has not been designed in detail but with off-the-shelf products. However, some special attention was needed for the shaft that connects the propeller to the engine. Because the propeller is located at the aft of the MUAV and the engine in front of the centre wing box, a long shaft is needed. To prevent buckling and moving of the shaft, a thrust bearing is placed.

- **Electrical system design**
  Even though the electrical system is directly related to the modularity of the MUAV, by means of uploading new flight control schemes, this subsystem is designed with a relatively low depth of detail. There are many off-the-shelf products that can be used to accommodate for interchangeable flight control schemes as well as sensors and data/communication handling components.

- **Landing gear design**
  The design of the landing gear has been done in detail. Both in structural and aerodynamics perspective the landing gear has been optimised. The landing gear is not directly related to modularity, however the propeller can be replaced by larger ones. This results in a higher clearance from the ground which should be provided by the landing gear.

- **Parachute design**
  For UAVs of this size, parachutes are custom made/adapted by specialised manufacturers. Here an initial sizing of the parachute was done using data of those manufacturers. The only relation with the modularity is its position. Due to the changing centre of gravity this has to be chosen carefully to make sure the MUAV always lands on the landing gear.

6.2.2 Technical resource budget allocation

The relevant technical resource budgets for this project concern cost, mass and power. Figure 6.1 shows the cost breakdown. First the material cost of all subsystems is added, next to that the labour costs are estimated based on an hourly rate of €35 for workshop personnel. On top of that €10,000 euro has been budgeted for the production facility, energy usage and machinery. A maximum manufacturing cost of €50,000 is required, therefore a contingency of €7,769 still remains.

The mass breakdown is given in table 6.2. The most recent weight estimation is compared to the estimations in the baseline and mid-term report. It can be seen that the MTOW has been growing faster than the contingency available. With a remaining 7.5% contingency for the detailed design taken into account the MTOW is currently estimated on 91.5 kg.

The distribution of the power budget is shown in table 6.3. All values in the table represent the maximum power. For example, the maximum power of an actuators is only needed for short amounts of time and probably not for all actuators at the same time. Therefore the engine has a healthy power reserve under normal operational conditions.

Table 6.1: Manufacturing cost breakdown

Subsystem	Material cost [€]	Labour cost [€]	Total cost [€]
Fuselage & payload bay	36	4000	4036
Wing	38	3000	3038
Empennage	17	3000	3017
Propulsion & power	6979	100	7079
Electrical systems	3361	1600	4961
Landing gear	2500	500	3000
Parachute	2000	100	2100
Assembly		5000	5000
Facility, energy, machinery			10,000
Contingency			7,769
Total	14,931	17,300	50,000

Table 6.2: Mass breakdown

Subsystem	Baseline weight [kg]	Mid-term weight [kg]	Current weight [kg]
Fuselage		19.8	16.8
Payload bay			3.00
Wing		15.1	20.86
Wing-fuselage interface			2.6
Empennage		3.76	3.76
Propulsion and power		7.23	8.50
Electrical		5.50	4.30
Landing gear		4.60	4.38
Parachute		1.00	2.90
Contingency		8.27	6.00
OEW	55.4	68.8	73.1
Fuel weight	0.90	0.90	0.90
Payload weight	20.0	20.0	20.0
MTOW	76.3	89.7	94

Table 6.3: Power breakdown

Subsystem	Initial estimate [W]	Current power [W]
Propulsion	11,000	13,000
Payload	1,000	1,000
Control systems	200	38.62
Actuators		293.7
Contingency	1,340	
Total	13,540	14,332

6.3 Flight characteristics

In this section the results of the flight performance analysis are presented, and it is shown whether the performance requirements are met. The first subsection covers the analysis and results of different load factors and the corresponding maximum allowable cruise speeds. In the second subsection the wing loading, power loading and flight performance characteristics are presented.

6.3.1 Load factor analysis

To show the stall speeds, manoeuvring speeds and maximum cruise speeds for gust intensity for the MUAV a V-n diagram has been created. This V-n diagram can be found in figure 6.6.

The V-n diagram in figure 6.6, shows the aerodynamic, structural and aeroelastic limit for the movable wing concept. The resulting characteristic speeds from these limits are presented in table 6.4.

6.3.2 Load diagram and performance characteristics

In figure 6.7, the load diagram of the MUAV can be found. From the load diagram, the maximum wing loading and the maximum power loading can be determined, which are 202 N/m^2 and 0.11 N/W respectively. The design space can be found in the left-bottom part of the graph, and is limited by the climb rate, landing distance, and the take-off distance.

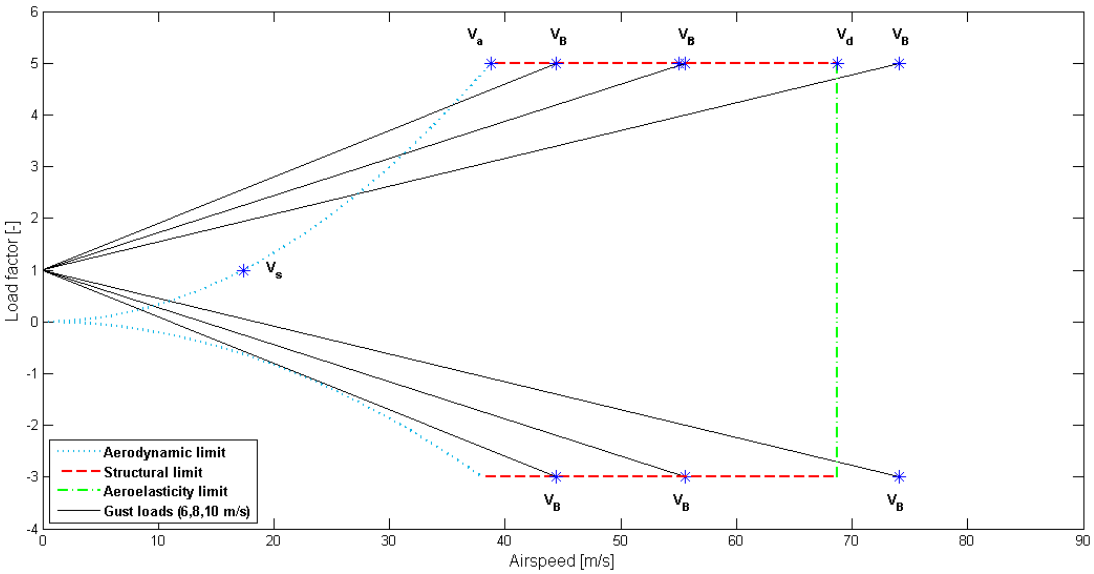

Figure 6.6: V-n diagram for the final design

Parameter	Symbol	Value	unit
Stall speed	V_s	17.1	m/s
Manoeuvring speed	V_a	37.78	m/s
Design cruise speed	V_c	55	m/s
Maximum dive speed	V_d	68.75	m/s
Maximum speed for gust (10 m/s)	V_B	43.05	m/s
Maximum speed for gust (8 m/s)	V_B	53.81	m/s
Maximum speed for gust (6 m/s)	V_B	> 55	m/s

Table 6.4: Characteristic speed results for the final design

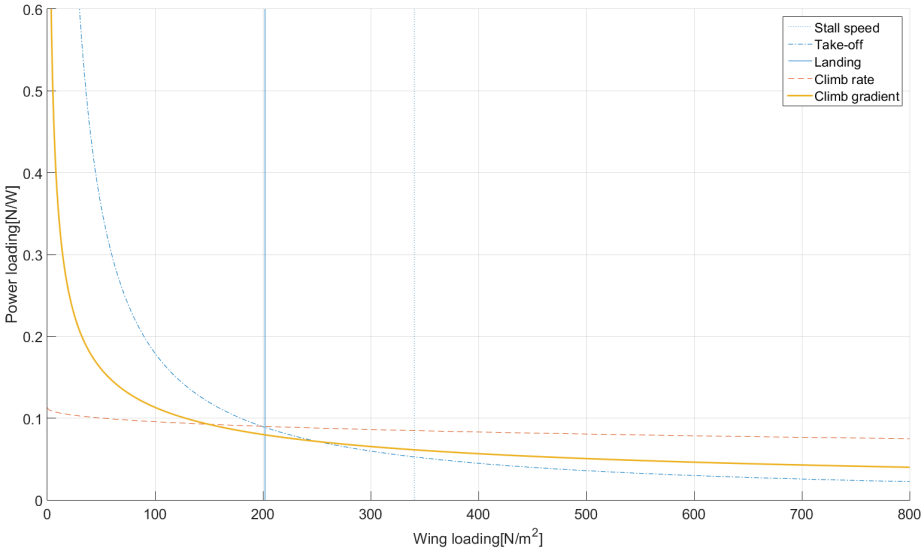

Figure 6.7: Load diagram of the MUAV

The performance characteristics are calculated using equations that can be found in the lecture slides of the course AE-2230I Flight Mechanics and in Raymer [4, 3]. The MUAV performance characteristics can be found in tables 6.5, 6.6, and 6.7. The touch down speed, approach speed, screen speed and lift of speed are all related to the stall speed as 1.15,1.30,1.20, and 1.10 times the stall speed respectively [4].

Table 6.5: Performance parameters part 1/2

Parameter	**Symbol**	**Value**	**unit**
Weight	W	922	N
Touch down speed	V_{TD}	19.9	m/s
Approach speed	V_A	22.5	m/s
Screen speed	V_{scr}	20.8	m/s
Lift off speed	V_{Lof}	19.1	m/s
Landing speed	V_{Sland}	17.6	m/s

Table 6.6: Performance parameters part 2/2

Parameter	**Symbol**	**Value**	**unit**
Take-off distance	s_{TO}	129.8	m
Landing distance	s_{land}	139	m
Climb rate	c	6.65	m/s
Climb gradient	c/V	32	deg
Maximum cruise speed	$V_{CruiseMax}$	59	m/s

Table 6.7: Breakdown of the total landing and take-off distance of the MUAV

Parameter	**Symbol**	**Value**	**unit**
Landing ground distance	$s_{groundland}$	88.7	m
Landing airborne distance	$s_{airland}$	50.3	m
Take-off ground distance	$s_{groundTO}$	33.5	m
Take-off airborne distance	s_{airTO}	96.2	m

Table 6.6 shows the total take-off and landing distance, while table 6.7 shows a break down of the total take-off and landing distances into the ground and airborn part. Table 6.7 shows a relatively short take off distance compared to initial estimations. This allows the MUAV to take-off from other sites than only a dedicated runway. Also the ground landing distance shows a promising value of 113.4m, which is calculated assuming worst case scenario settings (wet unpaved runway). The take-off airborne distance has been calculated assuming a minimum climb gradient of 8.5 degrees restricted by regulations (CS-23.65). The minimum take-off airborne distance is that when a climb gradient of 32 is assumed, resulting in a distance of 27 meters.

6.4 Aerodynamic characteristics

In this section the aerodynamics characteristics of the MUAV are presented. First an analyses of the drag is presented in subsection 6.4, which is followed by an analysis of the general aerodynamic properties of the MUAV in subsection 6.4

Drag analysis

Drag is an important parameter as it restricts the performance in many ways. To be able to asses the performance of the current design, a superposition method is used in which all the different contributors to the total drag have been evaluated separately. The total drag can be broken down in two major classifications: induced drag and zero-lift drag. The first one is related to the total lift coefficient, whereas the second is related to the speed of the plane.

Table 6.8: Drag coefficients for all components in cruise conditions

Component	C_{d0}	Contribution
Fuselage	0.0063	30.1%
Wing	0.0056	26.8%
Horizontal tail	0.0036	17.2%
Vertical tail	0.0036	17.2%
Landing gear	0.0003	1.4%
Struts	0.0013	6.2%
Trim	0.0002	1.0%
Total	0.0209	100%

For the wing, the total drag contribution is calculated from the drag breakdown given in XFLR5[1]. The other contributing elements of the MUAV to the total drag are given in table 6.8. From this table it can be seen that the highest two contributions to the drag come from the fuselage and the wing. This is logical, due to the fact that these components have the most contact with the airflow. What is important for the design, is that these values for the landing gear and the struts are based on highly efficient structures. If conventional circular beams are chosen for the design, the value for C_{D0} will drastically increase. The total resulting drag parameters are given in table 6.9.

Table 6.9: Drag coefficients and total drag in cruise conditions

C_{DiW}	C_{D0W}	C_D	D
$6.3338 \cdot 10^{-4}$	0.0054	0.0209	174.44

Main Aerodynamic performance parameters

There are many design choices that influence the wing and its performance. A summary of a the main design characteristics and their values is given in table 6.10. From these values the main aerodynamic

Table 6.10: Main design parameters wing

Parameter	Value	Remark
Wingspan	6 m	Given as a requirement
Aspect ratio	10 –	Given as a requirement
Taper ratio	1 –	For user friendliness(Effects are small)
Twist angle	0 deg	Already favourable stall characteristics
Incidence angle	0 deg	Not as relevant for unmanned missions

parameters for a 3D finite wing can be found. An overview of these parameters is given in table 6.11

In figure 6.8 the most important polars for the whole wing are given. In figure 6.8a the lift coefficient is plottted against the the angle of attack from stall speed up until cruise. In figure 6.8b the lift coefficient is plotted againt the drag coefficient for the same speed range.

[1] XFLR5 v6.02 Beta

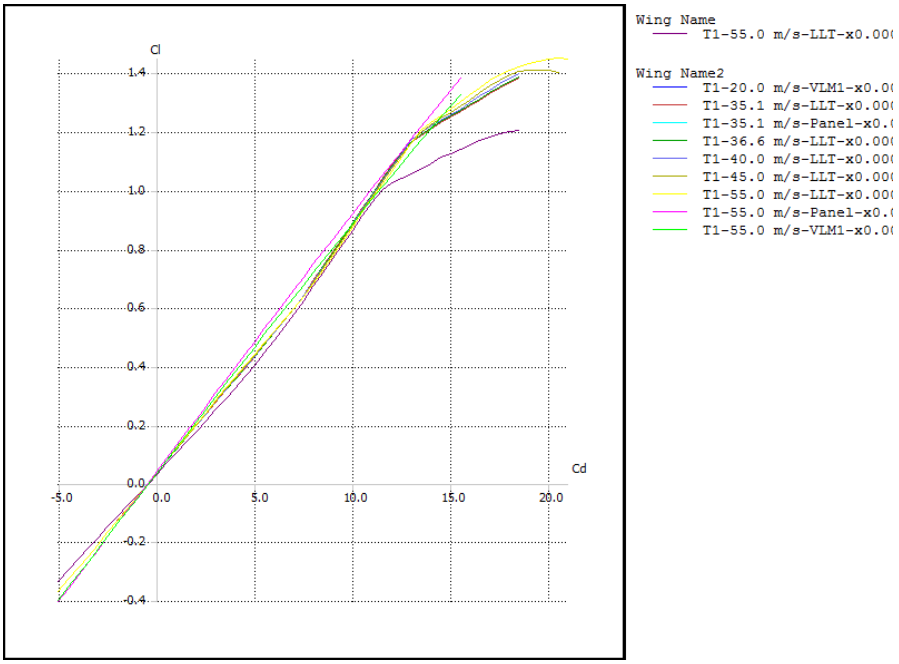

(a) C_L versus α

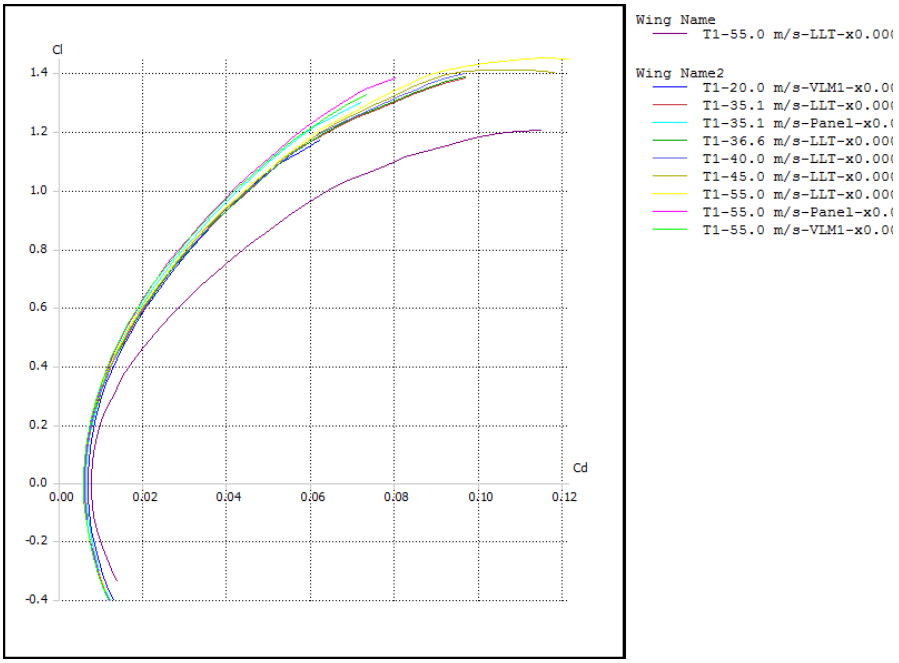

(b) C_L versus C_D

Figure 6.8: Polars for the 3D wing

Table 6.11: Summary of the main aerodynamic performance parameters for both the wing and airfoil

Parameter	Wing	Airfoil
$C_{L\alpha}$	0.0664 °	0.1097 °
C_{Lmax}	1.39	1.588
α_{stall}	22.5°	17°
α_{trimm}	1.65 °	0.5 °
α_{0L}	$-0.5°$	$-0.5°$

In this paragraph the most important conclusions from the table will be discussed. The first conclusion is that the maximum lift coefficient for the 3D case is lower compared to the 2D case shown in figure 4.1b. This lower value stems from the fact that there is efficiency loss in a finite wing due to pressure differences. Although lower, the value for C_{Lmax} is still high enough to provide sufficient lift during take-off at a stall speed of 20 m/s. The second important conclusion is that the stall angle increases substantially, which is favourable because it increases the freedom of the user.

6.5 Sensitivity analysis

Aside from the subsystem sensitivity analysis, system wide sensitivity analysis should be done to make sure that the product itself has a stable design point. If designed correctly the product should be reasonably forgiving to designer and customer mistakes. The sensitivity to some driving product parameters will be treated in this section.

Some subsystems are sensitive to changes in the design parameters while others are not. The electrical system does not really depend on design parameters for example, and is mostly driven by stakeholder needs. The most sensitive subsystems are the load bearing subsystems, which are the wing, fuselage, landing gear, and partly the empennage. These subsystems will be analysed on their sensitivity to certain changes in design parameters. Most parameter changes ultimately lead to an increase in MTOW, The general effect of parameter changes can be seen in the following items.

- **Payload/module mass**
  Increasing the payload or module mass effectively increases the MTOW which drives the structural design of the fuselage, wing, and empennage. This also has influence on the IDS as the c.g. of the payload bay is positioned in the fuselage after the nose cone and before the centre wingbox.

- **Endurance**
  Increasing the endurance will lead to a higher fuel mass. The fuel fraction is small so increases in fuel weight will not have a drastic effect on the MUAV. Doubling the endurance means at least twice the amount of fuel is necessary, which comes down to and added weight of around 1[kg] of fuel. This is a slight increase in MTOW which effects the fuselage and wing weight.

- **Cruise speed**
  Changing the cruise speed has effects on all the subsystems. Different cruise speed means a different propulsion power is required, this different power requires a different engine choice which leads to a change in MTOW. Cruise speed also has a big influence on the fuel consumption as the drag is a function of the velocity squared. so an increase in cruise speed not only leads to more engine mass, but also mure fuel mass.

- **IDS**
  Changing the IDS will change the range of configurations for which the MUAV has to be designed. This mainly concerns the stability and controllability of the MUAV, which influences the tail length(increases fuselage weight) and tail size(increases tail weight). This effect has been studied extensively in section 4.4.

- **c.g.**
  changing the c.g. has effects on the stability, controllability, and landing gear location. More information on this effect can be found in section 4.4. Ultimately the tail size will have to change with a change in IDS which leads to an increase in fuselage weight.

From these items it is clear that MTOW is the main parameter that changes with the other parameters. The effect of MTOW changes has been investigated for the subsystems that are most sensitive to MTOW changes: fuselage, wing structure, and landing gear. The empennage has been excluded since it does not have the same level op depth considering structural design. The results of the sensitivity analysis towards MTOW changes can be found in table 6.12. The fuselage design was mostly driven by the boxwing

Subsystem	Fuselage	Wing structure	Landing gear
Subsystem weight increase for 10% MTOW increase [%]	< 1	5.8	5.9

Table 6.12: Structural designed subsystem sensitivity to increase of MTOW

torsional loads, of which the MTOW sensitivity is not known at this point. However, the fuselage design process closely resembles the wing structural design and as such the wing structure sensitivity will be relied on at this point. The results for wing structure and landing gear sensitivity indicate that the payload mass fraction can possibly be increased at higher MTOW since the snowball effect is damped. Table 6.12 shows a promising sensitivity of the structural subsystems to the MTOW. This sensitivity analysis verifies the subsystem design as it ensures a stable design point. Small changes to important parameters will have a small effect on the subsystem designs, but it will not influence the design choices made to get the current design. More research should be put into the sensitivity of the fuselage structure as this has not been analysed with enough detail.

This concludes most of the MUAVverification. The only thing left is to cross-reference the design results with the requirements to see if all the requirements were met. This will be discussed in the next section.

6.6 Requirement compliance matrix

This section includes the requirement compliance matrix as well as a feasibility analysis of the requirements that were not met. The requirement compliance matrix has been divided into three tables. Table 6.14 contains the systems requirements, and in tables 6.15 and 6.16 the subsystem requirements can be found. The latter two tables contain the ID of the subsystem requirements, and are not written out. To understand which ID belongs to which subsystem requirement, the reader can use the requirement specification document [1] that will accompany this report. For clarification, table 6.13 contains an overview of the notation that is used to link a subsystem to a requirement. Most of the system requirements are linked to one or more subsystem requirements, and therefore these system requirements are met when all the subsystem requirements corresponding to that system requirement are met. A checkmark is used when a requirement is met and an X is used when a requirement is not met. There are some wing requirements that have not been evaluated due to the depth of detail at which the wing is designed, these requirements have been marked with an $\sim$. The parent corresponding to these subsystem requirements are however check marked (when all the other subsystem requirements are met). How the system requirements are coupled to the subsystem requirements can be found in the requirement specification document. The feasibility analysis is performed in order to rationalise why the design does not meet the requirement(s), or which modifications would be required in order to meet the requirement(s). When a requirement is not met, the actual value of this requirement is stated in the value column of the requirement compliance matrix.

Table 6.13: Link between an ID and a subsystem

Notation	Subsystem
F	Fuselage
W	Wing
C	Centre wing box
L	Landing gear
P	Power and propulsion
B	Payload bay
E	Electronics
S	Parachute
T	Empennage

6.6.1 Feasibility analysis

There are three systems requirements that have not been met. These requirements are listed below, and it is rationalised why these requirements have not been met.

- **M2RU-SYS-SO2-06: Maximum take-off weight shall be lower than 80 kg**
  The reason why this requirement has not been met is that the requirement itself has not been defined properly. It is either the OEW shall not be higher than a certain value, or the MTOW shall be at least a certain value.
- **M2RU-SYS-SO5-01: The propulsion system shall have zero emission**
  This requirement has not been met due to the fact that power suppliers which have zero emission are simply too heavy. It is therefore that the choice fell on bio-fuel. Even though bio-fuel does not have zero emission, it does have zero net emission. In order to meet this requirement, the maximum OEW requirement must be increased. The zero emission and maximum OEW requirements simply do not go hand-in-hand with each other.
- **M2RU-SYS-SO5-02: The vehicle shall be 100% recyclable at the end of its life**
  Based on reference data, it is expected that the MUAV shall be 90 % recyclable at the end of its life. The MUAV is built out of many sorts of materials, and there are always materials that can be recycled. Technology is simply not that advanced to guarantee a 100 % recyclable aircraft, and so no recommendations can be given.

Table 6.14: Systems requirement compliance matrix

ID	Requirement	Compliance	Value
M2RU-SYS-S01-01	The empennage shall be fixed	✓	
M2RU-SYS-S01-02	Undercarriage shall be fixed to the fuselage	✓	
M2RU-SYS-S01-03	It shall be possible to attach various leading edge, trailing edge and winglet concepts to the wing box	✓	
M2RU-SYS-S01-04	The vehicle shall be able to be equipped with different wing concepts	✓	
M2RU-SYS-S01-05	The stability margins of the vehicle shall be variable	✓	
M2RU-SYS-S01-06	Experimental investigation of various high-lift devices shall be possible	✓	
M2RU-SYS-S01-07	Experimental investigation of various types of active and passive winglets shall be possible	✓	
M2RU-SYS-S01-08	Assessment of control strategies for active load alleviation using high-lift devices shall be possible	✓	
M2RU-SYS-S01-09	Assessment of control strategies for flight dynamic control shall be possible	✓	
M2RU-SYS-S01-10	Evaluation of flow control devices shall be possible	✓	
M2RU-SYS-S01-11	Evaluation of various types of propellers shall be possible	✓	
M2RU-SYS-S01-12	Three-axis control of the vehicle shall be provided by the empennage	✓	
M2RU-SYS-S01-13	Vehicle configuration shall be adjustable within 90 minutes	✓	
M2RU-SYS-S01-14	Leading edge of the wing box shall have a sweep angle of 0 degrees	✓	
M2RU-SYS-S01-15	The fuselage shall be fixed	✓	
M2RU-SYS-S01-16	The fuselage shall be able to carry the telemetry, the data acquisition system, the fuel and the propulsion system	✓	
M2RU-SYS-S01-17	The vehicle shall be able to accommodate measurements/sensors for the modular devices used	✓	
M2RU-SYS-S01-18	The vehicle shall be able to accommodate a wing with a surface area between 1.5 and 4 m^2	✓	
M2RU-SYS-S01-19	The vehicle shall be able to accommodate a wing with a taper ratio between 0 and 1	✓	
M2RU-SYS-S01-20	The vehicle shall be able to accommodate a wing with an aspect ratio between 5 and 15	✓	
M2RU-SYS-S01-21	The vehicle shall be able to accommodate a wing with a sweep angle between -10 and +15 degrees	✓	
M2RU-SYS-S02-01	Cruise speed shall be higher than 55 m/s	✓	
M2RU-SYS-S02-02	Stall speed shall be lower than 20 m/s	✓	
M2RU-SYS-S02-03	The wing shall have an aspect ratio of 10	✓	
M2RU-SYS-S02-04	The maximum load factor shall be at least 5 g	✓	
M2RU-SYS-S02-05	The vehicle shall have an endurance of at least 30 minutes cruise in basic configuration	✓	
M2RU-SYS-S02-06	Maximum take-off weight shall be lower than 80 kg	X	94
M2RU-SYS-S02-07	Maximum payload mass shall be at least 20 kg	✓	
M2RU-SYS-S02-08	The wingspan shall be at least 6 meters	✓	
M2RU-SYS-S02-09	The vehicle shall be able to take-off and land without any assistance	✓	
M2RU-SYS-S03-01	The vehicle shall be unmanned	✓	
M2RU-SYS-S03-02	A safety margin of 1.5 shall be applied	✓	
M2RU-SYS-S03-03	A parachute system shall be included in case of in-flight failure	✓	
M2RU-SYS-S03-04	Onboard electronics shall survive impact loads during crash	✓	
M2RU-SYS-S03-05	Flight altitude shall be below 100 m above ground level	✓	
M2RU-SYS-S03-06	The vehicle structure must be able to support limit loads without detrimental, permanent deformation. At any load up to limit loads, the deformation may not interfere with safe operation	✓	
M2RU-SYS-S03-07	The vehicle structure must be able to support ultimate loads without failure for at least three seconds	✓	
M2RU-SYS-S04-01	Manufacturing costs shall be lower than €50,000	✓	
M2RU-SYS-S04-02	Vehicle shall be able to be transported over public road	✓	
M2RU-SYS-S05-01	The propulsion system shall have zero emission	X	Biofuel
M2RU-SYS-S05-02	The vehicle shall be 100% recyclable at the end of its life	X	90%
M2RU-SYS-S06-01	The vehicle shall be operated within the line of sight of the operator	✓	

Table 6.15: Compliance matrix for the subsystem requirements (part 1 of 2)

ID	Compliance	Value	ID	Compliance	Value	ID	Compliance	Value
F1	✓		W5	✓		W9	✓	
F1.1	✓		W5.1	✓		W9.1	✓	
F1.2	✓		W5.2	✓		W10	✓	
F1.3	✓		W5.3	✓				
F2	✓		W5.4	✓				
F2.1	✓		W5.5	∼	-			
F2.2	✓		W5.6	∼	-			
F3	✓		W5.7	✓		C1	✓	
F3.1	✓		W5.8	✓		C2	✓	
F3.2	✓		W5.9	✓		C3	✓	
F3.3	✓		W5.10	✓		C4	✓	
F3.4	✓		W5.11	✓		C4.1	✓	
F3.5	✓		W6	✓		C4.2	✓	
F3.6	✓		W6.1	✓		C4.3	✓	
F4	✓		W6.2	✓			✓	
F4.1	✓		W6.3	✓		L1	✓	
F4.2	✓		W6.4	✓		L1.1	✓	
F5	✓		W6.5	∼	-	L1.2	✓	
F5.1	✓		W6.6	∼	-	L1.3	✓	
			W6.7	✓		L1.4	✓	
W1	✓		W6.8	✓		L2	✓	
W1.1	✓		W6.9	✓		L2.1	✓	
W1.2	✓		W6.10	✓		L2.2	✓	
W1.3	✓					L3	✓	
W2	✓		W7	✓		L3.1	✓	
W2.1	✓		W7.1	✓		L4	✓	
W2.2	∼	-	W7.2	✓		L4.1	✓	
W2.3	✓		W7.3	✓		L4.2	✓	
W2.4	✓		W7.4	✓		L4.3	✓	
W2.5	✓		W7.5	∼	-	L5	✓	
W2.6	✓		W7.6	∼	-	L5.1	✓	
W3	✓	-	W7.7	✓		L5.2	✓	
W3.1	∼	-	W7.8	✓		L5.3	✓	
W3.2	∼	-	W7.9	✓		L6	✓	
W4	✓		W8	✓		L6.1	✓	

Table 6.16: Compliance matrix for the subsystem requirements (part 2 of 2)

ID	Compliance	Value	ID	Compliance	Value	ID	Compliance	Value
L6.3	✓					E3.1	✓	
			B1	✓		E3.2	✓	
P1	✓		B1.1	✓		E4	✓	
P1.1	✓		B1.2	✓		E4.1	✓	
P2	✓		B1.3	✓		E4.2	✓	
P2.2	✓		B1.4	✓		E5	✓	
P3	✓		B2	✓		E5.1	✓	
P3.1	✓		B2.1	✓		E5.2	✓	
P3.2	✓		B3	✓		E5.3	✓	
P3.3	✓		B3.1	✓		E6	✓	
P3.4	✓		B3.2	✓		E7	✓	
P3.5	✓		B3.3	✓		E7.1	✓	
P3.6	✓		B3.4	✓		E7.2	✓	
P3.7	✓		B4	X		E7.3	✓	
P3.8	✓		B4.1	X	3	E8	✓	
P4	✓		B5	✓		E8.1	✓	
P4.1	✓		B5.1	✓		E8.2	✓	
P5	✓		B5.2	✓		E9	✓	
P5.1	✓		B6	✓		E9.1	✓	
P5.2	✓		B6.1	✓		E9.2	✓	
P5.3	✓		B6.2	✓		E10	✓	
P6	✓					E10.1	✓	
P6.1	✓					E10.2	✓	
P6.2	✓					E11	✓	
P7	✓		E1	✓		E11.1	✓	
P8	✓		E1.1	✓		E11.2	✓	
P8.1	✓		E1.2	✓				
P8.2	✓		E1.3	✓		S1	✓	
P8.3	✓		E2	✓		S1.1	✓	
P9	✓		E2.1	✓		S1.2	✓	
P9.1	✓		E2.2	✓		S1.3	✓	
P10	✓		E2.3	✓		S1.4	✓	
P11	✓		E2.4	✓		S2	✓	
P12	✓		E3	✓		S2.1	✓	
P12.1	✓		E3.1	✓		S2.2	✓	
P12.2	✓		E3.2	✓		S2.3	✓	

Chapter 7

Integration of risk and RAMS analysis in the design process

In the design process of a new product, it is crucial to identify and assess risks in the earliest stage possible. Once the risks are identified and assessed, they can be anticipated upon and incorporated in the design of the new product. To do this in a systematic way a risk management system is used. This risk management system itself is described in section 7.1.1, whereas the way risk mitigation is incorporated into the design is described in section 7.1.2. Additionally a Reliability, Availability, Maintainability and Safety (RAMS) analysis and optimisation is provided in section 7.2. This will give an indication of the reliability, availability, maintainability and safety of the product. Next to the RAMS analysis the design choices inspired by RAMS considerations are presented in section 7.2.5.

7.1 Risk management

In this section the risk management process used during the design is discussed. First a systems of the tools we used for risk management is discussed in section 7.1.1. Followed by a discussion on how the risk analysis has affected or inspired various design choices.

7.1.1 Risk management system

During the project each week the risks are assessed. This is done by identifying new risks and assessing existing risks that might have changed due to design changes, decisions or external parameters. The risks are recorded in the risk register and the risk map (see appendix D). A identifier is assigned to every risk as well as a cause,risk event, consequence, likelihood, effect and mitigation method. To asses the priority of the risk, a risk assessment matrix is drawn up which can be found in the risk map. The risk assessment matrix positions the risks based on their impact and likelihood. Risks with high values for both should be given the highest priority. From this risk assessment matrix the top three technical risks are found, these are presented in table 7.1.

7.1.2 Incorporation of risk mitigation into the design process

To give an insight into the way the risk mitigation is intertwined into the design process, the mitigation methods for the top three technical risks provided in table 7.1 are presented here. The mitigation methods are focused on preventing the risk event from happening or on reducing the consequence of the risk. Starting of with the risk of structural failure due to high gust loadings. To mitigate this risk, two options were available in the design process. The first option was to increase the maximum load factor, to make sure the aircraft would be able to cope with higher gust loadings. As this is disadvantageous in terms of structural weight and the exact data for vertical gusts to base this load factor on was not available, a different approach was chosen. To mitigate this risk a program will be developed. This program enables

Table 7.1: Top three technical risks

#	Risk event	Likelihood	Effect	Mitigation method
32	Structural failure	medium	Catastrophic	pre-flight wind check
30	Unpredicted dynamic behaviour	Medium	Critical	Good engineers, good product manual, pre-flight checks
27	Loss of lift in-flight	Low	Critical	Parachute, design for higher loadings

the user to decide on what the maximum cruise speed can be flown at with a certain gust speed. For the second highest risk a similar procedure was followed. To avoid unpredicted dynamic behaviour, a stability tool will be created. With this stability tool the user is able to check for stability based on their configuration. Furthermore the empennage is designed to ensure stability for the entire IDS. The third highest risk is deemed to be the loss of lift in flight due to failure of wing components. To mitigate this risk, the wing box is designed in such a way that the modules that can be attached upon it, do not have to carry any loads. A second measure to anticipate the failure of wing components, is that the wing is designed to be able to land and take-off without the use of high lift devices. So in case of a failure for these systems the wing will still provide enough lift. In case any of the mitigation methods presented would prove to be inadequate an additional safety system is build in by means of a parachute. The risk mitigation is done in an analogous procedure for the remainder of the identified risks.

7.2 RAMS engineering

A RAMS analysis is required to identify how well the MUAV can perform its intended function and how this can be optimised. In this section the reliability of the MUAV is assessed in subsection 7.2.1, the maintainability in subsection 7.2.2 and the availability in subsection 7.2.3. Finally the safety will be assessed in subsection 7.2.4 by looking at the Failure Mode and Effect Analysis (FMEA) together with the risks identified in the previous section. The analysis in this section is based on a lifetime of 10 years, in which 10 tests of 30 min will be performed each week throughout the academic year of 40 weeks. This leads to a system life time of 2000 hours and cycle life time of 4000 hours.

7.2.1 Reliability

In this subsection the reliability of the MUAV is assessed. Reliability is the ability of a component or system to fulfil its intended function [27]. The reliability of a system depends on the reliability of the components included in the system as well as the relationship between the failure of components. The total combination of these relationships and the individual reliability of the components leads to the reliability of the total system.

The reliability of an individual component can be described by its Mean Time To failure (MTTF). This parameter describes the time during which the component is expected to perform its function successfully. Another performance measure for the reliability of a system is the failure rate λ_r. The failure rate is the inverse of the MTTF. The failure rate over the lifetime is observed to follow a bathtub curve as can be seen in figure 7.1 [27]. This curve consists of a burn in region, chance failure region and a wear-out failure region. During the burn in region the failure rate shows a decreasing pattern, whereas in the wear-out region the failure rate is increasing. In the chance failure region the failure rate remains reasonably constant. If the chance failure region is large compared to the other two regions, which is the case for electronic and structural components, the failure rate can be assumed to be constant.

The reliability of a component can be modelled with various failure distribution models. If a constant failure rate is assumed the failure distribution can be modelled with an exponential probability distribution [28]. The reliability of an individual component can be found with equation 7.1. The reliability of a component can be improved highly effective by adding identical standby redundant components. When

Figure 7.1: Typical bathtub curve.

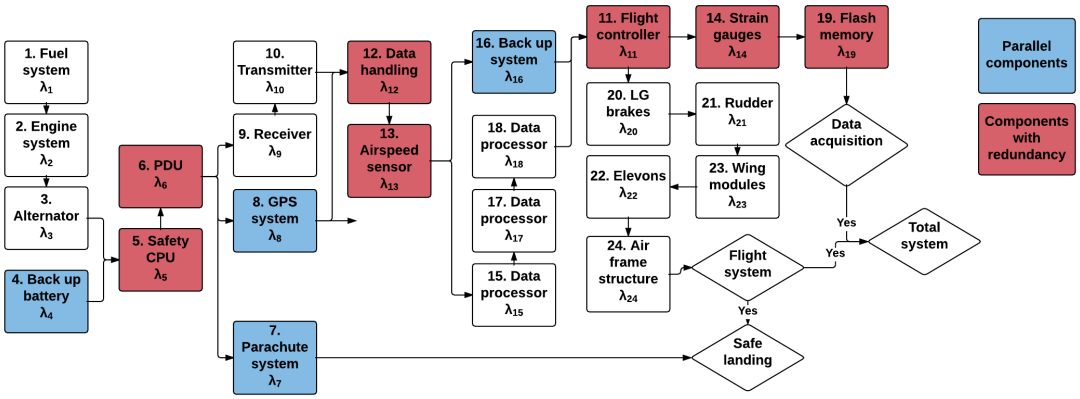

Figure 7.2: Reliability block diagram system

assuming that the switch is perfect the MTTF of the standby redundant system can be found by equation 7.2.

$$R(t_s) = e^{-\lambda_r t_s} \tag{7.1}$$

$$MTTF_s = \frac{N_c}{\lambda_r} \tag{7.2}$$

The reliability of the total system follows from failure relations within the system. The reliability block diagram in figure 7.2 gives a clear view on these relations. The reliability of a system in series, where if one component fails the entire system fails, is lower than the reliability of a parallel system where all systems in parallel have to fail. So different equations are required to determine the reliability of these different systems. For the reliability of a system in series equation 7.3 is used, whereas for a parallel system equation 7.4 is used.

$$R_s(t_s) = \prod_{i=1}^{n} R_i(t_s) = \prod_{i=1}^{n} e^{-\lambda_r t_s} \tag{7.3}$$

$$R_s(t_s) = 1 - \prod_{i=1}^{n} \left[1 - R_i(t)\right] = 1 - \prod_{i=1}^{n} \left[1 - e^{-\lambda_r t_s}\right] \tag{7.4}$$

Reliability block diagram

The reliability block diagram, which can be seen in figure 7.2, combines parallel and serial configurations. Parallel systems are indicated in blue and the red blocks indicate that redundancy has been added of that component. To calculate the reliability of this system, first the total reliability for every set of components in series leading up to a parallel system is calculated with equation 7.3. Then the total reliability of the systems in parallel is calculated, with equation 7.4. The system now consists of the different total reliabilities of the parallel systems, which are in series. So now the total reliability can easily be calculated with equation 7.3.

To give a better insight into the reliability per different function, the total system reliability is calculated as well as the reliability for the different functions. The different functions for which the reliability is calculated is the flight system functioning, the data acquisition functioning and the safe landing function. Furthermore the reliability is calculated for the system without parallel components and standby redundancy, for the system with only the parallel components added and for the system with parallel components as well as standby redundancy. This is done to be able to get an insight into the effect of the two measures to improve the reliability of the system. These results are displayed in table 7.2.

Function	Reliability (series)	Reliability (parallel)	Reliability (redundancy)	MTTF
Flight system	<1%	50.6%	68.9%	5369 hrs
Safe landing	<1%	93.1%	96.3%	53048 hrs
Data acquisition	<1%	23.9%	47.4%	3733 hrs
Total system	<1%	12.1%	32.7%	2679 hrs

Table 7.2: Reliability results from block diagram

It is clear from table 7.2 that the system reliability for a purely serial system in column one is too low. The addition of parallel components such as the back up processor, back up battery, Global Positioning System (GPS) and parachute system greatly improve the reliability for its different function, as can be seen in column two. The additional reliability for redundancy is achieved by adding a standby redundant component for the electrical components 5,6,11,12,13,14,19 in the reliability block diagram, see figure 7.2. The standby redundant electrical components do not contribute significant weights, while improving the reliability of the total system by 20.6 percent. The absolute values of the reliability are on the lower bound, because the failure rate data is for the most part data from before the year 2000 [29]. Since the reliability has improved significantly since then, the actual reliability will be higher.

The MTTF is given in the last column of table 7.2. This value represents the expected mean time before failure to occur. As can be seen in table 7.2, the MTTF for the total system is higher than the systems lifetime, which means the system is expected to fail at a time beyond the system lifetime.

Fault tree

A fault tree consists of a top event which is the number one undesired event that can occur. In the case of the MUAV it is the event that the MUAV mission is a failure. The events leading to this top event are systematically deduced. The fault tree of the MUAV is shown in figure 7.3. The symbols used are explained in [27]. It does not contain all possible failure modes of the system, therefore it is not an exhaustive logic tree. Only the events that are considered important for the failure of the system are included. Based upon the evaluation of the tree, important systems in terms of failure can be identified. In this case the fault tree is used to give the logic of the system with minimum understanding of the overall functionality and logic of the system. It was used to help identify the systems that will impact the mission the most when failure occurs. More in depth analysis of this tree and further development of the system logic are tasks for later design stages of the MUAV.

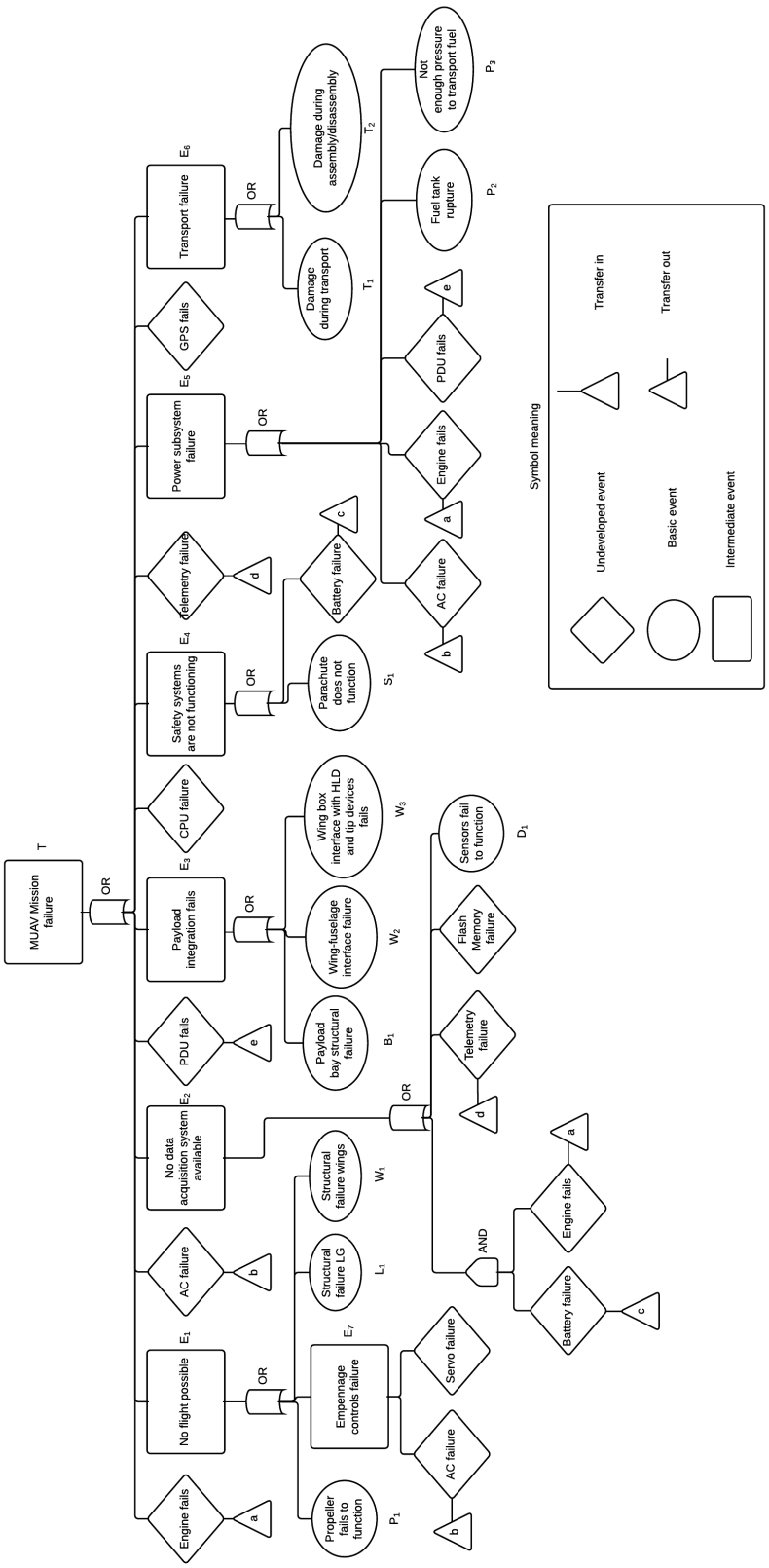

Figure 7.3: Fault tree of the MUAV mission

7.2.2 Maintainability

In this section an estimation is made on the amount of maintenance required for the MUAV. The estimation is based on the data from a US Air Force database. This database, the "Acquisition management Aircraft historical Reliability and Maintainability Data" documents the maintenance data for air planes from the US Air Force fleet [1].

From this data the applicable subsystems are selected and the associate MTBMs and manhours are presented in table 7.3. The type 1 MTBM and Man Hours stands for the inherent maintenance. This consists of unscheduled and on-equipment maintenance. The type 2 MTBM and Man hours stands for the induced maintenance, which is maintenance caused by external factors rather than an internal failure pattern. The type 3 stands for maintenance with no defect, so these are scheduled maintenance actions. To measure the maintainability the MTBM(C) and the DMMH/FH parameters are suggested [30], which can be calculated by equations 7.5 and 7.6 respectively. Where TFH is denoted as the total flight hours, TCMA is denoted as the total corrective maintenance action and TCMH is denoted as total chargeable man-hours in equations 7.5 and 7.6. The first factor stands for the total corrective mean time between maintenance, which includes the types 1,2 and 6. With the calculation for the applicable systems of the reference aircraft the MTBM becomes 975.6 hours. The second term stands for direct maintenance man hours per flight hour and is 1.58 Man hours per flight hour for the total of the subsystems applicable to the MUAV.

Table 7.3: AFALD PAMPHLET 800-4 maintenance data in hours

System	MTBM 1	MTBM 2	MTBM 6	MH 1	MH 2	MH 6
Airframe	20.7	20.01	97.96	4212	1523	1011
Landing gear system	21.14	64.03	93.09	3344	925	2001
Flight controls	33.15	83.08	56.28	2821	509	1132
Electrical power supply	177.38	656.3	375.03	2896	81	194
Fuel system	128.69	570.7	172.71	1610	108	830
Instruments	190.23	820.38	120.42	295	29	388
Autopilot	144.24	2187.67	226.31	391	2025	285
Radio navigation	125.01	1458.44	729.22	590	26	87
Emergency equipment	1312.5	4375.33	1875.14	15	20	55

$$MTBM(C) = \frac{TFH}{TCMA} \tag{7.5}$$

$$DMMH/FH = \frac{TCMH}{TFH} \tag{7.6}$$

7.2.3 Avalability

The availability of a system is defined by the ratio of the uptime over the uptime plus downtime together. The system downtime of the MUAV differs from a regular aircraft due to the fact that the several subsystems of the MUAV need to be assembled and disassembled before flight and before transportation. The assembly times can be found in table 7.4. Furthermore the system is not able to fly at desired cruise speeds for certain vertical gust speeds, meaning the systems are not available at those days. More research should be done for these factors to get a more accurate estimation of these times.

7.2.4 Safety by FMEA analysis

FMEA is a powerful tool to asses the reliability and safety of the system. It can be used in all design phases and from system functions to component level. The FMEA that is made for this project is one that

[1] AFALD PAMPHLET 800-4 `http://ntrs.nasa.gov/archive/nasa/casi.ntrs.nasa.gov/19920000819.pdf`

Table 7.4: Time to adjust configuration breakdown

Step	Description	Time estimation (min)
1	Attach the wings	15
2	Attach and connect the payload	40
3	Connect the data and power systems	10
4	Perform payload checklist	15
	Total	80

is of the highest level: system functions. The FMEA of the MUAV can be seen in figure 7.4 and in figure 7.5. In these figures the first column is the column where the system functions of the MUAV are listed. A failure has occurred and this function can not be fulfilled anymore. The potential failure mode(s) are listed in the second column. The potential effect of the failure on the MUAV is described in the third column. The severity of the failure, the probability of occurrence and the detectability are identified as described in section 4.5 of [27] from a scale of 1 to 10 (with 10 being the worst case) and are listed in the fourth, sixth and eighth column respectively. The potential causes of the failure and the current design controls are recorded in the fifth and seventh column respectively. Finally a Risk Priority Number (RPN) rating can also be determined for each failure mode and its effect. This rating is based on the severity, probability of occurrence and detectability. The RPN is listed in the ninth column, failures that have a high RPN rating are considered high risk items and have to be mitigated. This tool is closely related to the risk register and the risk map already discussed in section 7.1.1. In other words the items in the FMEA are also items in the risk register that represent technical risks. The downside of the FMEA is that it provides very little insight into the reliability of the system and assesses only one failure at a time. On the other hand it provides valuable qualitative information about the system design and operation. In the detailed design phase an FMEA can be made on component or sub-component level as well. From the FMEA it can be concluded that currently no further action has to be taken with respect to the failures listed in figure 7.4 and figure 7.5. Most of the failures were already considered in the conceptual design phase and the mitigation methods described in section 7.1.2 were incorporated in system and subsystem design. Therefore the RPN rating in the ninth column of the FMEA is not high for any item listed, considering this rating can reach a value of 1000.

7.2.5 RAMS inspired design choices

There was close communication during the subsystem design phase in order to make sure the RAMS of the MUAV was as good as possible without sacrificing performance. Several subsystems had their design modified in order to improve the RAMS. The choices made in these designs will be treated in this subsection.

Electrical system redundancy

The RAMS had influence on the topology of the electrical system. The electrical system was already fully designed after it was found out the system did not meet the expected safety standard. There was no parallel redundancy and no override computer to ensure safe operation in case of failure. Suitable redundant components as well as a watchdog unit to monitor the performance of each component were selected to improve the reliability of the electrical subsystem and the MUAV as a whole.

Untapered wing box

After the conceptual design phase a tapered wing box was chosen for the default wing. However during the RAMS analysis it became apparent that the use of an untapered wing box would make it easier for the customer to design and attach their wing box modules. Therefore an untapered wing box was chosen for the default wing.

System: MUAV
Subsystem:
Component:
Design Lead:
Core Team: 01-DSE group

Potential Failure Mode and Effects Analysis (Design FMEA)

Key Date:

FMEA Number: Project M2RU
Prepared By: Roeland de Breu
FMEA Date: 18/01/2016
Revision Date:
Page 1 of 5

Item / Function	Potential Failure Mode(s)	Potential Effect(s) of Failure	Sev	Potential Cause(s)/ Mechanism(s) of Failure	Prob	Current Design Controls	Det	RPN	Recommended Action(s)	Responsibility & Target Completion Date	Action Results: Actions Taken	New Sev	New Occ	New Det	New RPN
1	2	3	4	5	6	7	8	9	10	11	12	13	14	15	16
Provide enough fuel to power up the engines and the electrical generator	Not enough fuel avaiable for the power generation	No lift-off, No thrust, undesired decent	8	Insufficient pressure to force the fuel from the tank to the engine	1	System analysis modeling vehicle inegration testing	2	**16**							
Provide enough shaft power to attain the required thrust settings	Not enough shaft power	No lift-off, Not enough thrust to maintain airspeed or continue mission abort	8	Engine malfunction	2	System analysis modeling vehicle inegration testing	2	**32**							
Provide enough electrical power for the subsystems and/or payload systems	Not enough electrical power	Systems will not power-up, mission abort	8	Alternator malfunction	2	System analysis modeling vehicle inegration testing	2	**32**							
Provide back-up to major subsystems for save landing in-case of power failure	No back-up power available	No back-up battery available	4	Insufficient power left on the battery (end-of-life), battery leakage, battery malfunction	3	System analysis modeling vehicle inegration testing	2	**24**							
Provide the computational power to process the data obtained on-board	No CPU available	Uncontrallable vehicle	9	No power and back-up power available, CPU burnout	1	System analysis modeling vehicle inegration testing	1	**9**							

Figure 7.4: FMEA of the MUAV for top level functions (part 1)

Regulate the power to each subsystem	PDU not available	No power to the subsystems, mission abort	8	PDU malfunction	2	System analysis modeling vehicle inegration testing	2	**32**							
Transmit data to ground station	No data is being send	Inability to monitor the vehicles progress	9	Broken transmitter, software routine malfunction	1	System analysis modeling vehicle inegration testing	3	**27**							
Receive data from the ground station	No data is being received	Inability to control the vehicle	10	Broken receiver, software routine malfunction	1	System analysis modeling vehicle inegration testing	3	**30**							
Track the GPS coordinates of the vehicle	No GPS coordinates are being recorded	Inability to locate the exact position of the vehicle	9	GPS malfunction	2	System analysis modeling vehicle inegration testing	3	**54**							
Provide 3-axis control of the vehicle	Controls are unresponsive or not desired	No adequate control to continue the mission	9	Flight controller malfunction or software routine malfunction	2	System analysis modeling vehicle inegration testing	3	**54**							
Provide power to the LG brakes	Brakes are not working sufficiently	Not enough rolling friction on the main landing gear wheels to stop within the desired landing distance	7	Servo's malfunction or software routine malfunction	2	System analysis modeling vehicle inegration testing	3	**42**							
Provide data storage	Flash memory not available	Loss of data	7	Flash memery malfunction	1	System analysis modeling vehicle inegration testing	2	**14**							
Provide sensors to measure relevant parameters	Sensors not available	Not sufficient data acquisation	7	Sensor malfunction	1	System analysis modeling vehicle inegration testing	1	**7**							

Figure 7.5: FMEA of the MUAV for top level functions (part 2)

Module integration fasteners

The wing box modules will be changed frequently which makes the way these are fastened an important design choice. The maintainability especially has to be taken into account here as repeatedly fastening a structure might compromise its rigidity. Therefore coupling bolts have been selected which is a bolting couple consisting of one bolt with internal thread and one bolt with external thread. This way screw threads in the wing box are avoided which would otherwise decrease the maintainability.

Fuselage doors

The fuselage doors can be opened by a one-click-system and thus reducing the time needed for refitting modules inside the payload bay. This improves the availability of the system.

Payload bay size

19-inch racks are frequently used to house electrical components such as computers and other electrical equipment. As these are widely known and available, making it an attractive choice for the payload bay size. Sizing the payload bay to account for the accommodation of 19-inch racks increases the availability and maintainability.

Chapter 8

Business case

The MUAV design has thus far only been discussed with regards to the stakeholder needs and engineering practises. However, the MUAV should also be made appealing for possible investors and customers. By having a proper business case, production planning, and design approach more customers and investors will be attracted to the product.

In this chapter the reader shall first be provided with a look into the future of this design project in section 8.1. Next is section 8.2 with a market analysis to appeal to possible investors. To give the customer an insight in the use of the MUAV, the operations and logistics will be discussed in section 8.3. A preliminary production plan has been laid out in section 8.4 to create an evenly distributed workload with few bottlenecks. In section 8.5 this chapter will be concluded with a discussion on the approach to sustainability during the design of the MUAV.

8.1 Future project

This report is called the 'Final report', however that does not mean the project is finished. In this section will focused on the steps that have to be taken before the final product can enter series production, and the costs involved with it. In figure 8.1 these steps are shown in a block diagram and appendix C shows an initial estimate of the time needed for each step. Finally the costs involved in all pre-production steps are shown in figure 8.2. To estimate the cost for personnel an hourly rate of 75 euros was used for engineers and 35 euros for workshop personnel.

On a few subsystems the preliminary design of the MUAV should still be finished. Especially the structural design needs some attention. The structure of the empennage should still be designed, while the wings and fuselage should be optimised. On top of that the stability and controllability should be iterated and optimised for the latest subsystem weights. When the preliminary design is done wind tunnel test should be performed to find the stability derivatives. The time needed to finish these steps was estimated based on the experiences of the last 10 weeks. The cost for the wind tunnel are based on the rates of the University of Washington[1].

When the preliminary design the MUAV should be designed up to the last detail in the detailed design phase. This phase will take a lot of time, the detailed design phase is typically 90% of the total design duration [31]. In this case this might be less, since a lot of off-the-shelf components were used. After that, a prototype has to be built and tested. Evaluation of this prototype might lead to changes in the design. Building a prototype is estimated to cost twice the manufacturing cost of the final product. When the performance and reliability of the prototype are satisfactory, the preparation for series production can start. In parallel with the design and testing phase, the potential costumers should be made aware of the product and the user manual and software should be developed.

As can be seen in figure 8.2 the development costs are estimated to be more than 3.6 million euros. This could be lowered by using students instead, who do not need to be payed. The development can be

[1] Services & Rates, Aeronautics and Astronautics, `https://www.aa.washington.edu/AERL/KWT/rateguide`, Accessed: 18-1-2016

done in projects which are part of the curriculum or a separate student project can be started. Another way to minimise the required investment for the DUT is finding other parties. Other institutions can be approached to cooperate in development and share the costs.

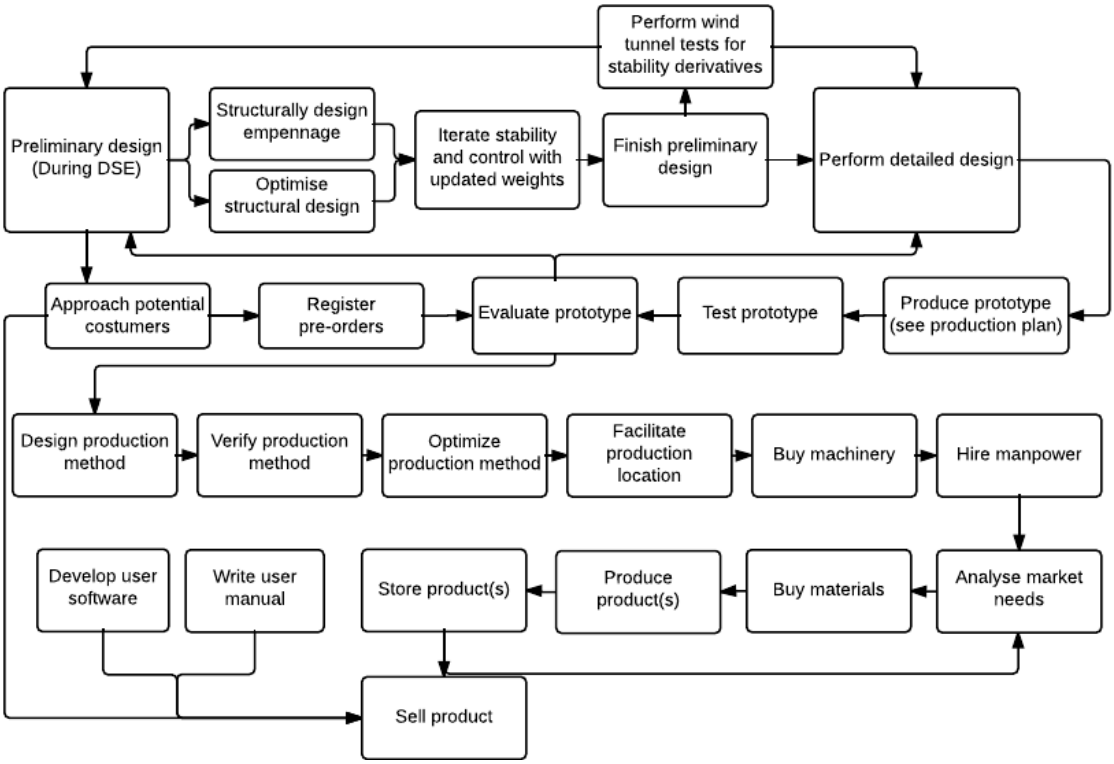

Figure 8.1: Project Design and Development logic

8.2 Market analysis

In this section the business potential of the project will be discussed. Since this is not the specific field of expertise of the team, Mr. Johan Spaans of the faculty of Technology, Policy and Management of Delft University of Technology has been contacted for advice. First there will be made a Strengths Weaknesses - Opportunities Threats (SWOT) analysis of the product after which a customer profile will be determined. Using that customer profile the market is sized, this section is concluded with a proposed strategy for pricing the MUAV.

8.2.1 SWOT analysis

This section provides an overview of the strengths, weaknesses, opportunities, and threats (SWOT) of the business venture. These four categories represent combinations of positive and negative, internal and external circumstances that influence the chance of success of the project.

Strengths

- **Purpose built**. This MUAV is the only one that has specifically been designed for the purpose of in-flight testing of aeronautical concepts. This implies that there are no direct competitors.
- **Low pricing**. If the manufacturing costs will be indeed lower than €50,000, a retail price between €80,000 and €200,000 will provide decent gross margins in the range of 37,5% to 75%. These

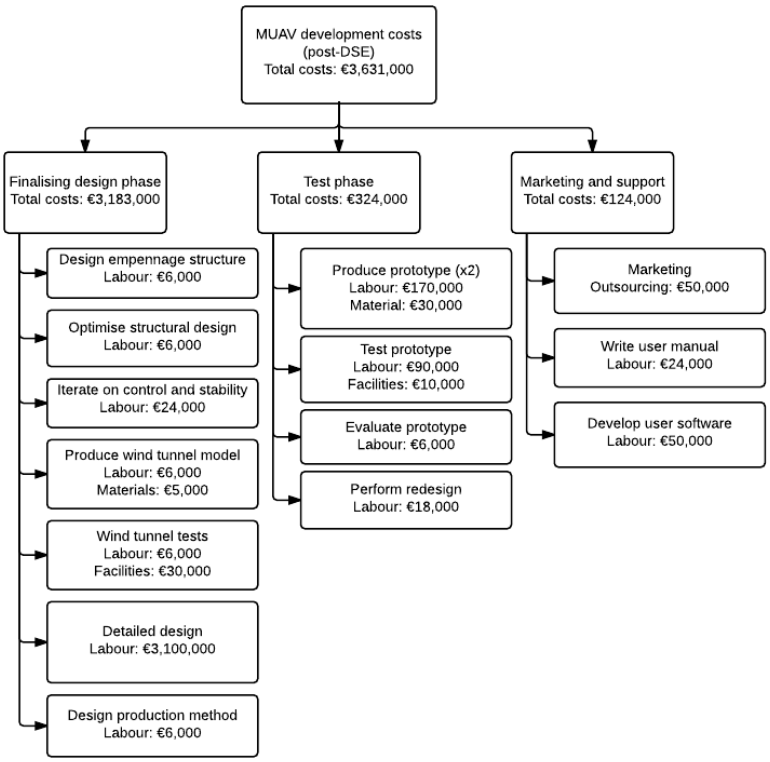

Figure 8.2: Cost Breakdown structure

figures are, however, rather low for UAV's this size. This low price will attract a broad customer base.

- **Sustainability.** Sustainability of the MUAV will provide potential buyers with a better position when lobbying for subsidiaries, permission to use airport facilities et cetera. Moreover, it will be good for the general image of the buyer.

Weaknesses

- **Built by other university.** Buying equipment form another university is not completely an economical decision. Customers might be reluctant to buy technology from other universities and prefer developing it themselves. This will provide interesting projects (like the one this team is on), might save costs and can gain positive publicity.
- **Size.** Six meters is not very small, posing potential problems in logistics and flying permission (see 'threats', below).

Opportunities

- **Growing demand for air travel.** In various densely populated developing countries such as India and China, large portions of those populations will soon get over the critical level of wealth enabling them to use air traffic as means of transportation. This will not happen overnight, but it is certain that it will happen, stressing demand for aviation technology and aeronautic research.
- **Competitive pertaining to manned flight.** UAV technology is highly competitive with respect to manned flight due both a lower investment and lower operational costs. Surely, it cannot take over all tasks of manned aerial research, but it can save costs significantly in the fields where the researcher is not required to be in the aircraft.

Threats

- **Public opinion.** UAV's are commonly associated with ethically challenging applications such as air raids and espionage. This makes society highly sceptic of drones flying over urban areas. The large wingspan of 6 meters and low cruising altitude of 100 meters do not contribute to a positive sentiment.
- **Regulations.** As a result of public scepticism and lack of expertise of governments, regulations on UAV use are strict and lagging massively behind technological development. Also, regulations vary widely per country. This induces great threats to the business case since it is fully dependent on the global market.

8.2.2 Customer profile

In order to size the market for the MUAV, a customer profile is required. Though specifically build for a technical university, the MUAV will be more widely deployable. Also it has been determined in a previous report [32] that focusing exclusively on universities does not yield enough market potential. The entire market for the MUAV has been determined to consist of the following customers:

1. Educational institutions such as DUT.
2. Government funded and independentent research facilities such as Netherlands Aerospace Centre (NLR).
3. Aircraft (part) manufacturers.

Still it can be hard to estimate the market size bottom up, as information is often classified in the aviation industry. Therefore another way of quantifying the market size of aeronautical experimental equipment is deployed.

8.2.3 Market size

As mentioned in the project description, current experiments with aircraft concepts make use of either wind tunnels or manned aircraft. One can assume that all potential customers of the MUAV make use of those facilities, luckily it is relatively easy to determine the presence of wind tunnels in a region (it is harder to determine how many experimental aircraft are present). This data provides useful information on the size of the aeronautical research market in that area. The reader should note that this does not mean that only institutes with wind tunnels are potential customers, many aeronautical companies rent test hours because a private wind tunnel is not profitable. The MUAV will be many times less capital intensive than a wind tunnel, therefore its customer base will be broader. Still, the number of wind tunnels is a good indicator of the size of the market. To avoid counting all the world's wind tunnels, data is extrapolated over three regions. This yields the following information[33]:

1. High wind tunnel density, first world. Regions: North America, Europe, Oceania, South Korea, Japan and Taiwan. One wind tunnel per 8 million inhabitants. Population: 1.4 billion. Estimated number of wind tunnel institutes: 175.
2. Medium wind tunnel density, second world. Regions: South-America, South Africa and the rest of Asia. One wind tunnel per 150 million inhabitants. Population: 4.8 billion. Estimated amount of wind tunnels: 32.
3. Low wind tunnel density, third world. Regions: Rest of Africa. Density unknown. Population: 1.1 billion. Amount of wind tunnels is assumed to be negligible.

An estimate should be made on what the presence of a wind tunnel says about the size of the market for MUAV. This is unavoidably arbitrary, To limit this the following additional factors are taken into account (besides the SWOT analysis and the three customer profiles enumerated above): a retail price

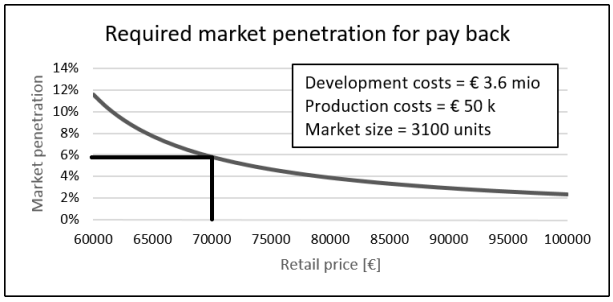

Figure 8.3: Required market penetation as a function of the retail price.

around €100,000, the fact that wind tunnels rent their facilities to many customers and the possibility that a customer acquires multiple MUAVS. The result is an estimated market size of fifteen sales per wind tunnel. Therefore it is estimated that the market sizes of the first and second world are respectively (approximately) 2600 and 500 pieces. The total market size is therefore estimated to be around 3100 pieces.

8.2.4 Pricing

Regarding the pricing of the UAV, two requirements have been set. First, the production costs cannot exceed €50,000 per unit. Second, the maximum pay back period is set on five years. As can be seen in figure 8.2, the latest estimate for development costs is determined to be €3,600,000. Figure 8.3 shows the relation between the retail price and required market penetration for payback.

Assuming for example a retail price of €70,000, it can be observed that the required market penetration is 6% for payback. This yields a monthly production of $60/(6\% \cdot 3100) = 3.1$ units per month. In figure 8.4 the costs are specified for this case. The production costs are based on material costs (both raw and off-the-shelf) and labour costs. It is assumed that workshop labourers cost €35 per hour. Also, the €10,000 depreciation on facilities and equipment is based on reference data from industrial projects. Multiplying with a fictional production of 200 units yields €2,000,000 in funds available. This seems sufficient, if not high. The assumption is therefore safe. Still, there is €8,000 contingency in production costs while staying within the €50,000 requirement. We can conclude that it is reasonable to believe that both requirements can be met.

The reader should note that increasing the retail price does not influence the production costs, it will only increase the gross profit. Since a requirement is set on the pay back period and no investments are made, the entire gross profit will be used for investment relief. To determine the exact retail price it is recommended to hold an extensive survey among potential customers.

Besides the cost for buying the MUAV itself, the manufacturing cost for modules should be considered. As examples, the default wing and the SHLD, discussed in section 4.1 and 5.2, can be considered. The cost of these modules are estimated to be €3038 and €2800 respectively. To put this numbers in some perspective, they can be compared to the costs of wind tunnel tests and flight testing. As can be seen in figure 8.2 using a wind tunnel facility for testing one model, already costs €30,000, while building the model will not be cheaper than building a module. The operational cost of a Cessna Citation, as used by the TU Delft, are around €1500 per hour[2].

It can be concluded that using the MUAV is much cheaper than both wind tunnel test and full-size flight testing. On top of that, it offers new test possibilities. Therefore, the current pricing is considered to be competitive.

[2]Typical Operating Cost, `www.sijet.com/download/charts.pdf`, Accessed: 26-01-2016

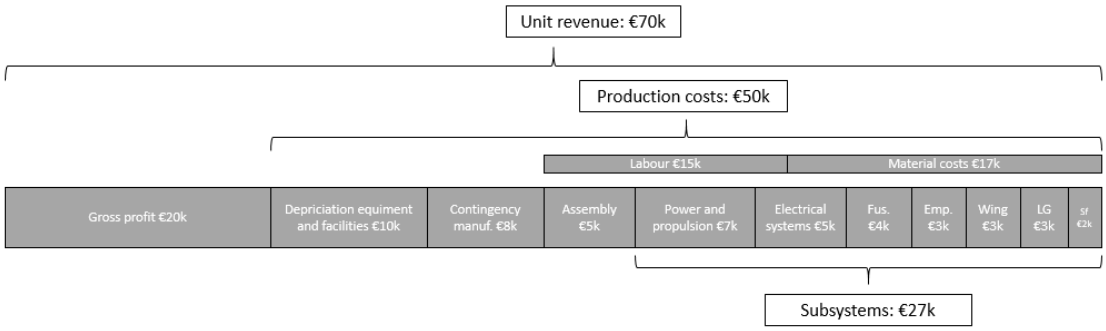

Figure 8.4: Unit cost specification for 6% market penetration for payback.

8.3 Operations and logistics

In this section the MUAV will be discussed from a user perspective. First all modular components and their limitations will be discussed in section 8.3.1. After that the limits to operating the MUAV as a whole are treated in section 8.3.2. After that some information will be given on the required test location, fuel and logistics in sections 8.3.3, 8.3.4 and 8.3.5 respectively.

8.3.1 Modules

In this section the possibilities and limits of each modular part will be discussed. First wings and wing devices will be treated, after that the payload, propeller and control strategies.

Wings

The main modularity of the MUAV lies in the possibility to mount a large variation of wings. One standard set of wings will be supplied, other configurations have to be produced by the user. Of course there are some limitations in what wings can be mounted.

The maximum weight of one wing is 20 kg. The centre wing box has 5 mounting points with a distance of 18.6 cm between them. The standard wings use two of them, therefore the wing can be mounted in 4 different positions. The user can also decide to design wings with a large root cord using more mounting points, sacrificing the ability to move the wing. The wing mounting points can be accessed via the hatch above the centre wing box.

As mentioned in section 4.4 the MUAV has been designed to be stable with wings with parameters from the IDS. This means that the user can design any wing he wants within this design space. A wing configuration outside of this design space might be possible as well. However, this should first be analysed.

It has to be noted that all performance calculations were done using the standard wing. Mounting other wings with other aerodynamic properties will result in different performance characteristics. The user manual shall include a table in which the maximum performance with certain lift and drag coefficients are shown. The default wing with, a surface area of 3.6 m^2, needs a C_L of 1.02 to take-off. Therefore it can be concluded that a wing needs at least a $C_L \cdot S$ of 3.672 to be able to take-off.

Wing devices

On the standard wing box it is possible to attach LE, TE and wing tip devices. As discussed in section 4.1.2 a standard mounting system can be used for this. Since the wing is not tapered each interface is basically a rectangular plate, simplifying the production process of modules. On each wing 10 kg of modules can be placed. It does not matter whether these are placed on the TE, LE or tip, as long as the total weight is 10 kg maximum.

Besides the structural aspect, the electrical should be taken into account as well. The standard wings are equipped with strain gauges which are connected to a dedicated sensor node. Since this node is fully programmable and has additional pins, more sensors, actuators or flow control devices can be connected as well. These connections can be accessed via the same hatch as the wing mounting. To power the actuators and flow control devices 7.4 and 24 V sockets are available. It has to be taken into account that the power used here is part of the 1 kW available for payload.

Payload

As mentioned in section 4.3 the design of the payload bay is based on a 19 inch rack. Five units of 44.45 mm are available. The instrumentation can have a depth of 500 mm maximum. The maximum weight that can be stored in the payload bay is 15 kg. A maximum of 1 kW of power is available on 5, 7.4 and 24 V. To be able to connect the payload both mechanically and electrically, the payload bay can be accessed by removing the nose cone and opening the the hatch in the top of the fuselage.

Propeller

The standard propeller has a diameter of 28 inch. To make sure the propeller does not hit the ground during landing a ground clearance of 15 cm is considered. In case the user wants to mount a slightly larger propeller he should take into account that this margin decreases. On top of that any mounted propeller should be able to rotate at 8500 rpm and weigh no more than 500 g.

Control strategies

The standard flight computer is fully programmable and therefore the user is able to upload his own control scheme. Since the flight computer is mounted in the payload bay, it can be disconnected and replaced by a different controller as well. This gives the user complete freedom in what controller and control scheme is used.

The MUAV can be manually controlled via a fully programmable controller. So in case extra modules are attached these can be activated via this controller as well.

8.3.2 Limits of operation

Besides the limitations for specific modules, there are some limitations for operating the MUAV as a whole. Those will be discussed in this section. First some stability issues will discussed, after that some considerations concerning gusts will be given.

Stability

Static and dynamic stability requirements have a big influence on the design of an aircraft. Therefore the stability characteristics of the MUAV vary depending on the modules attached to it. For a given wing configuration the c.g. location might have to be adjusted. To make sure the MUAV does not crash due to mistakes in the configuration, a software tool shall be supplied in which the user can fill in the characteristics of the configuration to be tested. The tool gives the stability characteristics as an output. With this tool it can also be evaluated whether it is possible to fly with a wing configuration which is outside of the IDS. It should also be used to select the correct wing and payload location when using a wing configuration within the IDS.

Gusts

The MUAV is designed for a load factor of 5g. Therefore some caution is required with regards to gust loadings. In figure 8.5 the maximum allowed cruise speed is plotted for multiple wing configurations at a gust intensity of 8 m/s. It can be seen that for large wings with a large aspect ratio the maximum cruise speed has to limited. The user manual shall include these kind of figures for different gust intensities. Very little data is known about gusts on the flight altitudes of the MUAV.

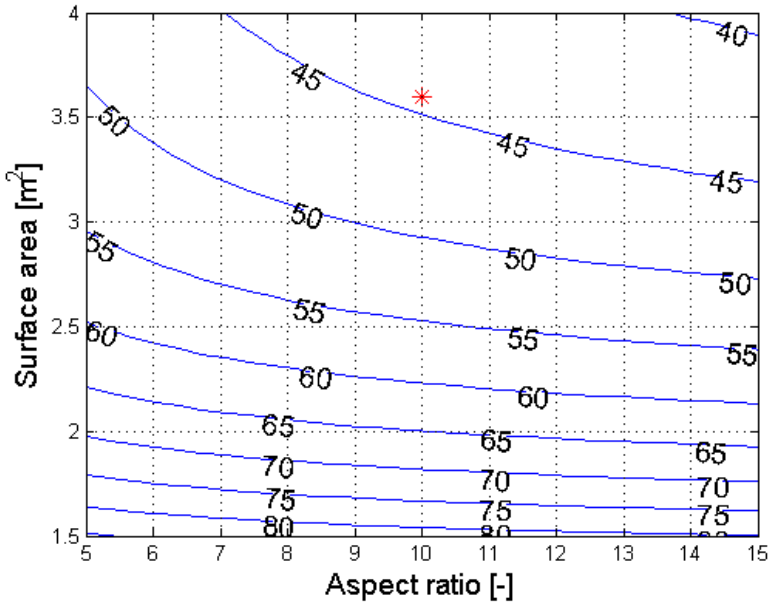

Figure 8.5: Maximum cruise speed for modularity range for gust intensity of 10 m/s

8.3.3 Test location

Due to regulations it is not allowed to fly the MUAV over populated areas or near airports. On top of that the aircraft should always be within line of sight of the operator or dedicated observers. Therefore the test location should be a big and empty piece of land. These kind of areas are not very common in the densely populated areas where most universities are located. Therefore the test equipment will most likely have to be transported from the university to the test location.

An additional test location requirement comes from the take-off distance. As discussed in section 6.3 the MUAV needs a runway of about 139 m. The runway does not have to be paved, but it should be reasonably flat.

From a users perspective the amount of equipment needed at the test location should be minimised. For operating the MUAV not a lot of equipment is required. As mentioned in section 8.3.1, the MUAV comes with a controller. The same system takes care of the telemetry and can be connected to a regular laptop, on which the data can be analysed. Besides that some tools are needed in case the wings and payload have to be moved/replaced and some extra fuel for multiple test flights should be taken along.

8.3.4 Fuel

When multiple test flights have to be performed on one day, the MUAV should be refuelled on the test location. It has been decided that a combustion engine will be used in combination with bio-fuel. Refuelling this type of fuel is very straightforward. The test crew can simply take for example a jerrycan and pour some extra fuel in before a flight. For an endurance of 30 minutes, only 1.14 L of bio-ethanol is needed, so taking enough fuel for multiple tests is not a problem. The availability and price of bio-fuel can differ per country. Since the TU Delft is an important stakeholder the Netherlands are used as an example here.

In the Netherlands bio-ethanol can be bought at around 25 fuel stations, which is not a lot. However, bio-ethanol is also used as a fuel in applications like fire places and torches. Therefore it is also being sold in small bottles at department stores, for example. Since only a bit more than a liter is required for one test flight this might well be an option as well. At fuel stations bio-ethanol costs about €1.50 per liter, at department stores it is about two times as expensive.

As mentioned before, this situation is different in other countries. However, combustion engines can be adapted to run on different types of fuel. Therefore it is possible to make the MUAV work with the

type of fuel most available in the region the costumer is located.

The MUAV is equipped with a 5 l fuel tank, therefore the user can also test with longer endurance or lower density fuel. It has to be noted that in case more than 1.14 l of fuel are taken, the extra weight is considered to be payload weight. Which means less other payload can be mounted.

8.3.5 Logistics

To make sure the MUAV can be transported in an affordable way it should be legal to do that over public roads. Here the modularity is a very useful feature. Since it is possible to dismount the wings anyway, this can be used for transportation in the same way as it is done with gliders. The fuselage of 4 m and two wings of about 3 m length can easily be placed on a trailer or in a small truck. Because of the low weight of the UAV the car-trailer combination can even be driven without trailer license.

While not being used, the MUAV should be stored indoors. On top of that the sensors should be covered. Selling a cover that fits nicely over the complete modular platform or standard wings might be a good option.

8.4 Production plan

It is important to look into the production activities of the MUAV in order to make sure that the product is producible within the allocated budgets. In this section the activities leading from the product blueprints to a physical product will be treated. In subsection 8.4.1 will be elaborated on the general production activities. Finally, in subsection 8.4.2 a Manufacturing Assembly and Integration (MAI) chart giving a more elaborate insight to the production activities will be shown.

8.4.1 General activities

To be able to make a profit the production process should be as efficient as expected. This can be achieved by manufacturing the required quantity of a product, of the required quality, at the required time using the best and cheapest method [34]. This highlights the importance of proper production planning.

Before the parts can be ordered a thorough preparation is needed. The product technical drawings need to be verified, workers need to be hired, product need should be analysed, and a production facility should be arranged. From a costs perspective it is advised to manufacture most of the parts at the Faculty of Aerospace Engineering in Delft.

After making the necessary preparations the first production activities can begin. Raw materials, off-the-shelf components, and outsourced components should be ordered in the right amount depending on the product need. The materials will have to be formed according to the designed components such as stringers, ribs, and skin material. To finalise the component production holes should be drilled where necessary and electrical components such as strain gauges should be attached while their location is still easily reachable.

With all the components produced the subsystem assembly can begin. All the components and outsourced parts should be ready by this point. The subsystems will be assembled and have their wiring laid out. Some subsystems can already be connected such as the payload bay and fuselage. When all the subsystems have been assembled the wiring should be connected and finally the product is assembled.

During component production, subsystem assembly, and product assembly quality checks are an important activity to ensure product quality. Each component should be checked thoroughly to verify whether they are accurate to the technical drawings and subsystem designs.

8.4.2 Production chart

To give an insight in the time span and order of the production processes a MAI chart was made. This plan gives an insight to the preliminary production schedule. All activity dependencies are shown which can help with identifying bottlenecks in the production of the MUAV. The MAI is shown in figure 8.6 with a colour identification for interconnected activities. Three major bottlenecks can be identified from

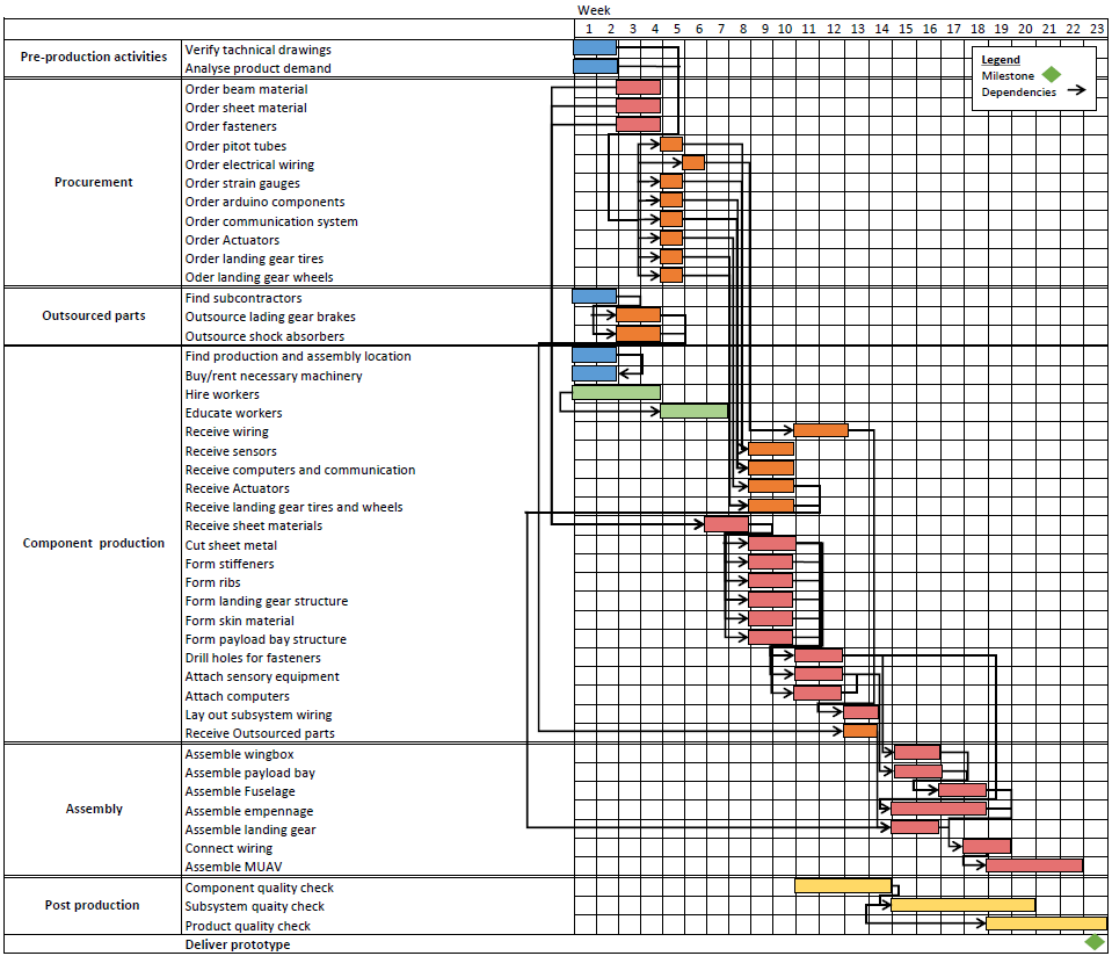

Figure 8.6: MAI chart with all the production activities following after the design phase up to the first prototype

the MAI. First the drawings have to be verified, if not the products can not be ordered. Secondly, the receiving of the raw material, if this is delayed the workers can not start forming the material and this will add cost because the workers are already hired. Lastly, for the assembly the outsourced materials have to be received and the produced parts have to be ready to assemble the subsystem.

8.5 Sustainability approach

Although the concept of sustainability is now widely adopted among many different companies, the actual integration of sustainability in the final product remains challenging because of the broad range of environmental, economic and social factors that need to be considered. The aim of this section is to present a reflcetion on integration of a realistic sustainability approach defined within the scope of the project.

8.5.1 Environmental impact of different power and propulsion systems

The emission of an aircraft is the aspect with the highest environmental impact. Up until now the most commonly used fuel for an aircraft is fossil fuel, as a result of its high energy density. However, due to the high environmental impact of fossil fuels, the need for alternatives with a lower environmental impact arises. The two most widely used alternatives for fossil fuels are using electrical power and bio-fuels.

The following subsection will discuss these two alternatives and how the sustainability is implemented in the propulsion system for the MUAV.

Electrical

Electrical propulsion is the most obvious alternative to the use of fossil fuels as batteries have no emission. However that does not mean that when using batteries, there is no environmental impact. The environmental impact of an electric propulsion system greatly depends on the source of the energy. If renewable energy is used, the relative advantage of an electrical system greatly increases.

On top of that, an electrical propulsion system uses a lot of batteries to be able to store all the energy needed. A battery in itself is harmful for the environment, however the relative impact is low when compared to the total life-cycle of the propulsion system. Studies show that the impact of operation is the largest when looking at the whole cycle of transportation systems [35, 36]. This is supported by the fact that for the most common batteries, the Lithium-Ion batteries, the relative amount of Lithium is very low. [37] So if the batteries are charged with renewable fuel the electrical propulsion system is a very clean and good alternative to the conventional fossil fuel system.

Unfortunately, battery technology is not yet feasible to function as main energy source for this MUAV. This is because the amount of batteries required for the operation of the MUAV, increase the total weight in three-fold.

Bio-fuels

As batteries are no option, further research is done in the most sustainable form of propulsion available within the requirements. One of these considerations are bio-fuels. Bio-fuels have several advantages over fossil fuels. The most important one is the fact that they are produced using a renewable source. These sources can be classified in three generations. The first generation bio-fuels are produced using beets and corn. The sugars from these vegetables can be used to create bio-ethanol. There are however many drawbacks to this kind of fuel production. One of the drawbacks is that studies suggest that using first generation bio-fuels actually has a larger impact on the environment than using fossil fuels [38, 39]. Another major drawback is the fact that these dedicated corn and beet farms directly compete with the world food market. The desire for new initiatives has lead to the development of the second and third generation bio-fuels, which are produced through a variety of feed stocks and conversion technologies. The first step in this development is the second generation bio-fuels, which are produced from bio-waste and other inedible crops. Although this process does not directly compete with the food production the overall efficiency of the second generation bio-fuels is lower. The third, and most promising, generation produces bio-fuels from algae.

Application of fuel considerations to the MUAV

In the design, an low environmental impact is one of the major concerns. If that was the only concern than the choice was easily made for the use of batteries. However, the weight penalty is so severe that the MUAV will have to fly on a liquid bio-fuel system.

8.5.2 Recycling of the UAV

In the following subsection a brief overview of recycling in the aviation industry will be given, followed by the incorporation of recyclability in the design of the MUAV.

Recycling in the aircraft industry

Although the concept of recycling aircraft as an end of life solution is relatively new, it has quickly become a key concern during the design process. Currently the aircraft industry does not operate in a closed loop fashion. Traditionally a significant portion of aircraft components is dumped on graveyards and left to decay. Major changes have been implemented and using current technology 80% of the mass of the 12,000 aircraft which will be retired in the next two decades can be recycled. This is expected to

rise to 90% by 2016 [3]. The main difficulties encountered in recycling aircraft parts are the complexity of the systems on one hand and the number of different materials on the other. The materials range from long and short fibre composites, aluminium, titanium and steel alloys to foam and textiles. Subsystems are intricate where many small parts consisting of different materials are combined making it difficult to separate these during recycling.

Application to the MUAV

In the design of the MUAV, the recyclability is incorporated in the design through the proper selection of highly recycable materials and simplicity of the modules. This was one of the driving parameters in the choice for aluminium as aluminium is much better recyclable than carbon structures. It is also chosen to use only one kind of aluminium alloy, to allow for easier recycling and a lower loss in material grade. On top of that, hatches were located in such a way that they provide maximum accessibility in order to be able to make changes to all parts within the MUAV.

8.5.3 Sustainability and modularity

In this section an overview is given on the effects of modularity on the sustainability ambitions. This is split up in the effects on the sustainability of the platform itself, and the effects this platform can have on the entire aircraft industry.

Effects of modularity on a sustainable design of the MUAV

On of the most important assets of the aircraft considering sustainability, is the modular design in itself. Although it requires a little more material to achieve this amount of modularity, it creates many opportunities. One of these is the fact that all components can be upgraded and changed one at a time. This means that a specific End of Life (EOL) solution can be designed for every separate component of the aircraft. On top of that, only the components that need to be changed will be replaced. Last is that the access and modularity make repair much more easy, this saves energy and material.

Effects of MUAV on sustainability of the aircraft industry

On top of that, this research platform can and will be used for the testing of concepts that can make the aircraft industry more efficient, and therefore more sustainable. Research on concepts that in theory can greatly reduce the aerodynamic drag that is encountered during flight, such as the boxed wing concept and SHLD, will likely get a boost. This research platform greatly facilitates the testing of sustainable innovations.

8.5.4 Effects of modularity on a sustainable use of the MUAV

Apart from the effects the MUAV has as described in the previous chapters, the actual concept of the MUAV is in itself a highly sustainable concept. Due to its nature of being a multi-purpose vehicle, the environmental impact of the MUAV is much lower than buying a new UAV for every research project. This means that it can replace the much more demanding simulators and private aircraft currently used for testing.

[3] Aircraft Recycling Directory, Aircraft Fleet Recycling Association, `http://www.afraassociation.org`, 2015, accessed: 10-12-15

Chapter 9

Conclusions

Many facilities are available at the Delft University of Technology (DUT) for testing and evaluation of aeronautic concepts. Among these are various wind tunnels and a Cessna citation research aircraft for in-flight testing. The wind tunnels provide valuable data for research and development but, by their nature, will always provide an approximation of actual flight. The Cessna Citation available for flight testing has very high operational costs and test modules must meet extensive certification requirements. The purpose of the presented project is to fill the gap between wind tunnel testing and full-scale flight testing with a low cost modular platform for in-flight testing of aeronautical concepts.

Within nine weeks a preliminary design of the MUAV was made. The MUAV is 4 meters long, the default wing has a span of 6 meters, and it has a MTOW is 992.5 N. The payload capacity is 20 kg which can be used for leading edge, trailing edge, or tip modules on the default wing. The default wing can also be replaced entirely by a custom design. A planform with any parameter combination is allowed for a sweep between minus ten and fifteen degrees, a taper ratio between zero and one, an aspect ratio between five and fifteen and a surface area between 1.6 and four square metres. Planforms outside of these parameters can also be accommodated, but not unconditionally. To make sure the aircraft can be stable in any configuration, both the payload and wing position can be changed. Up to 15 kg of payload can be carried in the fuselage payload bay for data acquisition and processing. For control system and auto-pilot testing any part of the entire control system can be replaced with custom units. The manufacturing costs are estimated to be €42000,- with a contingency of €8000,-. Furthermore the structure is designed to be able to withstand a limit load of at least 5g. The empennage has a vertical stabiliser with a rudder for yaw control and a full moving horizontal stabiliser for pitch and roll control. In case of a critical failure in-flight, a parachute will be deployed to reduce the crash loads and preserve the electrical systems on-board with the help of a well designed payload bay.

Since the platform can accommodate various payload modules as well as various wing planforms, it can be used for flight testing of a large number of concepts. The production and operational costs are significantly reduced compared to a Cessna Citation and no official certification of payload modules is required. To demonstrate the capability of the platform two payload modules have been designed. A set of seamless high lift devices demonstrate the capability of the default wing and an entire box wing demonstrates the flexibility of the aircraft in testing entire wing concepts.

Chapter 10

Recommendations

It has become clear from the the previous chapters that a modular concept for a UAV has a lot of potential. As the design of the MUAV was done within a limited time frame, there is still room for improvement. The following paragraphs will reflect on the design process and identifies the areas that can be improved. This first section will focus on the technical recommendations, whereas the second section will focus on the project wide recommendations.

10.1 Technical recommendations on the design

Although the initial results look promising, there is still much to be done to make the MUAV an airworthy platform. The first recommendation stems from the fact that the level of depth for the calculations done is not yet detailed enough. An example for this is the material selection, for the current design the range of values for the maximum allowable stress is rather high. This resulted in more material used than needed as the lowest value is calculated with. Furthermore, different materials than aluminium should be considered and a new trade-off has to be made. Two driving reasons behind the choice of aluminium was the fact that it currently is more difficult to recycle carbon fibre composites and the higher cost associated with production. More research has to be done on the environmental impact of the use of a carbon fibre composite structure. Because the current value for MTOW is higher than the requirement (922.5 N instead of 785 N), this could be a viable option. On top of that, the use of composites would counter the manufacturability limitations currently encountered by the aluminium wing skin. Another example of a subsystem that requires a better analysis, would be the fuselage and especially its structure. Not all loads on the fuselage are fully investigated and the optimisation sequence for the wing was used. Therefore a better structural design of the fuselage is needed before further steps in the design process can be taken. This is even more true for the empennage. Although the stability criteria are thoroughly researched, the structure itself has not yet been designed.

The second recommendation that can be made is the use of optimisation and iteration techniques. As there was little time in the design of this project, only one major system wide design iteration was done. This means that for many subsystems the knowledge over a possible optimum is limited. On top of that, the dependencies between the different design parameters should be made more intelligible. An example is the ratio of tail length versus tail surface area for which an optimisation was made. The sensitivity of the subsystems and their variables with respect to the tail length was not further investigated.

10.2 Project wide recommendations on the design

The main purpose of the MUAV is to provide the possibility for realistic in-flight testing of new concepts, these test must be as accurate as possible. However, the restrictions to the design that follow from this requirement make the design of the MUAV more challenging. An example of one of these requirements is the wing span. As the OEW requirement of the MUAV is only 60kg, the corresponding wing

span of 6 m leads to a very low wing loading. The result of this low wing loading is that the weight fraction of the wings are very high, with only a skin of 0.7 mm the total weight percentage of the wing is 62%.

Another requirement that makes the design of the MUAV challenging, are the requirements on the sustainability of the vehicle. For the design, sustainability is taken into account as much as possible, within the boundaries of a reasonable design. If in a more mature design stage of the MUAV an ambition to more intensively incorporate sustainability arises, extensive research must be done to the possibilities and the implications this has on the design. At this point in time, a 100% recyclable UAV is not yet possible, neither is a UAV with zero-emission for this mission profile.

The design of the MUAV includes an initial design of the boxed wing concept. Although the boxed wing looks promising, the MUAV in its current form is not the most optimal way to test this design. If there is a real motivation to develop a MUAV with the possibility of a boxed wing concept, the whole configuration should be reevaluated to be able to test the boxed wing with its full potential.

Although the design space for the MUAV is large, it would be more efficient to incorporate a tail with a variable tail length, for example a boom tail. This would set in motion a chain of reactions, for example the location of the propeller should be reassessed, which in itself could have severe implications on the rest of the design. Also the relation between tail size and tail surface is an interesting subject for the future, where lies the optimum to cover both the design space, as well as being as light as possible.

The final recommendation is that we would advice to carry on in the development of this project. This concept has a lot of potential, and with the innovations that lie ahead, could prove to be a very successful product.

Bibliography

[1] D. group 1. “Requirement specification”. In: (2016).

[2] G. L. Rocca. *Systems Engineering and Aerospace Design*. 2014.

[3] D. Raymer. *Aircraft Design: A Conceptual Approach*. 3rd ed. AIAA, 1999.

[4] M. Voskuijl. *AE-2230I Flight mechanics*. Lecture slides. 2012.

[5] J. Anderson. *Fundamentals of Aerodynamics 5th edition*. McGraw-Hill, 2011.

[6] J. Markish. *Valuation Techniques for Commercial Aircraft Program Design*. AIAA. 2002.

[7] J. Roskam. *Airplane Design. Part VIII: Airplane cost estimation: design, development, manufacturing and operating*. The University of Kansas, 1990.

[8] M. C.Y.Niu. *Airframe structural design*. Hong Kong conmilit press LTD., 1997.

[9] D. Mclean. *Wingtip devices: What they do and how they do it*. 2005.

[10] L. falcao. *Aero-structural Design Optimization of a Morphing Wingtip*. 2011.

[11] Anon. “ESDU F.05.01.01: Normal force on flaps and controls”. In: (1973).

[12] M. D.Maughmer. “The design of winglets for low speed aircraft”. In: (2001).

[13] T. Megson. *Aircraft Structures for Engineering Students*. Elsevier Ltd, 2007.

[14] E. Bruhn. *Analysis and design of flight vehicle structures*. 2nd ed. Jacobs publishing, 1973.

[15] S. Levy. “NACA Technical Note No. 846: Bending of rectangular plates with large deflections”. In: (1942).

[16] M. Sadraey. *Aircraft design : a systems engineering approach*. Wiley, Hoboken, New Jersey, USA, 2012.

[17] A. in ’t Veld. *AE-3202 Flight dynamics*. Lecture notes. 2013.

[18] R. Finck. *United States Air Force Stability and Control DATCOM*. McDonnell Douglas Astronautics Company, 1978.

[19] A. Ravi. *UAV Power Plant Performance Evaluation*. Tech. rep. Master Thesis. Oklahoma State University, 2010.

[20] J. Roskam. *Airplane Design. Part IV: Layout design of landing gear and systems*. The University of Kansas, 1989.

[21] J. M.C. Butler and R. Montanez. *How to select and qualify a parachute recovery system for your UAV*. 2002.

[22] L. Prandtl. “Induced Drag of Multiplanes”. In: *Technische Berichte* (1924), pp. 1–23.

[23] R. Emanuelle. *Optimization methods applied to the preliminary design of innovative, non conventional aircraft configurations*. 2007.

[24] E. Torenbeek. *Synthesis of Subsonic Airplane Design*. Delft University Press, Delft, 1982.

[25] S. G. *Kinematic Simulation and Structure Analysis of a Morphing Flap*. Tech. rep. Master Thesis. Cranfield University, 2013.

[26] H.Monner. *Smart High Lift Decives for Next Generation Wings*. 2013.

[27] M. Modarres, M.Kaminskiy, and V. Krivtsov. *reliability Engineering and Risk Analysis*. Marcel Dekker, Inc., 1999.

[28] C. Ebeling. *An Introduction to Reliability and Maintainability Engineering*. Waveland Press, Inc., 2010.

[29] B. Ayyub. *Risk Analysis in Engineering and Economics*. CRC Press, 2003.

[30] M. A. Bourcier. "Logistics Test and Evaluation in Flight Test". In: *Flight Test Techniques Series* 20 (2001), pp. 11–13.

[31] R. Vos and B. Zandbergen. *AE-1201 Aerospace Design and Systems Engineering Elements I*. Lecture slides. 2011.

[32] D. group 1. "Baseline report". In: (2016).

[33] M. Goodrich. *Aeronautical Wind Tunnels in Europe and Asia*. NASA Aeronautics Research Mission Directorate, 2006.

[34] H. Nagare. *Machine shop production planning*. Welingkar institute, India, 2007.

[35] H. MacLean and L. B. Lave. "Life Cycle Assesment of Automobile/Fuel Options". In: *Enviromental Science and Technology* 37.17 (2003), pp. 5445–5452.

[36] G. Schwelmer. "Life Cycle Inventory for the Golf A4". University of Kassel, 2000, pp. 5445–5452.

[37] D. Notter et al. "Contribution of Li-Ion Batteries to the Environmental Impact of Electric Vehicles". In: *Enviromental Science and Technology* 44.17 (2010), pp. 6550–6554.

[38] J. Fargione et al. "Land clearing and the biofuel carbon debt." In: *Science* 319 (2008), pp. 1235–1237.

[39] T Searchinger et al. "Use of U.S.croplands for biofuels increases greenhouse gases through emissions from land-use change." In: *Science* 319 (2008), pp. 1238–1240.

Appendix A

Who-Did-What

Table A.1 contains the work distribution of the final report. It shows who wrote what, and also the contribution of each team member to a certain section is.

Table A.1: Who-did-what

Section/subsection	Reporting	Contribution	Reviewer
Introduction	Ruud		Patrick
Summary	Patrick		
2.1	Jerry		Patrick
2.2	Jerry	Ruud (diagrams)	Patrick
2.3	Patrick		Jerry
2.4	Jerry	Ruud (FFD)	Patrick
2.5	Jerry		Patrick
2.6	Matthias		Patrick
3.1	Mart		Matthias
3.2	Mart		Matthias
3.3	Mart, Matthias (3.3.2)		Matthias
3.4	Mart		Matthias
3.5	Mart		Matthias
4.1	Jos		Mart
4.2	Storm		Mart
4.3	Ruud:4.3.1 Steven:4.3.2-4.3.3	Milan	Jerry
4.4	Matthias 4.4.1, 4.4.2 (v.tail stability), 4.4.4, 4.4.5 Jasper 4.4.2 (except v.tail),4.4.3, 4.4.5	Matthias, Jasper	Steven
4.5	Mart		Jerry
4.6	Patrick	Mart	Jerry
4.7	Jerry		Ruud
4.8	Mart		Ruud
5.1	Milan		Ruud
5.2	Patrick		Milan
6.1	Ruud		Milan
6.2	Storm		Milan
6.3	Ruud		Milan
6.4	Milan	Ruud	Milan
6.5	Ruud		Milan
7.1	Patrick		Jasper
7.2	Patrick	Jos (load diagrams)	Jasper
7.3	Patrick		Jasper
7.4	Patrick		Jasper
8.1	Jerry		Jasper
8.2	Jos	Jerry(FMEA, fault tree)	Jasper
9.1	Mart	Matthias	Patrick
9.2	Matthias		Patrick
9.3	Mart	Jos (gust loading)	Patrick
9.4	Patrick and Jasper		Patrick
9.5	Milan		Patrick
Conclusion/Recom.	Jerry (Concl.) Milan(Recom.)		Patrick(C), Jerry(R)
Requirement specification	Ruud	Jerry,Steven, Storm	

Appendix B

Reference data

Table B.1: Reference data part A, '-' indicates unknown data

Aircraft #	Type	Manufacturer	Wingspan [m]	Length [m]
1	Arcturus T-20	Arcturus	5.2	2.8
2	RQ-7B Shadow	AAI	6.7	3.4
3	RQ-21 Blackjack	Boeing Insitu	4.9	2.5
4	Lipan M3	Argentine Army	4.6	3.55
5	yarara	Nostromo	4	2.472
6	Sojka 3	-	4.12	3.78
7	Niti	Armstechno	5.38	3
8	RQ-2 Pioneer	AAI	5.2	4
9	FOX	CAC	4	2.75
10	Nearchos	EADS 3 Sigma	5.1	3.95
11	Mastiff	Tadiran	4.25	3.3

Table B.2: Reference data part B (continued), '-' indicates unknown data

Aircraft #	MTOW [N]	OEW[N]	PW[N]	FW[N]	PW+FW[N]
1	823	490	-	-	333
2	1667	824	-	-	843
3	600	363	-	-	237
4	588	-	-	-	-
5	220.725	152	49	19.62	68.62
6	1422.5	-	294	-	-
7	588.6	-	-	-	-
8	2011	-	-	370	-
9	1324	716	294.3	313.92	608.22
10	1079.1	588.6	-	-	490.5
11	1353.8	706.32	363	284.48	647.48

Table B.3: Reference data part C (continued), '-' indicates unknown data

Aircraft #	**Powerplant [-]**	**Power [kw]**	v_{cruise}**[m/s]**	v_{max}**[m/s]**	**Endurance[hours]**
1	190cc 4 Stroke	7.5	-	47	1
2	Wankel UAV Engine 741	28	36	56	9
3	EFI Piston Engine	6	28	38	16
4	-	-	-	47	5
5	Piston, Wankel	6	32	40	6
6	-	-	36	50	-
7	3W 106iB2 Two-cylinder engine	8	30	33	-
8	2-cylinder piston engine	19	-	-	-
9	Limbach L275E	16	-	50	5
10	Piston engine	28.34	-	61	8
11	-	-	-	51.4	7.5

Appendix C

Gantt chart for future development

Figure C.1: Gantt chart for futur development

Appendix D

Risk register

#	Risk ID	Category	Cause	Risk event	Consequence	Likelihood	Effect	Approach	Mitigation method
1	RID-W2-01	Business	Inability to find suitable manufacturing facilities	manufacturing costs exceed requirement by 50%	Marketing position degradation	low	critical	Research	-
2	RID-W2-02	Commercial	Unavailable technology	Not 100% sustainable	Marketing position degradation / requirements not met	very high	marginal	Research	-
3	RID-W2-03-B	Communication	Inadequate communication	Discrepant input data	Unviable design	Medium	catastrophic	Mitigation	Appoint data manager and set up data tracking infrastructure
4	RID-W2-04-B	Communication	Inadequate systems engineering	Mismatch of subsystems	Unviable design	Medium	catastrophic	Mitigation	Appoint systems engineer
5	RID-W2-05	External	Legislative change	Permit declined	No certification	low	critical	Watch	-
~~6~~	~~RID-W2-06~~	~~Project management~~	~~Inadequate project management~~	~~Congestion in workflow~~	~~Project delay~~	~~medium~~	~~critical~~	~~Mitigation~~	~~Appoint project manager~~
7	RID-W2-07	Project management	Lack of project control	Overlooked subjects	Longer development time	medium	critical	Mitigation	Appoint project manager and employ SE tools
8	RID-W2-08-B	Project management	Lack of validation	Improper validation	Not meeting requirements	Low	catastrophic	Mitigation	Set lead engineer responsible, V&V methodolgy
9	RID-W2-09-B	Project management	Lack of verification	Improper verification	Unviable design	Low	critical	Mitigation	Set lead engineer responsible, V&V methodolgy
10	RID-W2-10-C	Technology	Use of (too) new technologies	Teething problems	Longer development time	Low	critical	Mitigation	Off the shelf products and extrapolated from existing design approach
11	RID-W2-11	Technology	Unreliable supplier	Inadequate of-the-shelve technology	Need for new supplier	low	negligible	Research	-
12	RID-W2-12	Technology	Bad weight management	OEW 50% too high	Too high OEW	high	marginal	Watch	-
13	RID-W2-13	Technology	Inadequate cost tracking	Manufacturing costs exceed requirement by 50%	Marketing position degradation	medium	marginal	Watch	-
~~14~~	~~RID-W2-14~~	~~Technology~~	~~Inadequate conceptual design phase~~	~~Incomplete design option tree~~	~~Non-optimum design~~	~~low~~	~~critical~~	~~Watch~~	-
15	RID-W2-15	Technology	Too tight schedule	Not being able to fulfil all requirements	Concessions on meeting customers need	very high	marginal	Mitigation	Good communication with customer
16	RID-W2-16-B	Technology	Non proven flight design	Crash tolerance requirement not met	Longer development time	Medium	catastrophic	Research	-
17	RID-W3-17-B	Project management	Bottlenecks	Concept trade-off/Sensitivity analysis/ midterm report/ system definition takes too long	Project delay	low	critical	Mitigation	Set deadlines and keep track by project manager
18	RID-W3-T01	Technical	Sharp objects on runway	Flat nose tire	Crash (impact) during take-off or landing	Low	Critical	Mitigation	Use solid wheels or another nose tire, or check the runway before use
19	RID-W3-T02	Technical	Engine malfunction	No more engine power	No thrust and power to electrical power generation	Low	Marginal	Mitigation	Engine test before take-off
20	RID-W3-T03	Technical	Generators malfunction, wiring failure	No more electrical power	Not enough power to continue mission	Low	Critical	Mitigation	Checklist, check battery power
21	RID-W3-T04-B	Technical	Transmitter/receiver failure	No communication	No Low control	Low	Marginal	Mitigation	Automatic landing procedures when communication is lost, parachute
22	RID-W3-T05	Technical	Control surface failure	No axis control	Not enough control	Low	Critical	Mitigation	Checklist, abort mission
23	RID-W3-T06-B	Technical	Landing gear failure or not reaching appropriate speeds	Unsuccessful take-off or landing	Unstable roll and pitch	Low	Marginal	Mitigation	Validate system design by testing, use of checklists
24	RID-W3-T07	Technical	Control loss during take-off or landing/ no propeller clearance	Injury with persons	Damage on both MUAV and person	Low	Marginal	Mitigation	Landing/take-off instructions, control surface and control check before take-off
25	RID-W3-T08	Technical	Not receiving data from gps antenna or circuit board	GPS failure	No exact location of MUAV is known	Low	Marginal	Mitigation	Check connection before using an autopilot, control the aircraft manually
26	RID-W3-T09	Technical	Crash, short circuit or battery puncture	Fire	MAUV destruction and environmental damage	Low	Critical	Mitigation	No exposed wires, batteries secured, fire extinguisher always on site, off-road vehicle available to get to the crash site

Figure D.1: Risk register(part 1)

#	Risk ID	Category	Cause	Risk event	Consequence	Likelihood	Effect	Approach	Mitigation method
27	RID-W3-T10-B	Technical	Wing structural failure in-flight due to high loads (by gusts or manoeuvres)	Loss of lift in-flight	Unstable aircraft, barely controllable, crash	Low	Critical	Mitigation	Parachute, design for higher loadings
28	RID-W3-T11	Technical	Crash, landing gear failure	High impact load	Expensive electrical systems damaged	Low	Catastrophic	Mitigation	Parachute, high safety factor (1.5)
29	RID-W5-T12	Technical	Not well mounted	Structural breakdown	Emergency operations	Low	Catastrophic	Mitigation	Optimise design for user friendliness, train ground personnel, parachute
30	RID-W5-T13	Technical	Wrong performance analysis	Unpredicted dynamic behaviour	Unstable vehicle	Medium	Critical	Mitigation	Good engineers, good product manual, pre-flight checks
31	RID-W5-T14	Technical	Payload not well mounted	C.g. Moves in-flight	Unstable vehicle	Low	Critical	Mitigation	Good design, pre-flight checks
32	RID-W5-T15	Technical	High gust loading	Structural failure	Emergency operations	medium	Catastrophic	Mitigation	pre-flight wind check
33	RID-W5-T16	Technical	Cables not well connected	Electrical failure	No power to various subsystems	Low	Critical	Mitigation	pre-flight cable check, well trained workers
34	RID-W5-T17	Technical	High complexity	Autopilot malfunction	Uncontrollable vehicle	Low	Marginal	Mitigation	Manual control, parachute
35	RID-W5-T18	Technical	Parachute deployment	Structural breakdown	(partial) crash	Low	Catastrophic	Mitigation	Well designed vehicle
36	RID-W5-01	Project management	High complexity	Exceeding time budget	Higher costs	Low	Marginal	Mitigation	Less complex design, more off the shelves products, better contingency management
37	RID-W5-02	Project management	High complexity	Weight exceeding requirements limits	Unsuccessful product	Low	Catastrophic	Mitigation	Less complex design,. Better contingency management
38	RID-W7-T19	Technical	Bad control scheme	Flight controller failure	Uncontrollable vehicle	Low	critical	Mitigation	Validate control scheme, good planning (programming)
39	RID-W7-T20	Technical	Sensor damage or fatigue	Sensor failure	False data	Low	Marginal	Mitigation	Redudancy, on board data analysis

Probability	Negligible	Marginal	Critical	Catastrophic
Very High		2 15		
High		12		
Medium		13	7, 10, 30	3, 4, 16, 32
Low	11	19, 21, 23, 24, 25, 34, 36, 39	1, 5, 9, 14 , 17, 18, 20 ,22, 26, 27, 31, 33, 38	8, 28, 29, 35, 37

Consequence

Doc. Version	Entry nr.	Date	Change	Reason
0.1	1	25/11/2015	Added new risk RID-W3-17	Identified risks from PERT charts
0.2	2	26/11/2015	Risk RID-W2-06 can be replaced	RID-W3-17 is more specific
0.3	3	03/12/2015	RID-W3-T04	Added parachute as mitigation method
0.4	4	09/12/2015	Naming of likelihood	Consistency
0.5	5	10/12/2015	Added concept risks entry number 29-37	Concept risk identification
0.6	6	13/12/2015	Updated project risk: RID-W2-03, RID-W2-04, RID-W2-10 and RID-W2-16	Mitigation approach is working
0.6	7	13/12/2015	RID-W5-T10	Added mitigation approach
0.7	8	16/12/2015	RID-W3-T06	Assesed to be medium likelihood instead of high
0.8	9	07/01/2016	RID-W2-08 and RID-W2-09	Likelihood less due to integrated V&V methodology
0.8	10	07/01/2016	RID-W2-10-B	Likelihood less due new mitigation method
0.8	11	07/01/2016	RID-W2-14	NA anymore
0.8	12	07/01/2016	RID-W3-17	Lower likelihood because good planning
0.9	13	08/01/2016	RID-W7-T19 and RID-W7-T20	Added risk (from electrical system design)

Figure D.2: Risk register and map and change record (part 2)

Appendix E

Document change record

Table E.1: Document change record

Revision:	Date:	Affected Section:	Description of Change:
0	04-01-2016	-	Document created
1	20-01-2016	-	First round of editing completed
		-	Removed acronym explanations from table of contents
		-	Removed page number from blank page after the tile page and correct the acronym list (in alphabetic order) as well as improved the list of symbols
		-	Fixed grammar and spelling in every chapter
		(old) 7.0	Removed chapter about verification and validation, redistributed over report.
		1	corrected spelling
		2.3	Changed subsection to subsubsection and change the intro to 2.3 Test profiles
		2.4	Improved the consistency between the FFD and FBS
		2.7	Moved the methodology of verification and validation to the mission outline from section (old) 7.1, Validation method revised, sensitivity analysis added.
		4	Moved wing design in front of the fuselage design in the subsystem design chapter , For every subsystem added verification and validation methods used and sensitivity analysis for load bearing subsystems
		4.1.3	Added EDS considerations to wing-fuselage interface loads.
		4.1.4	Explained distinction between primary and secondary assumptions, replaced wing box render with top view and cross section technical drawings.
2	25-01-2016	4.7	Changed the order of input and output table, replaced 'landing gear' with 'subsystem' on multiple places within this section, added V&V method and sensitivity analysis
		4.4.3	Equations for aspect ratio and wing lift coefficient and other geometry removed. explained in text
		4.4.3	For the dynamic stability the plot for alpha is removed because alpha is assumed to be constand. And the eigenvalues, frequency and damping ratio is added.
		4.4.5	An extra sensitivity analysis is performed for a change in wing position. The change in airspeed is compared.
		4.2.1	Shear and moment diagrams added, plus the addition of clarifying pictures and verification and sensitivity analysis added
		5.2	Updated SHLD weight estimation.
		5.2.5	Added cost estimation for SHLD.
		6	Moved section technical drawings to front of chapter, and added overview of the system including subsystems, Added sensitivity analysis
		6.4, 4.1	Moved airfoil selection to 4.1.
		6.4	Removed equations, to comply with style of rest of report.
		6.3	Updated and fixed values of table 6.8.

Table E.2: Document change record cont.

Revision:	Date:	Affected Section:	Description of Change:
		7	Introduction rewritten, added subsection for risk integration, rewritten content
		7.2.2	Changed equations 8.6 and 8.7 to be more readable
		7.2	Test case defined in the introduction, design influence added, block diagram changed (added colour scheme), rearranged sections and subsection to be more logical and added introduction
2	25-01-2016		
		8.2.4	Added cost comparison with wind tunnel and flight tests.
			Changed table lay-outs for uniformity.
		8.3	Added lift requirement for take-off.
		9	Revised conclusion
		10	Revised recommendations
3	26-01-2016	4.2.1	changed size of loading diagrams
		Nomenclature	Latex magic caused the nomenclature to have disappeared. Magicked the nomenclature back into existence.
4	26-01-2016		